03095

UNIVERSIDAD NACIONAL AUTÓNOMA DE MÉXICO

PROGRAMA DE POSGRADO EN CIENCIAS DE LA TIERRA

ESTUDIO PALEOMAGNETICO INTEGRADO DE ROCAS VOLCÁNICAS PLIO-CUATERNARIAS DE MÉXICO E ITALIA

T E S I S

QUE PARA OBTENER EL GRADO DE

DOCTOR EN CIENCIAS

P R E S E N T A :

GENNARO CONTE FASANO

DIRECTOR DE TESIS:

DR. JAIME URRUTIA FUCUGAUCHI

MÉXICO, D.F. 2004

A Sandra
che malgrado la distanza,
le incomprensioni e le
tentazioni, ha saputo
aspettarmi.

Agradecimiento

Para agradecer a toda la gente que en cualquier modo ha estado cerca de mí a lo largo de estos estudios aquí en México, necesitaría otro tomo como este. Sin embargo siento el deber y sobre todo el placer de agradecer a algunas de ellas y de antemano pido mil disculpas por no haber mencionado a todos, lo cual no representa una falta de atención sino el hecho de que Ustedes son muchos.

Un gracias particular va a mi Asesor, el Dr. Jaime Urrutia Fucugauchi por sus múltiples enseñanzas y las facilidades que me ha brindado, sin dejar atrás su amabilidad y su amistad. Un gracias también al Dr. Avto Goguichaishvili, por el tiempo que me ha dedicado y sus sugerencias que han sido fundamentales para llevar a cabo este trabajo doctoral. Gracias a él he tenido la posibilidad de participar en congresos internacionales que sin duda representan pilares indispensables para la formación de un Doctor. Al Prof. Alberto Incoronato de la Università di Napoli (Italia) van mis profundos agradecimientos por haber sido mi guía al conducirme a esta rama de Ciencias de la Tierra, "Paleomagnetismo". De igual manera agradezco a su asistente el Dr. Pasquale Tiano por su invaluable participación durante el trabajo de campo.

Miles de gracias a todas aquellas personas que por cualquier pregunta y/o duda mía siempre me han contestado en la forma más sencilla posible con el sólo objeto de trasmitirme sus enseñanzas, como por ejemplo el Dr. Mouloud Benammi, el Dr. Luis Alva, la Dra. Ana Maria Soler, la Dra. Glicinia Ortiz, la Dra. Ofelia Morton, Maria de la Luz, Antonio González (Toño) y todos aquellos y aquellas que como he mencionado arriba por espacio no voy a poner.

No cabe la menor duda de que la realización de cualquier trabajo, sobre todo en el extranjero, no depende solamente de las enseñanzas de los "grandes" sino de un conjunto de varios factores que influyen de modo directo en el bienestar de la persona en un País ajeno al suyo. Un gracias en particular a Gabriela Ramírez, quien fue la primera persona mexicana que conocí (vía internet), mil gracias porque me ayudó a descubrir a un País "MÉXICO" y a sus gentes, quienes son extremadamente amables y hospitalarias. Un gracias muy fuerte entonces a la Familia Ramírez (quienes desde hace 5 años me adoptaron en todos los sentidos) al igual que a mi familia de Italia.

Por esa misma razón, va un fuerte agradecimiento a todo el personal administrativo del Instituto de Geofísica, tal es el caso del Sr. Martín Espinosa que a parte ser mi colaborador en el campo ha sido mi confidente y amigo, a su hermano Lorenzo, a todas las secretarias, en un modo muy especial a la Señora Aída, Graciela, Laura y a las del Posgrado, al personal de la biblioteca.....y al final, pero no por último, a todos los estudiantes mexicanos que nunca me hicieron sentir extranjero brindándome todo su apoyo y cariño.

Gracias a todos, gracias a tí México.

INDICE

PREMISA

Esta tesis doctoral fue estructurada con una primera parte en idioma español en donde se da un panorama completo de los objetivos que se plantearon para la investigación, así como descripciones de la Geología de los lugares estudiados y la metodología empleada. Por ser introductiva, en ella no se muestran resultados.

La segunda parte está por cuatro artículos en inglés los cuales incluyen todo el material obtenido en este trabajo doctoral. En cada uno de ellos se exponen objetivos, resultados y conclusiones. Uno de los artículos ya fue publicado en *Internacional Geology Review* V. 46, el resto han sido sometidos en otras revistas internacionales.

Se termine la tesis con una tercera parte en español con una breve conclusión.

RESUMEN

En este proyecto doctoral se han estudiado flujos de lava de edad Plio-Cuaternaria de México e Italia. Para México Central se estudiaron 16 flujos de lava del complejo volcánico Popocatépetl y 24 volcanes del campo volcánico Michoacán-Guanajuato. Estas dos áreas pertenecen a la Faja Volcánica Trans-Mexicana, que se originó por medio de la subducción de la placa de Cocos debajo de la placa Norteamericana a partir del Mioceno superior. En Italia meridional, se estudiaron 14 flujos de lava del complejo volcánico Somma-Vesuvio, correspondientes a la actividad histórica (1631-1944).

Las muestras obtenidas en los flujos de lava se procesaron con métodos paleomagnéticos para determinar paleodirecciones y paleointensidades. La mineralogía magnética y propiedades magnéticas se estudiaron por métodos de magnetismo de rocas, como mediciones de susceptibilidad magnética a temperatura alta, ciclo de histéresis magnética y magnetización remanente isotermal (IRM). Estos estudios permitieron identificar los minerales magnéticos, tamaños de partículas y los estados de dominio magnético. Los minerales portadores de la magnetización remanente, en la mayoría de los casos están representados por titanomagnétitas pobres en titanio y predominantemente de dominio pseudo-sencillo.

Se determinó la paleodirección de la mayoría de los sitios a partir de estudios detallados de desmagnetización térmica y por campos alternos. Varios sitios mostraron una componente magnética secundaria (magnetización remanente viscosa, VRM) de magnitud baja, que fue generalmente eliminada alrededor de 200° C o 30 mT, mientras algunos, por presuntos fenómenos de relámpagos, presentaron una fuerte magnetización remanente con una alta dispersión en la dirección, y por eso fueron excluidos para el análisis estadístico final. A partir de un análisis detallado de los experimentos magnéticos, se pre-seleccionaron algunas muestras para ser tratadas con técnica Thellier-Thellier (Thellier & Thellier, 1959) y sus modificaciones (Coe et al., 1967; 1978) para determinar la paleointensidad.

Del los flujos de lava del volcán Popocatépetl se obtuvo un valor promedio de paleodirección de D=345.7, I=35.4, K=21, α_{95}=5.8, N=15 el cual se desvía

ligeramente (~20°) en el sentido contrario de las manecillas del reloj respeto al valor actual del campo geomagnético, y confirman una edad para el complejo volcánico menor de 0.78 Ma (Brunhes Chron). De las 25 muestras que fueron pre-seleccionadas y tratadas para la determinación de paleointensidad, solamente 14 (cuatro flujos) dieron resultados satisfactorios, reportando un valor promedio de VDM (Virtual Dipole Moments) de 7.2 ±1.4 ($10^{22}Am^2$).

En cuanto al campo volcánico Michoacán-Guanajuato, la mayoría de los sitios estudiados dieron resultados que se acercan a los esperados publicados en diferentes partes del mundo para este periodo, con un valor promedio de paleodirección de D=357.9, I=28.4, α_{95}=7.3, N=20. Sin embargo el estudio de paleointensidad proporcionó resultados satisfactorios solamente para dos flujos.

Todos los datos obtenidos de la Faja Volcánica Trans-Mexicana en este estudio, combinados con los publicados, documentan para los últimos 70,000 años una dispersión de variación secular, con valores de S_f=13.0, S_u=14.5 y S_l=11.8 (limite superior e inferior respectivamente), de acuerdo con el modelo teórico (Modelo G de McFadden 1988, 1991) excluyendo entonces que México Central pertenezca a la zona de baja magnitud no-dipolar del Pacífico como ha sido supuesto por algunos autores (Doell and Cox, 1971, 1972).

De los sitios del campo volcánico Michoacán-Guanajuato, se realizó un estudio metodológico de paleointensidad, investigando en detalle el uso de la técnica de microondas (Shaw et al., 1984, 1996, 1999) modificada por Kono & Ueno (1977), sobre lavas del volcán Paricutín (1943-1947). Desgraciadamente, a pesar que los flujos de lava son muy jóvenes (actuales) y entonces muy útil para poner a prueba el método, los resultados no fueron los esperados y las explicaciones de tal discrepancia son aún hipotéticos.

La mayoría de los resultados de paleodirecciones para en complejo volcánico Somma-Vesuvio están de acuerdo con la curva de variación secular de referencia para Italia meridional (Incoronato et al., 2002; Incoronato & Del Negro, 2004), sin embargo los datos de paleointensidad a pesar de la buena calidad, presentan valores de VDM entre de 7.86±0.2 a 13.5±0.4 ($10^{22}Am^2$) es decir bastante altos respecto a lo actual.

ABSTRACT

Results of a paleodirectional and paleointensity study of sixteen Popocatepetl lava flows are presented. Rock magnetic experiments show that remanence is carried in most cases by Ti-poor titanomagnetite, resulting from oxy-exsolution of original titanomagnetite during flow cooling; high coercivity minerals, likely hematite is also observed in some flows. Unblocking temperature spectra and intermediate coercivities point to 'small' pseudo-single domain (PSD) magnetic grains for these (titano)magnetites. Single-component, linear demagnetization plots characterize the remanence. A strong, lightning-produced magnetization overprint was detected for one site. Combining the new paleomagnetic data with selected previously published results (Carrasco et al., 1986) provides a mean paleodirection of I=35.4°, D=345.7°, k=21, α_{95}=8.5°, N=15 for the Popocatepetl volcano region; with flows showing normal polarity in agreement with a maximum age within the Brunhes chron. Twenty-five samples from flows were selected for Thellier palaeointensity experiments based on magnetic properties, stable single-component remanent magnetizations and reasonably reversible continuous thermomagnetic curves. Fourteen samples from four different flows, yield reliable paleointensity estimates with the flow-mean virtual dipole moments (VDM) ranging from 5.9 to 9.2 x10^{22} Am^2. The NRM fractions used for paleointensity determination range from 35 to 96%, and the quality factors vary between 3.4 and 46.9, being normally greater than 6. Mean VDM obtained in this study is 7.2 ± 1.4 10^{22} Am^2, slightly lower than the present-day dipolar value.

We report detailed rock magnetic, paleomagnetic and paleointensity studies of 24 Plio-Quaternary volcanic units from the Michoacan-Guanjuato volcanic field (MGVF), which is formed by over 1000 volcanic centers (almost 90% of them are cinder cones). Rock magnetic experiments show that remanence is carried in most of cases by Ti-poor titanomagnetites, resulting from oxy-exsolution of original titanomagnetite during flow cooling. Unblocking temperature spectra and high coercivities point to "small" PSD magnetic grains for the titanomagnetites. Single component, linear demagnetization plots define a characteristic magnetization; seven sites yield reverse polarity magnetization while fifteen volcanoes are normally

magnetized. The mean paleodirection obtained in this study is I=28.4°, D=357.9°, k=21, α_{95}=7.3°, with a mean paleomagnetic pole position P_{lat}=85.7°, P_{long}=104.5°, K=27, α_{95}=6.4°. Site-mean directions are undistinguishable from the expected Plio-Quaternary paleodirections, as derived from reference poles for the North American polar wander curve and previously reported paleodirections for central Mexico. Absolute paleointensities obtained from twelve samples from two sites gave values close to the present geomagnetic field strength. The combination of new results obtained in this study with currently available paleomagnetic data from central Mexico yield S_F=13.0 with S_U=14.5 and S_L=11.8 (PSV statistical parameters for dispersion of virtual geomagnetic poles) for the last 70,000 years, which are in agreement with the latitude-dependent PSV model of McFadden (1988, 1991) for the last 5 Ma.

We report a microwave paleointensity study of historic lavas from Paricutin volcano, erupted during the period between 1943 and 1948 in southern sector of MGVF. Most samples are characterized by uni-vectorial orthogonal plots. Rock magnetic and microscopy studies indicate PSD titanomagnetites as remanence carriers. The microwave paleointensity technique was applied to selected samples using both Kono and Ueno (1977) and Coe et al. (1978) variants of Thellier method. Samples yielded technically high quality paleointensity results, though show high within-flow dispersion and are significantly different from the expected value of 45 μT. This is also seen in results using the Thellier method (Urrutia-Fucugauchi et al., 2004). Explanations for this behavior are explored, with reference to other historic lava studies.

We carried out an integrated paleomagnetic, rock magnetic and paleointensity study of fourteen uncertain-age lavas flows from the Somma-Vesuvius volcanic complex. The magnetic carriers consist in Ti-poor titanomagnetites, with PSD domain states. Characteristic magnetization directions determined from detailed stepwise alternating field and thermal demagnetizations give 14 new well-defined flow unit mean directions. Thirty nine samples from seven lava flows yield reliable paleointensity estimates with the flow-mean VDM ranging from 7.86 to 13.5 ($10^{22}Am^2$). Mean paleomagnetic directions of eleven lava flows may be correlated

with the Southern Italy Secular Variation Curve "SISVC" yielding new constraints on their ages. Paleodirections for nine lava flows out of twenty-four analyzed (Caraccedo et al., 1993; Gialanella et al., 1993; Hoye, 1981; This Study) appear to be related to the AD 1631 eruption, as indicated by their direct correlation to the early seventeen century segment of the SISVC, which supports that the AD 1631 episode was an explosive-effusive eruption.

INTRODUCCIÓN

El campo geomagnético es una propiedad global del planeta, como lo es el campo gravitacional. Este campo geomagnético se extiende al exterior de la atmósfera terrestre en el espacio por más de 60,000 km, cada parte del planeta es ocupado por las líneas invisibles de fuerza magnética. La información suministrada por los Observatorios Geomagnéticos a escala mundial ha permitido conocer los rasgos principales del campo geomagnético; estudios del campo geomagnético indican que este puede representarse por una función matemática armónica esférica o sea una función arbitraria definida sobre la superficie de una esfera. El análisis matemático del campo geomagnético pone en evidencia una de sus características más notables: la preponderancia de la armónica de grado uno, es decir, el termino dipolar el cual constituye el campo geomagnético principal. Los estudiosos del geomagnetismo, agrupados en la Asociación Internacional de Aeronomía y Geomagnetismo (IAGA), decidieron en 1960 proponer un modelo que sería adoptado por la comunidad científica internacional y que es denominado IGRF (International Geomagnetic Reference Field). El IGRF es una serie de modelos matemáticos del campo geomagnético principal y de su variación secular (Campos et al., 1991). En primera aproximación el campo geomagnético puede ser representado al 99% como un dipolo egocéntrico axial inclinado de cerca 11.5°C con respecto al eje de rotación de la Tierra. La discrepancia que todavía queda entre el modelo teórico del campo geomagnético principal y lo observado, nos indica la presencia de una porción del campo geomagnético denominada campo no-dipolar (armónicas secundarias en el modelo matemático). Una de las características más importantes de ese campo es su intensidad baja sobre el Océano Pacífico central y su migración hacia el Oeste con un desplazamiento del orden de los $0.12° \pm 0.03°$ por año, el cual podría ser producido por efecto de circuitos horizontales de corrientes eléctricas en el núcleo terrestre, próximo a la superficie de su límite exterior.

El campo geomagnético tiene variaciones temporales que lo afectan localmente, las cuales se conocen, de acuerdo con su duración, como variaciones secular, diaria y disturbios magnéticos. Las variaciones seculares se manifiestan lenta

y progresivamente con periodos de tiempo entre de 10^2-10^4 años, se presentan en todas las componentes del campo (dirección y intensidad) hasta la completa inversión. El comportamiento de estas variaciones a través del tiempo (por medio de mediciones directas) se ha observado que se desplazan sistemáticamente hacia el Oeste a una velocidad del mismo orden que la del campo no-dipolar. Todo eso sugiere que la variación secular del campo geomagnético se debe predominantemente a variaciones del campo no-dipolar (Valencio, 1977).

El registro instrumental de la variación secular se ha llevado a partir de 1600 en Londres y París mientras que para los demás lugares comenzó más tarde. Una manera para reconstruir la variación secular para periodos anteriores a 1600 es a través del paleomagnetismo, con las mediciones de la magnetización remanente grabada en las rocas y/o en los materiales arqueológicos (objetivos del paleomagnetismo). Estudios paleomagnéticos en secuencias de lavas en varias partes del mundo (Cox, 1969) permiten la estimación de la variación secular para períodos más allá del intervalo histórico, conocida con el nombre de variación paleosecular (PSV). Dichos estudios del pasado geológico permitieron observar que la magnitud de la componente no-dipolar ha sido casi completamente inexistente, en los últimos 800,000 años, para la región del Pacífico central (Low-Field) lo que ocasionó, a esa latitud, una baja dispersión de los polos geomagnéticos virtuales VGP (Creer, 1963; Doell and Cox, 1971, 1972; Cox, 1975; Coe et al., 1978; McWilliams et al., 1982; Miki el al., 1998). Según Creer (1963) y Doell y Cox (1972) esta zona de "Low-Field", incluiría también México Central. Posteriormente, Urrutia y Campos (1993) comparando los datos registrados por la estación Teoloyucan (en México) con el modelo de referencia IGRF para el período 1945-1990, encontraron una baja variación de los elementos del campo geomagnético que sugiere poca influencia del campo no-dipolar a esta latitud y concordaron con los autores anteriores en que el centro de México está en la zona de campo bajo. Sin embargo Steele (1985) y Herrero-Bervera et al. (1986) encontraron una dispersión de VGP en México Central igual a la esperada según el Modelo F de McFadden and McElhinny (1984). Posteriormente Bohnel et al. (1990) y Urrutia (1997) revisaron los datos paleomagnéticos y concluyeron que la dispersión de VGP para el centro de México es

baja, similar a la observada en la zona del Océano Pacífico (por ejemplo Hawaii) y demostraron que la discrepancia con los estudios de Steele (1985) y Herrero-Bervera et al. (1986) era debido a los criterios de selección de los datos paleodireccionales.

Unos de los objetivos de este proyecto doctoral es contribuir al estudio de la variación paleosecular del campo geomagnético para el centro de México, mediante el estudio de lavas plio-cuaternarias de la Faja Volcánica Trans-Mexicana integrando datos ya publicados y comparándolos con el modelo de McFadden et al. (1988, 1991). Con este fin se recolectaron muestras de rocas volcánicas del complejo volcánico Popocatépetl (16 sitios) y de 24 volcanes del campo volcánico Michoacán-Guanajuato. Todas las muestras fueron tratadas con las técnicas de desmagnetización térmica o por campos alternos para determinar la componente principal de la magnetización. Se efectuaron estudios de mineralogía magnética por medio de medición de susceptibilidad magnética, temperatura de Curie, ciclos de histéresis y adquisición de IRM. Para algunos lugares también se realizó un estudio geoquímico de los elementos mayores y de trazas (particularmente en el caso del complejo volcánico Popocatépetl). Además se contribuyó a la base de datos de paleointensidad para el centro de México al tratar las muestras consideradas "adecuadas" por medio de técnica Thellier-Thellier (Thellier 1959) y sus modificaciones (Coe et al., 1967, 1978). En el caso del volcán Paricutín, el estudio también se realizó utilizando la técnica de microondas (Shaw et al., 1984, 1996, 1999) modificada por Kono y Ueno (1977).

De la misma manera se estudiaron flujos de lava del complejo volcánico Somma-Vesuvio (Italia meridional). Se realizó un muestreo en 14 sitios de flujos de lava de erupciones históricas para conocer la distribución espacial de los productos emitidos reportados en el mapa vulcanológico cuya finalidad es verificar sus edades ya que según algunos autores presentan varios errores. De manera especial se ha estudiado paleomagnéticamente algunos flujos de lava asignados a la erupción de 1631 que según Rosi y Santacroce (1984, 1986) y Arno et al. (1987) fue de carácter explosivo (sin salida de lava). Sin embargo según otros autores (Le Hon, 1865; Johnston Lavis, 1884; Rolandi and Russo 1987, 1989, 1993; Rolandi et al., 1991) en esta erupción hubo salida de lava. El estudio del carácter de esta erupción (1631) es

muy importante para el fin de la previsión y análisis de actividad eruptiva y modelos predictivos (como la presunta próxima erupción del volcán). Para el complejo volcánico Somma-Vesuvio, se contribuyó a la base de datos de paleointensidad al tratar las muestras con técnica Thellier-Thellier. Cabe mencionar que este trabajo es un primer intento de obtener el registro de variación secular del campo geomagnético en ambos términos: direcciones e intensidades.

PRIMERA PARTE

Geología, Muestreo y Metodología de Laboratorio

GEOLOGIA y MUESTREO

1.1-Geología del complejo volcánico del Popocatépetl y muestreo

El volcán Popocatépetl se encuentra a 65 km al sureste de la ciudad de México (19 03' N; 98 35' W) y es uno de los estrato-volcanes más grandes de la Faja Volcánica Trans-Mexicana (FVTM). Está formado por un cono truncado grande. Su cima tiene una sección elíptica alineada NE-SW, y ejes de 450 y 650 m. Su evolución es muy parecida a los demás estrato-volcanes de la FVTM como por ejemplo el Nevado de Colima, Volcán de Fuego, Pico de Orizaba. El volcán fue construido en dos etapas: una fase inicial de formación del volcán primitivo y otra posterior que originó al cono principal del volcán actual.

Las etapas de construcción del complejo volcánico se determinaron por evidencias morfológicas, petrográficas y químicas obteniéndose columnas estratigráficas distintas en cada caso (Carrasco et al., 1986). Estas secuencias distintas corresponden a las formaciones Nexpayantla y Popocatépetl (Carrasco et al., 1986). La primera está constituida en su parte inferior por lavas andesíticas con textura afanítica, que van cambiando a dacitas microlíticas intercaladas con brechas de la misma composición, hasta terminar con lavas porfídicas de naturaleza riodacítica, que ocasionalmente presentan horizontes pumicíticos. Una discordancia separa esta formación de la Formación Popocatépetl, la cual está formada por andesitas microlíticas que se intercalan con brechas esencialmente pumíticas que en su parte superior, se van cambiando gradualmente a tobas de composición andesítica. Las emisiones más recientes son andesitas y dacitas porfídicas, así como depósitos piroclásticos tanto de caída libre como de flujo.

1.1.1- Evolución del Popocatépetl

El volcán primitivo (Nexpayantla), está formado predominantemente por rocas andesíticas. Sus emisiones iniciales originaron derrames de lava muy fluidas de naturaleza máfica y textura afanítica. En general dichas rocas presentan una paragénesis que consiste en: microfenocristales de magnetita (Mg) de cristalización precoz, olivino (Ol), clinopiroxeno (Cpx) del tipo de la augita y en ocasiones ortopiroxenos (Opx) del tipo de la hiperstena. Además abundantes microlitos de plagioclasa (Pl) cálcica a intermedia como la labradorita, andesina y oligoclasa. Conforme las lavas emitidas se fueron apilando, fueron apareciendo nuevas asociaciones mineralógicas. Las variaciones mineralógicas permiten suponer que al menos uno de los procesos que ocasionaron la evolución de estas lavas fue cristalización fraccionada, sin dejar de considerar la intervención de otros mecanismos de la diferenciación (Carrasco et al., 1986). Las andesitas y dacitas que se relacionan con tales paragénesis fueron derivadas de un magma básico que fue evolucionando y tuvo que ascender una distancia cada vez mayor para alcanzar la superficie. El aumento progresivo en la viscosidad de los productos pudo ocasionar la obturación temporal del conducto y dar origen a erupciones de gran explosividad que emitieron lavas riodacíticas (SiO_2=70.3%). Los productos piroclásticos fueron emitidos en gran volumen lo que provocó un vacío que desequilibró la cámara magmática que alimentaba el volcán, y produjo un colapso que incluyó una gran parte del cono. Una interpretación alternativa es que la destrucción fue por una explosión que voló parte del cono, originando una etapa de "precaldera" o "caldera incipiente". De acuerdo con las dimensiones estimadas, el cráter pudo haber tenido unos 2.5 km de diámetro. Después de un período prolongado de calma y erosión se reactivó el vulcanismo lo que dio origen a la edificación del cono actual del Popocatépetl. El nuevo magma expulsado, con una gran cantidad de productos piroclásticos, en contra de lo esperado, presentó una composición más básica, que sugiere un origen diferente o tal vez, debido a la mezcla del magma con una nueva cámara magmática, sobretodo, si tomamos en cuenta el grado de diferenciación que había alcanzado el magma anteriormente.

En cuanto a la edad, todavía no se sabe mucho del nacimiento del volcán Popocatépetl ni de su antecesor el volcán Nexpayantla, debido a la ausencia de fechamientos isotópicos. Sin embargo, la edad relativa entre los dos, fue estimada por cambios geomorfológicos debidos a las glaciaciones. El Nexpayantla está mucho más afectado por fenómenos de glaciaciones respecto al Popocatépetl. Estudios de paleomagnetismo de flujos de lava del complejo volcánico (Carrasco et al., 1986) reportan una polaridad normal y una actividad relacionada al crono Brunhes, no más vieja de 0,78 Ma. Nixon (1989) refiere algunos datos de fechamientos de flujos de lava del Iztaccihuátl (que cubren al Nexpayantla) de edad ~ 200 Ka, afirma que la actividad volcánica de la Sierra Nevada (la misma cámara magmática del Popocatépetl) no puede ser más vieja de 1 Ma. Sobre esta base, y considerando la actividad reciente del Popocatépetl, la actividad del Nexpayantla no pudo ser más vieja de 0,78 Ma y no más joven de 200 Ka. En cuanto a la actividad del volcán Popocatépetl, la edad mínima parece ser de 10,000 – 8,500 años o sea cuando se tuvo el último máximo glacial que afectó a la Formación Popocatépetl, la edad máxima la relaciona a 36,000 años, siendo la primera glaciación que se encontró en México Central (Carrasco et al., 1986). Por lo que la edad para el Nexpayantla, puede ser situada entre 0,78-0,036 Ma, ya que la actividad del Popocatépetl inició hace 36,000 años y continua en la actualidad.

1.1.2-Muestreo del complejo volcánico Popocatépetl

Los 16 sitios de muestreo se localizan alrededor del Complejo Volcánico del Popocatépetl, cerca de los pueblos Tochimilco, Metepec y S. Jerónimo, Atlixco (Fig. 1, carta INEGI 1:250.000 E14-2 CD DE MEXICO y E14-5 CUERNAVACA).

Con una perforadora portátil se obtuvieron 8-10 núcleos cilíndricos de rocas volcánicas por cada sitio con 10-15 cm de largo y un diámetro de 2,5 cm, previamente orientada con una brújula magnética, obteniendo aproximadamente 150 núcleos de rocas volcánicas.

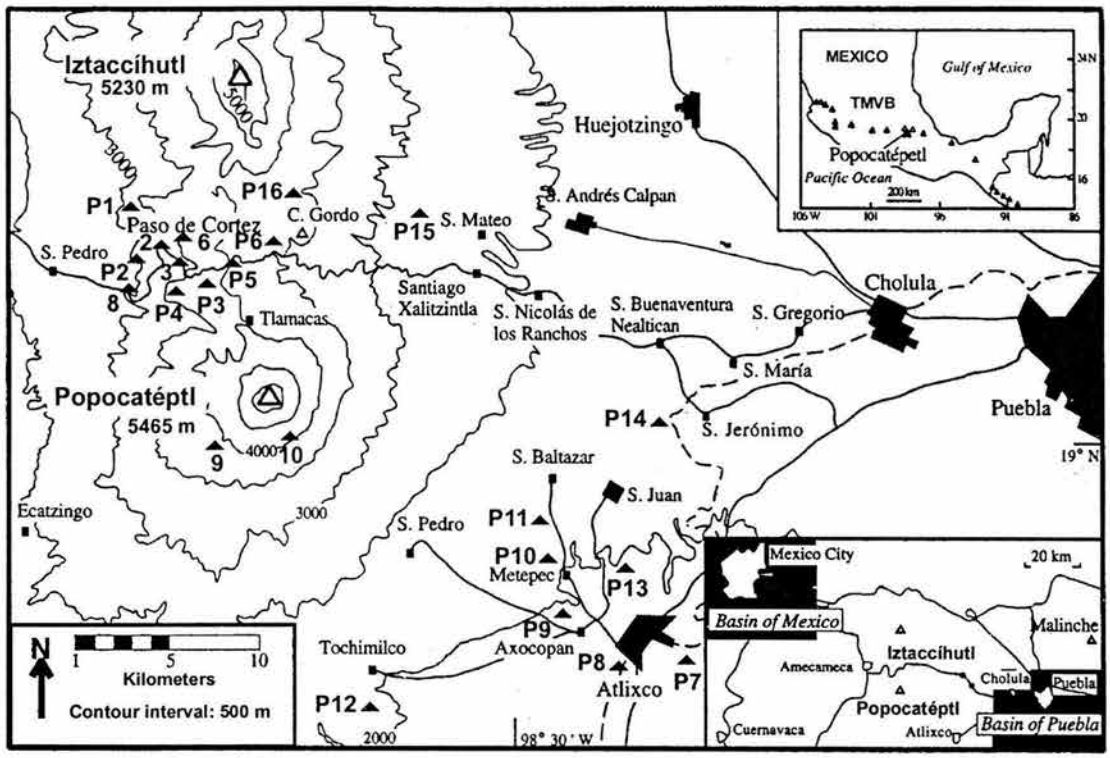

Fig. 1: Localización de los 16 sitios de muestreo etiquetados con letra P. Los sitios muestreados en un trabajo anterior (Carrasco et al., 1986) están representados solamente con los números.

1.2-Geología del Campo Volcánico Michoacán-Guanajuato y muestreo

El Campo Volcánico Michoacán-Guanajuato (CVMG), se localiza en el sector central-oeste de la FVTM, la cual está relacionada con la convergencia de las placas de Cocos y Rivera contra la placa Norte Americana, a partir del Mioceno superior. La FVTM se extiende desde las costas del Pacífico hasta las del Golfo de México con una distancia de más que 1 000 km y de ancho cerca de 100 km. A diferencia de la mayoría de los sistemas arco, no está paralela a la trinchera Mesoamericana (Middle America Trench), formando con esa un ángulo de 20° (Urrutia-Fucugauchi y Del Castillo, 1977; Urrutia y Bohnel, 1988) (Fig. 2). La mayoría de los aparatos volcánicos de la FVTM son de edad Cuaternaria pero también se encuentran centros volcánicos de edad pliocénica. Desde un punto de vista geoquímico, la FVTM es una provincia de composición calco-alcalina que se caracteriza por la abundancia de dacitas y andesitas, pero que también presenta productos alcalinos subordinados (Aguilar-Vargas y Verma, 1987). Los centros andesíticos mayores en la parte occidental de la FVTM que yacen sobre la porción subducida de la placa Rivera empezaron a evolucionar entre 0.6 y 0.2 Ma. Sin embargo, en las partes central y oriental del arco, donde está teniendo lugar la subducción de la placa del Cocos, las edificación de los conos andesíticos-dacíticos comenzó antes, aproximadamente 1.7 Ma. (Nixon et al., 1987). Junto a la FVTM, el volcanismo de México también está representado por la Provincia Alcalina del Golfo (Eastern Alkaline Province) (Oligoceno hasta el Cuaternario), Sierra Madre Occidental (Oligoceno hasta Mioceno) y la Provincia de California (Demant and Robin, 1975) (Fig. 2).

La porción oeste de la FVTM está caracterizada por tres sistemas de rift: Tepic-Zacoalco (NO-SE), Colima (N-S) y Chapala (E-O). El Campo Volcánico Michoacán-Guanajuato está localizado al Oeste del lago de Chapala, el cual constituye el eje del graben de Chapala. El CVMG, con un área de 40,000 km^2, está formada por más que 1,000 centros volcánicos monogenéticos de tamaño pequeño, de edad Cuaternaria, incluyendo: conos de ceniza y lava, maares, anillos de tobas, domos y flujos de lavas de los cuales la mayoría no presentan un centro eruptivo bien definido; todos presentan un carácter de calco-alcalino a alcalino (SiO_2 entre del 47% al 68%) con productos que varían de andesita-basálticas hasta basálticas (Hasenaka y

Carmichael, 1987; Hasenaka 1990, 1994; Hasenaka et al., 1994). La mayoría de ellos (75%) se encuentran entre 300 y 400 km de distancia de la Trinchera Mesoamericana (Fig. 3).

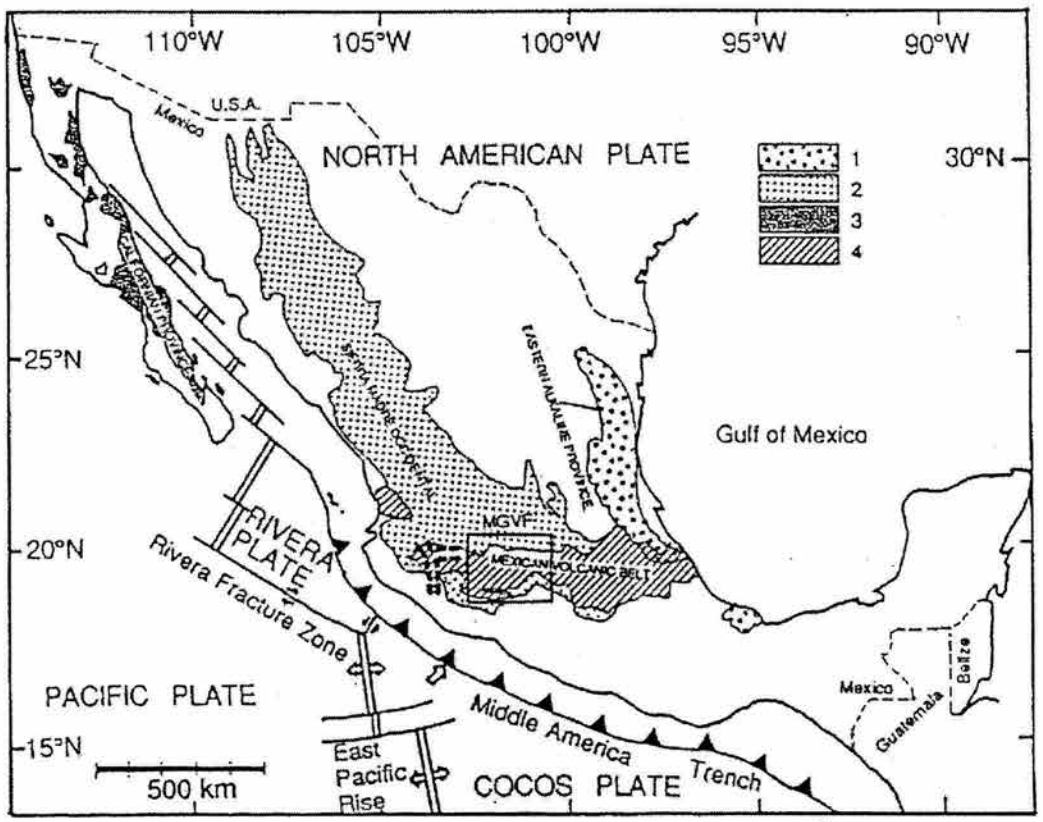

Fig. 2 Provincias volcánicas de México. En el rectángulo se ubica el Campo Volcánico Michoacán-Guanajuato (MGVF Michoacán-Guanjuato Volcanic Field).
Las cuatros provincias según Demant y Robin (1975) son: 1. Provincia Alcalina del Golfo (Eastern Alkaline Province, EAP), 2. Sierra Madre Occidental (SMO), 3. Provincia de California (CP), y 4. Faja Volcánica Trans-Mexicana (MVB).

En general los conos de ceniza y lava monogenéticos están activos sólo por una periodo muy corto, que va desde unos pocos meses hasta aproximadamente 15 años y rara vez vuelven a reactivarse. Dos conos de ceniza y lava se han formados en tiempos históricos: el Paricutín y el Jorullo (1943-1952 y 1759-1774 respectivamente). En el CVMG hay 400 volcanes de tamaño mediano con carácter calco-alcalino (SiO_2 entre del 55% al 61%) y productos andesíticos (Hasenaka y

Carmichael, 1985). Las lavas de estos volcanes son más diferenciadas respeto a los conos monogenéticos. Estos conos de tamaño mediano, son principalmente volcanes de escudo de tipo Iceland, con diámetro alrededor de 10 km. También se encuentran dos estrato-volcanes, el Volcán Grande y el Cerro Tancítaro. El CVMG es muy diferente respecto a la otra parte de la FVTM, la cual está formada por volcanes compuestos grandes como el Popocatépetl, Nevado de Colima y Pico de Orizaba.

Seis conos de ceniza y lava han sido fechados por medio del ^{14}C y se les calcula una edad entre de 3,800-29,000 años BP (Hasenaka y Carmichael, 1985), otros 71 más, parecen tener la misma edad (<40,000 años) dado que presentan el mismo grado de erosión. Ban et al. (1992) fecharon ocho volcanes escudo (tamaño mediano) y un estrato volcán por medio del K-Ar fechados con una edad entre 0.06 y 2.27 Ma, mientras Nixon et al., 1987, fecharon otros tres volcanes escudo (0.87-2.60 Ma), mediante K-Ar, llegando a la conclusión que los volcanes escudo presentan una edad mayor de 40,000 años.

Los centros volcánicos pequeños y medianos tienen una distribución bastante similar, excepto en la parte septentrional del CVMG en donde, los volcanes escudo son más frecuentes que los pequeños. Geomorfológicamente, los conos cineríticos en la parte Norte son más viejos que en la parte Sur, esto sugiere una migración de la actividad eruptiva hacia el Sur. Esta migración pudo ocurrir hace 1 Ma, ya que los volcanes escudos localizados en la parte Norte (latitud > 19°55') tienen una edad mayor a 1 Ma, a diferencia de los volcanes de la parte Sur que presentan una edad menor que 1Ma. Esta relación es observada tanto en los volcanes escudo como en los volcanes pequeños (Ban et al., 1992). El frente volcánico activo se encuentra en la parte Sur del CVMG (Hasenaka y Carmichael 1985).

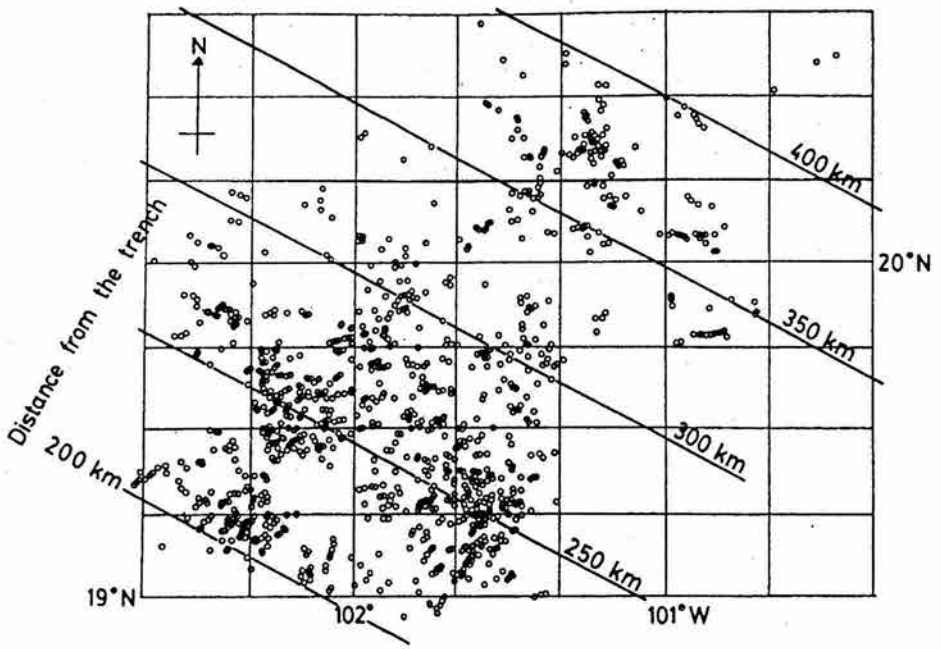

Fig. 3 Distribución de los volcanes en el Campo Volcánico Michoácan-Guanajuato.
Los círculos representan los centros volcánicos: conos cineríticos, maar, anillos de tobas, volcanes a escudos y flujos de lavas no asociados a centros eruptivos bien definidos (Hasenaka et al., 1985).

Dado que los conos monogenéticos del Campo Volcánico Michoacán-Guanajuato tienen una vida media de 15-20 años, son muy útiles para obtener información paleomagnética. Con ellos se pueden conocer las variaciones del campo geomagnético ya que sus flujos de lava han registrado los cambios del campo magnético terrestre con bastante precisión.

1.2.1-Muestreo del Campo Volcánico Michoacán-Guanajuato

En total se muestrearon 24 volcanes (conos de lava y escudos) (Fig. 4). Con una perforadora portátil se obtuvieron 8-10 núcleos cilíndricos de rocas volcánicas por cada sitio. Los núcleos son de 10-15 cm de largo, y tienen un diámetro de 2.5 cm y fueron orientados con una brújula previamente. En total se obtuvieron aproximadamente 230 núcleos de rocas volcánicas.

Las muestras sacadas fueron cortadas y marcadas en el Laboratorio de Paleomagnétismo del Instituto de Geofísica de la UNAM, se obtuvo por cada núcleo, cerca de tres muestras de 2.2 cm de largo (espécimen) con un total de 700 muestras.

De los 24 volcanes muestreados, 18 habían sido fechados con anterioridad (Ban et al., 1992; Hasenaka and Carmichael, 1985; Nixon et al., 1990). Uno de los objetivos del presente trabajo doctoral fue fechar los seis restantes por lo que se obtuvo un bloque de roca de cada uno de los puntos de muestreo lo más fresco posible de entre 1 y 2 kg para molerlos y para ser procesados mediante la técnica radiométrica K/Ar. Debido a la logística solo fue posible fechar él volcán "El Estribo" mediante la técnica antes mencionada obteniendo una edad de 25±4 ka (Herve Guillou, comunicación personal).

Con base a la paleodirección determinada y considerando que los volcanes que se encuentran más al norte del CVMG presentan una edad mayor a los 40,000 años, los cinco volcanes restantes fueron "fechados" de manera relativa.

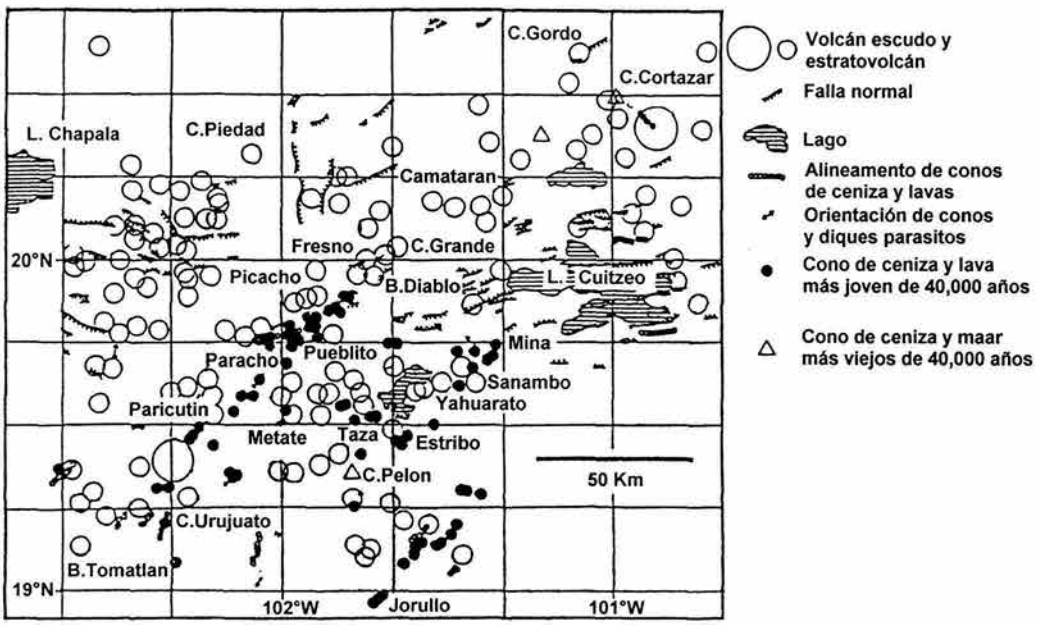

Fig. 4 Localización de los volcanes muestreados del campo volcánico Michoacán-Guanajuato.

1.3-Geología del complejo volcánico Somma-Vesuvio y muestreo

La Planicie Campana es una de las cuencas cuaternarias más extensas de Italia meridional y ocupa el fondo de un graben que ha rebajado por millares de metros las unidades meso-cenozoicas del Apenino Campano (Fig. 5). Esta depresión de origen tectónico, se extiende cerca de 70 km en dirección Apenínica (NO-SE). Las rocas mesozoicas forman los altos estructurales y morfológicos que delimitan la Planicie Campana, las tríasicas se encuentran en la parte oriental (Montes Lattari) en lo que queda de los relieves alrededor de la planicie, afloran secuencias jurásicas y cretácicas (Ortolani y Aprile, 1985). Los espesores de los depósitos carbonátados del Apenino Campano son notables; 1,500 metros para las rocas triásicas, 2,000 metros para las jurásicas y 1,500 metros para las cretácicas. Desde el plioceno tardio hasta el cuaternario, debido al proceso de subducción de la placa africana por debajo de la cadena Apenínica, se dio una actividad eruptiva intensa y compleja de naturaleza potásica con afinidad orogénica (Di Girolamo, 1978). Esto originó la "Provincia Potásica Romano-Campana", que se desarrolló a lo largo del borde Tirrénico, con centros eruptivos localizados en el Lazio (Vulsini, Vico, Sabatini) y en Campania (Roccamonfina, Campi Flegrei, islas de Ischia y Procida, Somma-Vesuvio). El basamento del complejo Somma-Vesuvio está representado por rocas sedimentarias mesozoicas y terciarias. Investigaciones geofísicas (Barberi et al., 1980; La Torre et al., 1982) han permitido reconstruir el perfil de la cima del sub-estrato.

El inicio de la actividad volcánica del complejo volcánico Somma-Vesuvio todavía no se conoce muy bien. Sin embargo los estudio estratigráficos y de fechamiento isotópico de algunos productos volcánicos y de paleosuelos, sugieren que la actividad más antigua del complejo fue hace 25,000 años.

El complejo volcánico Somma-Vesuvio está formado por dos estrato-volcanes. El más antiguo (Monte Somma), terminó su actividad con el colapso de la caldera. El más joven (Vesuvio) localizado en una posición ligeramente descéntrica dentro de la misma caldera.

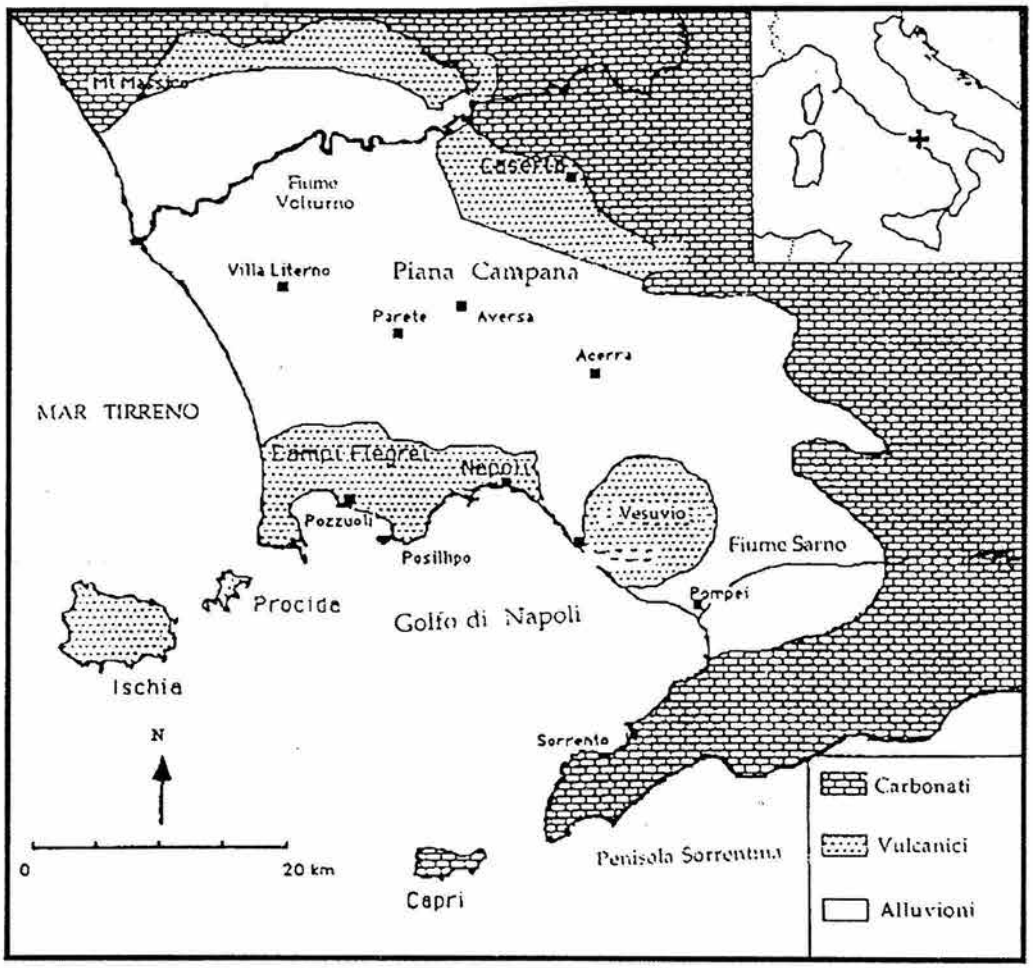

Fig. 5 Planicie Campana (Italia meridional).

Extrapolando los perfiles de los restos de la caldera (Monte Somma) se puede estimar una altura original alrededor de 2,000 metros. Además del cráter principal, alrededor del complejo volcánico se pueden encontrar algunos conos parásitos y bocas secundarias, generalmente situadas a lo largo de fracturas radiales del edificio volcánico. Entre los pueblos Torre del Greco y Torre Annunziata se pueden encontrar estas formas parásitas, como por ejemplo, el cono pre-histórico de los Camaldoli de la Torre y las bocas medievales del Viulo y de Fossamonaca.

La estratigrafía, el fechamiento isotópico de algunos productos volcánicos, así como el de los paleosuelos intercalados entre de ellos, han marcado varios ciclos de actividad eruptiva los cuales empiezan siempre con una erupción fuerte de tipo

pliniano y tienen una duración menor de 2,000 años. Los productos más antiguos del Somma aflorados, no tienen más de 25,000 años. A pesar de las varias actividades del complejo Somma-Vesuvio se pueden distinguir fundamentalmente tres tipos de actividad.

a) Erupción efusiva moderada.
b) Erupción fuerte, exclusivamente explosiva, de carácter "Subpliniano".
c) Erupción catastrófica, muy explosiva, de tipo "Pliniano".

El primer tipo está caracterizado por volúmenes pequeños de magma emitido (orden de 0.01 km^3), periodos cortos de calma precedentes a la erupción (orden de algunos años) y naturaleza del magma poco evolucionado. El segundo tipo está caracterizado por volúmenes de alrededor de 0.1 km^3, periodos de calma más grandes (decenas de años o siglos) y magma más evolucionado. El tercer tipo está asociado con grandes volúmenes de magma (1 km^3) y tiempos de calmas muy largos (siglos o miles de años).

Los productos aflorantes alrededor del complejo volcánico Somma-Vesuvio han permitido reconstruir la historia eruptiva del complejo volcánico, que puede ser dividida por tres períodos largos (Arnó et al., 1987; Santacroce R., 1987; Delibrias et al. 1979).

I-período

Este representa el periodo más largo y antiguo para el cual no hay datos de fechamiento isotópicos; por lo tanto las edades relativas se infieren de investigaciones geológicas-estratigráficas. Este periodo que va de cerca de 25, 000 años hasta el 79 d. C. (la gran erupción pliniana que destruyó Pompeya y Herculano) está caracterizada por varios episodios plinianos, cada uno marcan el inicio o el final de un nuevo ciclo de actividad volcánica. Las erupciones de este periodo se pueden agrupar en dos ciclos eruptivos: actividad pre-caldera con las erupciones de "Codola" (25,000 años), de "Sarno" (22,000 años) y "Basale" (17,000 años) y la actividad post-caldera con las

erupciones de "Pomici verdoline" (15,000 años), de "Lagno Amendolare" (11,000 años), del "Mercato" (8,000 años) y de "Avellino" (3,800 años).

II-período

La actividad post-caldera comenzó con el segundo periodo el cual, está mejor documentado. Esto incluye una serie de erupciones de diversa tipología que se manifestaron entre la famosa erupción del 79 d. C. y la del 1631. La primera erupción, bien documentada gracias a la descripción de Plinio el Joven es la del 79 d. C., fue de tipo pliniano y que destruyó Pompeya y Herculano. La escala temporal poco precisa, usada para la descripción de las erupciones en este período, generalmente no permite hacer correlación en el campo, además la ausencia de paleo-suelos, que indican períodos de pausas entre las dos erupciones, no permite separar cada uno de los eventos que, frecuentemente están caracterizados por los mismos productos volcánicos. Rosi y Santacroce (1986) han estudiado en detalle la erupción de hace 1500-1600 años atribuida al 472 d. C. Esta erupción sub-pliniana tiene las mismas características de la del 79 d. C. pero el volumen de magma extravasado es mucho menor. Las erupciones del 395 y del 512, han sido poco estudiadas.

La primera imagen del Vesuvio es del siglo VI, es una pintura encontrada dentro de las catacumbas de San Gennaro en Nápoles que ilustra al Santo entre el Monte Somma y el Vesuvio. Esta imagen es muy importante porque, muestra que el volcán ya tenía una morfología muy parecida a la actual. La mayoría de las erupciones que han caracterizado este segundo período son de tipo subpliniano.

III-período

Esto constituye el período más "joven" del volcán. Va desde la erupción de 1631 hasta la de 1944. Este período está bien documentado por medio de crónicas históricas que narran cada evento eruptivo. Con la erupción del 1631 que se dió después 500 años de moderada actividad, el Vesuvio entró en una nueva etapa de actividad casi continua. En 1841 se fundó el primero Instituto Vulcanológico del mundo, el Real Observatorio Vesuviano que permitió conocer bien la actividad eruptiva año por año.

La actividad reciente está bien estudiada por parte de los investigadores de la Universidad de Nápoles "Federico II" utilizando métodos estadísticos. Este estudio muestra que a partir de la erupción del 1631 hasta la del 1944 el volcán ha tenido 18 ciclos de actividad que se ha repetido periódicamente en el tiempo con períodos de pausas de siete años. Erupciones efusivas de importancia modesta se han presentado entre los ciclos (erupciones intermedias), mientras que las erupciones más grandes siempre se han dado al final de cada ciclo (erupciones finales). Estas ultimas erupciones están caracterizadas por una componente explosiva significativa, por medio de la cual, los productos emitidos se dispersan sobre una gran área; estas erupciones se han registrado en el: 1682, 1694, 1698, 1707, 1737, 1760, 1767, 1779, 1794, 1822, 1834, 1839, 1850, 1861, 1868, 1872, 1906 y 1944.

1.3.1-Erupción del 1631

Existe una gran discrepancia en las crónicas que describen la actividad eruptiva del 1631 en virtud de que, de las 250 existentes sólo algunas están completas. Se sabe que el volcán tuvo una etapa de tranquilidad de alrededor de 500 años ya que la erupción anterior fue en 1139.

La fase pre-eruptiva de la erupción del 1631 inició con un levantamiento del suelo los primeros días de diciembre. La actividad aumentó a partir del día 10 de diciembre y la erupción inicio el 16 con una explosión grande alrededor de las 13 ó 14 horas. Se desarrolló una columna eruptiva que se alzaba entre los 20-30 km de altura y se describen los diferentes colores que asumía la columna con el aumento de densidad de las partículas (Braccini, 1632). Marzo (en Riccio, 1883) narra una columna que parecía un gran árbol de pino con un tronco grueso.

Rolandi y Russo (1989), consideran esta primera fase como una erupción "pliniana". De Contreras (1633) y Braccini (1632) describen los productos que llegaron hasta el pueblo de Nola, como escorias por lo que, todo el sector oriental fue cubierto con estos productos. Posterior a este evento todos los autores coinciden en que se presentó actividad sísmica y posteriormente se dio una erupción nueva y diferente, la cual arrojó lava durante toda la noche del 16 terminando al amanecer del 17 de diciembre.

Todavía queda mucha duda sobre la naturaleza de este evento, algunos autores (Rosi y Santacroce 1984, 1986; Principe et al., 1987; Arno et al., 1987) sostienen que fue exclusivamente explosivo.

1.3.2-Muestreo del complejo volcánico Somma-Vesuvio

Se muestrearon 14 sitios alrededor del complejo volcánico Somma-Vesuvio, (Tabla 1, Fig. 6). Las presuntas edades de estos flujos se refieren al mapa Vulcanológico, el único actualmente disponible (Principe et al., 1987).

Uno de los objetivos de este trabajo es estudiar los flujos de lava cartografiados en el mapa Vulcanológico 79-1631 los cuales, según Principe et al. (1987) son todos los flujos de lavas que se depositaron después de la erupción del 79 d.C. y antes de la del 1631. Estos derrames están cubiertos por flujos piroclásticos de la erupción del 1631. Otros autores consideran que estos flujos de lava pertenecen a la erupción del 1631 (Burri and Di Girolamo, 1975; Rolandi et al., 1991; 1993).

El muestreo se hizo con una perforadora eléctrica, se tomaron 12 cilindros de roca lávica con una longitud de 10 a 15 cm y un diámetro 2.5 cm. Estos habían sido orientados previamente con una brújula solar.

Tabla 1

Sitio	Edad Presunta	Latitud (N)	Longitud (E)
V-45	79-1631	40°48,273'	14°20,431'
V-46	79-1631/1760	40°46,132'	14°25,141'
V-47	79-1631/1631	40°45,327'	14°24,552'
V-48	79-1631	40°45,543'	14°23,844'
V-49	1760	40°45,408'	14°25,277'
V-50	1760	40°46,644'	14°25,364'
V-51	79-1631	40°47,279'	14°21,719'
V-53	1872	40°48,880'	14°22,285'
V-55	1872/1944	40°50,075'	14°22,882'
V-57	1872/1944	40°50,075'	14°22,651'
V-61	1906	40°48,424'	14°26,120'
V-68	1872/1886	40°48,643'	14°24,665'
V-80	1858	40°49,430'	14°23,540'
V-81	1858/1895-99	40°49,410'	14°23,603'

Según el mapa Vulcanológico de Principe et al. (1987), 79-1631 son todos los flujos de lavas que se depositaron después de la erupción de 79 d.C. y antes de la del 1631. Estos están cubiertos frecuentemente por flujos piroclásticos de la erupción del 1631. Conforme el mapa, no hay lavas asociadas a la erupción del 1631.

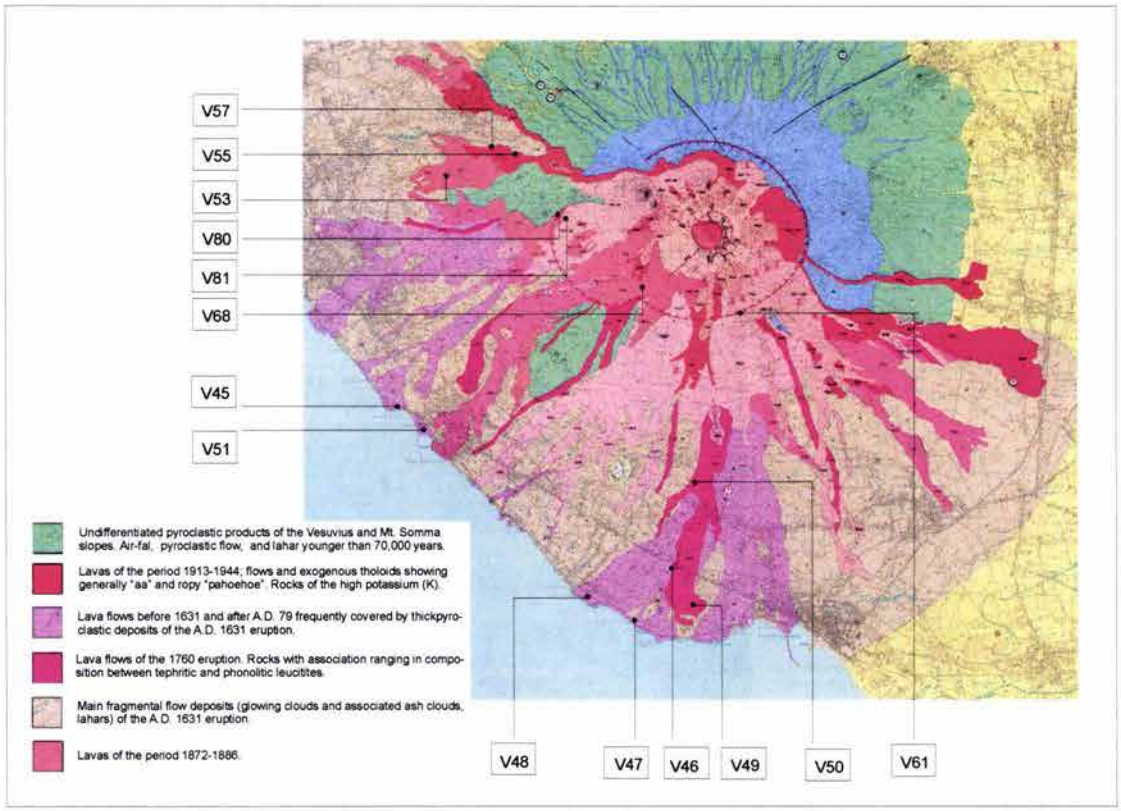

Fig. 6 Localización de los sitios muestreados alrededor del complejo volcánico Somma-Vesuvio. (modificado de Principe et al., 1987)

Referencias

Aguilar-Vargas and Verma, 1987. Composicion quimica (elementos mayores) de los magmas en el Cinturón Volcánico Mexicano. *Geofisica Internacional*, V. 26, pp. 195-272.

Arnó V., Principe C., Rosi M., Santacroce R., Sbrana A. & Sheridan M. F. (1987). Eruptive history. In Santacroce R. (Ed.) "Somma- Vesuvius" *Quaderni de "La ricerca scientifica"*. C. N. R. 114, 8, pp. 243

Ban M., Hasenaka T., Delgado-Granados H. and Takaoka N., 1992. K-Ar ages of lavas from shield volcanoes in the Michoacan-Guanajuato volcanic field, Mexico. *Geofisica International*, V. 31, pp. 467-473.

Barberi F., Ciappi D., Ghelardoni R., Nannini R., Sammaruga C. & Verdiani G. (1980). Integrated goethermal reconnaissance of the Somma-Vesuvius system. *2nd Intern. Sem. Results E.C. Get. Energy Res.*, Strasbourg.

Bohnel H., Urrutia-Fucugauchi J., and Herrero-Bervera. (1990). Paleomagnetic data from central Mexico and their use for paleosecular variation studies. *Phys. Earth Planet. Inter.*, V. 64, pp. 224-236.

Burri C., and Di Girolamo P. (1975) Contributo alla conoscenza delle lave della grande eruzione del Vesuvio del 1631. *Rend. Soc. Ital. Mineral. Petrol.*, 30 (2), pp. 705-739.

Braccini G. C. (1632). Dall'incendio fattosi nel Vesuvio a il IV di Dicembre MDCXXXI e delle sue cause ed effetti.

Campos-Enriquez J. O., Campos-Enriquez J. O. and Urrutia-Fucugauchi J. (1991). Variación secular reciente y cartas de los elementos del campo geomagnético en México. *Geof. Int.*, 30: 107-116 (1991).

Carrasco-Nuñez, G., Silva, L., Delgado-Granados, H., Urrutia-Fucugauchi, J., 1986. Geologia y paleomagnetismo del Popocatepetl. *Publ. Ser. Inv. Inst. Geofis.*, UNAM, 33, 1986.

Coe R. (1967). The determination of paleo intensities of the Earth's field with emphasis on mechanism which could cause non-ideal behavior in Thellier's method. *Journal of Geomagn. and Geolectr.*, V. 19, pp. 157-179.

Coe R., Gromme S. and, Mankinen E. A. (1978). Geomagnetic paleointensity from radiocarbon-dated lava flows on Hawaii and the question of the Pacific non-dipole Low. *Journal of Geophysical Research,* V. 83, pp. 1740-1756.

Cox A. (1969). A paleomagnetic study of secular variation in New Zeland. Earth Planet. Sci. lett., 6: 257-267 (1969).

Cox A. (1969). Confidence limits for the precision parameter k. *Geophys. J. R. astr. Soc.* V. 18, pp. 545-549.

Cox A. (1975). The frequency of geomagnetic reversals and the symmetry of the non dipole field. *Rev. Geophys. Space Phys.*, 13: 35-51 (1975).

Creer K. M. (1963). Geomagnetic and Paleomagnetic evidence of fósil axes of rotation of the Earth. *Nature*, 197: 122-126 (1963).

De Contreras A. (1933). Avventure del capitano Alfonso de Contreras (1582-1633).

Delibrias G., Di Paola G., Rosi M., and Santacroce R. (1979). La storia eruttiva del complesso vulcanico Somma-Vesuvio ricostruita nelle successioni piroclastiche del M.te Somma. *Rend. Soc. It. Mineral. Petrol.*, V. 35, pp. 411-438.

Demant A. and Robin C., 1975. Las fases del Volcanismo en México; una síntesis en relación con la evolución geodinámica desde el Cretácico. *Revista Inst. Geol.* UNAM, 75 (1), pp.70-83.

Di Girolamo P. (1978). Geotectonic setting of Miocene-Quaternary volcanism in and around the Easten Tyrrhenian sea border (Italy) as deduced from major element geochemistry. *Bull. Volcanol.*, V. 41, pp. 229-250.

Doell R., and Cox A. (1971). Pacific geomagnetic secular variation. *Science,* V. 71, pp. 248-254.

Doell R., and Cox A. (1972). The Pacific geomagnetic secular variation anomaly and the question of lateral uniformity in the lower mantle, in The Nature of the Solid Earth, edited by *E. C. Robertson, McGraw-Hill*, New York, pp. 245-284.

Hasenaka and Carmichael, 1985. A compilation of location, size, and geomorphological parameters of volcanoes of the Michoacan-Guanajuato volcanic field, central Mexico. *Geofisica Internacional*, 24-4: pp.577-607.

Hasenaka and Carmichael, 1987. The cinder cones of Michoacan-Guanajuato, central Mexico: petrology and chemistry. *J. Petrol.,* V. 28: pp. 241-269.

Hasenaka T. (1990). Contrasting monogenetic volcanism in Michoacan-Guanjuato, Mexico: Cinder cone group vs. schield volcano group. *Trans. Am. Geophys. Union (EOS)*, 71: 968 (1990).

Hasenaka T. (1994). Size, distribution, and magma output rate for shield volcanoes of the Michoacan-Guanajuato volcanic field, Central Mexico. *J. Volcanol. Geotherm. Res.,* V. 63, pp. 13-31.

Hasenaka T., Masao Ban and Hugo Delgado Granados (1994). Contrasting volcanism in the Michoacan-Guanajuato Volcanic Field, central México: Shield volcanoes vs. cinder cones. *Geofisica Internaciónal,* V. 33, (1), pp. 125-138.

Herrero-Bervera E., Urrutia-Fucugauchi J., Martin del Pozzo A., Bohnel H., and Guerrero J. (1986). Normal amplitude Brunhes paleosecular variation at low-latitudes: A paleomagnetic record from the Trans-Mexican Volcani Belt. *Geophysical Research Letters,* V. 13 (13), pp. 1442-1445.

J. Shaw and J. A. Share (1984). An automated superconducting magnetomer and demagnetizing system. Geophys J. R. astr. Soc., 78; 209-217.

J. Shaw, D. Walton, S. Yang, T. C. Rolph and J. A. Share (1996). Microwavw archaeointensities from Peruvian ceramics. Geophys. J. Int., 124; 241-244.

J. Shaw, S. Yang, T. C. Rolph and F. Y. Sun (1999). A comparison of archaeointensity results from Chinese seramics using microwave and conventional Thellier's and Shaw's methods. Geophys. J. Int., 136; 714-718.

Johnston Lavis H. J. (1884). The geology of the Mt. Somma and Vesuvius: being a study of volcanology. *Q. J. Geol. Soc. london*, V. 40, pp. 135-149.

Kono M., and Ueno N. (1977). Paleointensity determination by a modified Thellier method. *Phys. Earth Planet Int.*, V. 13, pp. 305-315.

La Torre P., Nannini R., and Sbrana A. (1982). Geothermal exploration in Southern Italy: geophysical interpretation of vesuvian area. *44 Meeting Cur. Explor. Geophys.*, Cannes.

Le Hon M. (1865). Histoire complete de la grande eruption du Vesuve de 1631. *Bulletin de l'Acadamie des Sciences, Lettres et Beaux Arts, Belge*, V. 20, pp. 483-538.

McFadden P., and McElhinny M. (1984). A physical model for paleosecular variation. *Geophys. J. R. Astrn. Soc.* V. 78, pp. 809-830.

McFadden P., Merrill T., McElhinny W. (1988). Dipole/Quadrupole Family Modeling of Paleosecular Variation. *Journal of Geophysical Research*, V. 93 (B10), pp. 11,583-11,588.

McFadden P.L., Merrill R., McEllhinny M. W., and Lee S. (1991). Reversals of the Earth's magnetic field and temporal variations of the dynamo families. *J. Geophys. Res.,* V. 96, pp 3923-3933.

McWilliams M., Holcomb R., and Champion D. (1982). Geomagnetic secular variation from ^{14}C dated lava flows on Hawaii and the question of the Pacific non-dipole low. *Phil. Trans. R. Soc. Lond.*, A, V. 306, pp. 211-222.

Miki M., Inokuchi H., Yamaguchi S., Matsuda J. I., Nagao K., Isekaki N. and Yaskawa K. (1998). Geomagnetic secular variation in Easter Island, the southeast Pacific. *Phys. Earth Planet Int.*, V. 106, pp. 93-101.

Nixon G. T., Demant A., Armstrong R. L. and Harakal J. E. (1987). K-Ar and Geologic Data Bearing on the Age and Evolution of the Trans-Mexican Volcanic Belt. *Geofisica Internacional,* V. 26-1, pp. 109-158.

Nixon, G.T. (1989). The geology of Iztaccihuatl volcano and adjacent areas of the Sierra Nevada and Valley of Mexico. Geol. Soc. Am. Sp. Pap., 219, pp. 58.

Ortolani, F., and Aprile, F. (1985). Principali caratteristiche stratigrafiche e strutturali dei depositi suprficiali della Piana Campana. *Boll. Soc. Geol. Italiana*, V. 104, pp. 186- 205.

Principe C., Rosi M., Santacroce R., Sbrana A. (1987). Explanatory Notes to the Geological Map of Vesuvius. *Quaderni de La ricerca scientifica, CNR, Rome 114* V. 8 pp. 11-51.

Riccio L. (1883). Nuovi documenti sull'incendio vesuviano dell'anno 1631. Archivio Storico per le province napoleane, anno XIV, 3, Napoli.

Rolandi G. and Russo F. (1987). Contributo alla conoscenza dell'attivita' storica del Vesuvio. La stratigrafia di Villa Inglese (Torre del Greco). Rendiconti della *Accademia delle Scienze Fisica e Matematiche, Napoli*, V. 54, pp. 123-157.

Rolandi G. and Russo F. (1989). Contributo alla conoscenza dell'attivita' storica del Vesuvio: dati stratigrafici e vulcanologici nel settore meridionale tra Torre del Greco, localita' Villa Inglese, e Torre Annunziata. *Bollettino della Societa' Geologica Italiana*, V. 108, pp. 521-536.

Rolandi G. and Russo F. (1993). L'eruzione del Vesuvio del 1631. *Bollettino della Societa' Geologica Italiana*, V. 112, pp. 315-332.

Rolandi G. Barrella A., Borrelli A., and D'Alessio G. (1991). The 1631 Vesuvian eruption. *Int. Conf. on Active Volcanoes and Risk Mitigation. Abst.,* 91.

Rosi M. and Santacroce R. (1986). L'attivita' del Somma-Vesuvio precedente l'eruzione del 1631. Dati stratigrafici e vulcanologici. In: Albore Livadie C. (ed.) Tremblement de terre, eruptions volcaniques et vie des hommes dans le campanie antique. *Biblioteque d'Institute Français Naples*, 7, pp. 15-33.

Rosi M., and Santacroce R. (1984). The famous AD 1631 eruption of Vesuvius: a revised interpretation in light of historical and volcanological data. *Workshop on Volcanic Blast, Mount St. Helena, abstr.*

Santacroce R. (1987). Somma-Vesuvius. *CNR Quader. Ric. Scient.*, 114, V. 8, pp. 251

Steele K. W. (1985). Paleomagnetic constraints on the volcanic history of Iztaccihuatl. *Geofisica Internacional,* V. 24 (1), pp. 159-167.

Thellier E. and Thellier O. (1959). Sur l'intensite de champ magnetique terrestre dans le passe historique et geologique. *Ann. Geophys,*. V. 15, pp. 285-376.

Urrutia-Fucugauchi J. (1995). Constraints on Brunhes low-latitude paleosecular variation-Iztaccíhuatl stratovolcano, basin of Mexico. *Geofisica Internacional,* V. 34 (3), pp. 253-262.

Urrutia-Fucugauchi J. (1997). Comment on "A new method to determine paleosecular variation" by D. Vandamme. Phys. Earth Planet. Inter., 102: 295-300 (1997).

Urrutia-Fucugauchi J. and Bohnel H. (1988). Tectonics along the Trans-Mexican volcanic belt according to palaeomagnetic data. *Phys. of Earth and Plan. Int.*, 52: 320-329 (1988).

Urrutia-Fucugauchi J. and Campos-Enríquez O. (1993). Geomagnetic secular variation in Central Mexico since 1923 AD and comparison with 1945-1990 IGRF models. *Journal Geomagn. Geoelectr.,* V. 45, pp. 243-249.

Urrutia-Fucugauchi J., and G. L. del Castillo, (1977). Un modelo del Eje Volcánico Mexicano. *Bol. Soc. Geol. Mexicana,* V. 38, pp. 18-28.

Valencio D. A. (1977). El magnetismo de las rocas (Libro). *Editorial Universitaria de Buenos Aires* (1977).

TECNICAS DE LABORATORIO y METODOLOGÍA

A continuación se describen los métodos empleados en los estudios paleomagnéticos y de paleointensidades en México e Italia. Los detalles de los estudios se presentan en cada uno de los artículos.

2.1-Preparación de las muestras

Las muestras paleomagnéticas, correspondientes a los cilindros de roca volcánica, fueron cortadas y marcadas en el Laboratorio de Paleomagnetismo del Instituto de Geofísica de la UNAM. Se obtuvieron por cada núcleo tres muestras de 2.2 cm de largo (espécimen) lo que nos dio un total de 450 muestras del complejo volcánico Popocatépetl, 700 muestras del campo volcánico Michoacán-Guanajuato y 450 para el complejo volcánico Somma-Vesuvio.

2.2-Mineralogía Magnética

El estudio de la mineralogía magnética, ayuda a conocer los minerales magnéticos portadores de la magnetización remanente natural (MRN) de la roca así como sus propiedades magnéticas (tamaño de partícula y estado de dominio). Estos estudios se realizaron en el Laboratorio de Paleomagnetismo del Instituto de Geofísica de la UNAM en donde se midió:

- Susceptibilidad magnética a alta temperatura
- Histéresis magnética
- Magnetización Remanente Isotermal (IRM)

La susceptibilidad magnética se midió con un equipo Bartington MS2 equipado con un horno. A cada muestra se le calentó hasta los 600°C con una tasa de 20°C/min. Posteriormente se enfrió a temperatura ambiente con la misma tasa. Las curva termomagnéticas obtenidas sirvieron para establecer las temperaturas de Curie las cuales se encuentran entre los 530°-590°C, lo que sugiere como portador magnético a una titanomagnetita rica en magnetita. Las muestras que presentaron una

curva sumamente reversible durante el calentamiento y enfriamiento fueron empleadas posteriormente para la determinación de paleointensidad.

Las mediciones de las curvas de histéresis y de las curvas de magnetización remanente isotermal (IRM) se obtuvieron con un equipo AGMF Micromag lo que permitió la determinación de los parámetros de histéresis y la construcción de los diagramas Day (Day et al., 1977) donde se observa que la mayoría de las muestras están caracterizadas con dominios magnéticos PSD (Pseudo-Single Domain) o más bien una mezcla entre MD (Multi-Domain) y SD (Single Domain).

2.3-Estudio Paleomagnético

A diferencia del método clásico (pilot study) todas las muestras en estos estudios fueron tratadas con todos los pasos de desmagnetización utilizando la técnica térmica y la de campos alternos (Gialanella et. al., 1993; Incoronato et. al., 1996).

Para elegir el tipo de desmagnetización más adecuada se seleccionaron dos muestras por cada sitio y se desmagnetizaron, una térmicamente y la otra por campos alternos. La desmagnetización por campos alternos llega hasta a 100 mT, por lo que si los gránulos magnéticos de la roca tienen una coercividad menor a este valor, este tipo de desmagnetización es posible, de lo contrario se opta por la desmagnetización térmica, la cual aunque no tiene ningún vínculo, se corre el riesgo de afectar la mineralogía magnética de la roca debido a las temperaturas altas. Por lo que después de cada paso en el cambio de la temperatura, se mide la susceptibilidad magnética de la muestra para verificar si esta se alteró.

La desmagnetización por campos alternos se realizó con un equipo MOLSPIN LIMITED. Los intervalos de desmagnetización fueron muy cortos en un inicio (para detectar la componente secundaria VRM) y luego se agrandaron. A cada paso de desmagnetización se midió la magnetización remanente a todos los datos obtenidos (después de todo el tratamiento) se les aplicó una corrección, mediante un programa de cálculo con respecto a las coordenadas geográficas de cada muestra por lo que todos los valores de inclinaciones y declinaciones de los momentos magnéticos de las muestras se referenciaron al norte geográfico.

La desmagnetización térmica (Thellier, 1938), se realizó mediante un horno SCHONDSTEDT, el cual se encuentra aislado del campo geomagnético por medio de bobinas Helmhotz. Este horno está conformado por dos partes, una para calentamiento y la otra para enfriamiento, el cual se realiza con un sistema interno de ventilación. El horno puede soportar como máximo 40 muestras.

A diferencia del tratamiento de campos alternos, los pasos utilizados, son más pequeños hacia la parte final de la desmagnetización (50-25°C), debido a qué la Magnetización Térmica Remanente (TRM) se adquiere durante los primeros 100 a 200°C por debajo de la temperatura de Curie (Thellier, 1959). Se midió la magnetización remanente de la muestra después de cada paso de desmagnetización hasta alcanzar la temperatura de Curie o bien cuando esta ya no se desmagnetizó más del 90% de la NRM inicial.

Todos los datos finales de desmagnetizaciones (térmica o por campos alternos), fueron procesados mediante un programa de cálculo para efectuar el análisis de componentes principales PCA (Zijderveld, 1967; Dunlop, 1979; Kirschvink, 1980), tomando en cuenta solo la parte alta del espectro (térmico y/o de coercividad) y considerando un MAD < 3 grados (Incoronato et al., 1996).

El análisis de componentes principales PCA a través del gráfico As-Zijderveld es una operación con un alto grado de dificultad el cual debe hacerse necesariamente tomando en cuenta también la representación estereográfica de los datos, para tener una visión más completa de la desmagnetización o, dicho de otra manera, de su variación direccional.

De manera muy general, la mayoría de los sitios estudiados presentan una sola componente direccional y la mayoría de las magnetizaciones fueron removidas alrededor de los 520°-570° C con el tratamiento térmico. Esto demuestra la presencia de titanomagnetita pobre en titanio como portador principal de la magnetización remanente, así como la MDF (Median Destructive Field) al utilizar el tratamiento por campos alternos el cual fue de 30-40 mT (véase los detalles de cada estudio).

2.4-Estudio de Paleointensidad

La determinación de la paleointensidad por medio del método Thellier-Thellier modificado (Coe et al., 1967; 1978) tiene algunos requisitos, como por ejemplo la presencia de una sola componente de la magnetización NRM (análisis del grafico de Zijderveld) y la capacidad de la roca a no alterarse con las altas temperaturas, es decir a tener una curva termomagnética lo más reversible posible. A través de un análisis de los gráficos de Zijderveld y de las curvas de susceptibilidad magnética de las muestras de cada sitio, se seleccionaron algunos sitios para ser tratados mediante técnica Thellier-Thellier modificada por Coe et. al. (op. cit.).

Se tomaron seis muestras en cada uno de los sitios seleccionados y los pasos de temperatura utilizados fueron de 50° hasta la temperatura de 450°, de 25° hasta los 500° y de 20° hasta la desmagnetización completa de la muestra. A lo largo del proceso, se efectuaron cinco chequeos (*check-pTRM*). El valor del campo magnético de laboratorio utilizado fue de 30 microTeslas.

El criterio utilizado para la determinación de la paleointensitdad es similar al empleado por Goguitchaichvili et al. (1999, 2000, 2001, 2002).

1) Seleccionar por lo menos seis puntos de la curva NRM-TRM correspondientes a una fracción de la NRM mayor a un 1/3,
2) Un factor de calidad (Coe et al., 1978) de 5 o más,
3) Los chequeos tienen que ser positivos (desviación de pTRM menor del 15%).

De las muestras procesadas, no todas proporcionaron los resultados óptimos esperados, por lo que fueron desechadas para el cálculo estadístico final.

Además de la técnica Thellier-Thellier modificada, en las muestras de los flujos de lava de volcán Paricutín también se utilizó la técnica de microondas (Shaw et al., 1984, 1996, 1999) modificada por Kono y Ueno (1977). Al igual que el método anterior no todas las muestras proporcionaron los resultados óptimos esperados (véanse los detalles de cada estudio).

Referencias

Coe R. (1967). The determination of paleo intensities of the Earth's field with emphasis on mechanism which could cause non-ideal behavior in Thellier's method. *Journal of Geomagn. and Geolectr.,* V. 19, pp. 157-179.

Coe R., Gromme S. and, Mankinen E. A. (1978). Geomagnetic paleointensity from radiocarbon-dated lava flows on Hawaii and the question of the Pacific non-dipole Low. *Journal of Geophysical Research,* V. 83, pp. 1740-1756.

Day R., Fuller M., and Schmidt, V. A. (1977). Hysteresis properties of titanomagnetites: Grain size and compositional dependence. *Physics of the Earth and Planetary Interiors*, V. 13, pp. 260-267.

Dunlop, D. J., (1979). On the use of Zijderveld vector diagrams in multicomponent paleomagnetic studies. Phys. Earth Planet. Int. 20, 12-24 (1979).

Gialanella R., Incoronato A., Russo F., and Nigro G. (1993). Magnetic stratigraphy of Vesuvius products. I-1631 lavas. *Journal of Volcanology and Geothermal Research,* 58, pp. 211-215.

Goguitchaichvili A., Alva-Valdivia L., Rosasa-Elguera J., Urrutia-Fucugauchi J., Gonzalez J., Morale J., Solé J. (2002). An integrated paleomagnetic study of Rio Grande de Santiago volcanic succession (tras-Mexican volcanic belt): revisited. *Phys. Earth Planet. Inter.* V. 130, pp. 175-194.

Goguitchaichvili A., Camps P., and Urrutia-Fucugauchi J. (2001). On the features of the geodynamo following reversals and excursions: By absolute geomagnetic intensity data. *Phys. Earth Planet. Inter.* V. 124, pp. 81-93.

Goguitchaichvili A., Chauvin A., Roperch P., Prevot M., Vergra M., Moreno H. (2000). Paleomagnetism of the Miocene Farellones formation in Chile. *Geophys. Journal Int.* 140, pp. 357-374.

Goguitchaichvili A., Prevot M., and Camps P. (1999) No evidence for strong fields during R3-N3 Icelandic geomagnetic reversals. *Earth Planet. Sci. Lett.* V. 167, pp. 15-34.

Incoronato A., (1996). Magnetic stratigraphy in volcanic area: The experience at Vesuvius, in Paleomagnetism and Tectonics of The Mediterranean Region,

eds Morrins, A. & Tarling, D. H., *Geol. Soc. Spec. Publ.,* V. 105, pp. 367-371.

J. Shaw and J. A. Share (1984). An automated superconducting magnetomer and demagnetizing system. Geophys J. R. astr. Soc., 78; 209-217.

J. Shaw, D. Walton, S. Yang, T. C. Rolph and J. A. Share (1996). Microwavw archaeointensities from Peruvian ceramics. Geophys. J. Int., 124; 241-244.

J. Shaw, S. Yang, T. C. Rolph and F. Y. Sun (1999). A comparison of archaeointensity results from Chinese seramics using microwave and conventional Thellier's and Shaw's methods. Geophys. J. Int., 136; 714-718.

Kirschvink, J. L., (1980). The least-squares line and plane and the analysis of palaeomagnetic data. *Geophys. J. R. Astr. Soc.* 62, pp. 699-718.

Kono M., and Ueno N. (1977). Paleointensity determination by a modified Thellier method. *Phys. Earth Planet Int.*, V. 13, pp. 305-315.

Thellier E. (1938). Sur l'aimantation des terres cuites et ses applications geophysiques, *Ann. Inst. Phys. Globe, Univ. Paris Bur. Cent. Magn. Terr.*, V. 16, pp. 157-302.

Thellier E. and Thellier O. (1959). Sur l'intensite de champ magnetique terrestre dans le passe historique et geologique. *Ann. Geophys,*. V. 15, pp. 285-376.

Zijderveld, J. D. A.. (1967). A. C. demagnetization of rocks: analysis of results, in Methods in Palaeomagnetism. E*ds Colinson, D. W., Creer, K. M. & Runcorn, S. K., Elsevier, Amsterdam.* pp. 254-286.

SEGUNDA PARTE

Producto del trabajo doctoral

-Paleomagnetic Study of Lavas From the Popocatépetl Volcanic Region, Central Mexico.

-Paleomagnetism of Michoacan-Guanajuato Volcanic Field, (Central Mexico): Implications to the Paleosecular Variation of the Earth's Magnetic Field at Low Latitudes.

-Erroneous Results from Historic Lavas: A Microwave Paleointensity Analysis of Paricutin Volcano, Mexico.

-Paleosecular Variation of Geomagnetic Full Vector from Vesuvius (Southern Italy): with Special Emphasis on the 1631 Eruption.

International Geology Review, Vol. 46, 2004, p. 210-225.

Paleomagnetic Study of Lavas From the Popocatépetl Volcanic Region, Central Mexico

G. Conte[1], J. Urrutia-Fucugauchi[1], A. Goguitchaichvili[1], A.M. Soler-Arechalde[1] O. Morton-Bermea[1] and Alberto Incoronato[2]

[1] Laboratorio de Paleomagnetismo y Geofisica Nuclear, Instituto de Geofisica, Universidad Nacional Autonoma de Mexico, Ciudad Universitaria, 04510 México D.F., MEXICO

[2] Earth Science Department, University of Naples 'Federico II', Naples, ITALY

Printed in: International Geology Review V. 46, (2004), pp. 210-225.

Note
The version reported in this Thesis presents some modifications that are not in the original paper.

Abstract

Results of a paleodirectional and paleointensity study of sixteen Popocatepetl lava flows are presented. Popocatepetl is a tall, active dacitic-andesitic stratovolcano; it forms the southern end of a NS trending Quaternary volcanic range at the eastern edge of the basin of Mexico. Studied units are mainly andesites and one trachyandestite, and all possess similar trace and rare earth element compositions. Rock-magnetic experiments show that remanence is carried in most cases by Ti-poor titanomagnetite, resulting from oxy-exsolution of original titanomagnetite during flow cooling. Unblocking temperature spectra and high coercivities point to 'small' pseudo-single domain magnetic grains for these (titano)magnetites. Single-component, linear demagnetization plots were observed in most cases. A strong, lightning-produced magnetization overprint was detected for one site. Combining the new paleomagnetic data with a selection of previously published results (Carrasco et al., 1986), provides a mean paleodirection of I=35.4°, D=345.7°, k=21, α_{95}=8.5°, N=15 for the Popocatepetl volcano region. All studied flows yield normal polarity magnetization, which supports a maximum age within the Brunhes chron.

Twenty-five samples from flows were selected for Thellier palaeointensity experiments based on magnetic properties, stable single-component remanent magnetizations and reasonably reversible continuous thermomagnetic curves. Fourteen samples from four different flows, yield reliable paleointensity estimates with the flow-mean virtual dipole moments (VDM) ranging from 5.9 to 9.2 $x10^{22}$ Am^2. The NRM fractions used for paleointensity determination range from 35 to 96%, and the quality factors vary between 3.4 and 46.9, being normally greater than 6. Mean VDM obtained in this study is 7.2 ± 1.4 10^{22} Am^2, slightly lower than the present-day dipolar value.

Introduction

A rock-magnetic, paleomagnetic and paleointensity study has been carried out on 16 flows from the Popocatepetl volcanic region (Fig. 1). This study forms part of a long-term project to investigate geomagnetic field strength and paleosecular variation during the Late Pleistocene and Holocene. In addition, objectives of this study include investigations of the Quaternary tectonics and volcanic stratigraphy of the ranges bordering the basin of Mexico. Popocatepetl stratovolcano forms part of the active volcanic front of the magmatic arc in central Mexico.

Interest in studying the age and volcanic history of the Popocatepetl stratovolcano recently increased due to initiation of explosive eruptive activity in late 1994, which continues to the present. An increase in seismicity by October 1994 marked onset of the activity and on December 21, 1994 a swarm of volcano-tectonic earthquakes and tremor accompanied a tall ash plume that rose from the summit crater (Arciniega-Ceballos et al., 1999, 2003). More recent activity includes several episodes of dome growth and destruction, and frequent ash emissions have attracted considerable interest from the scientific community and government agencies. Areas on the flanks of the volcano and its immediate vicinity are heavily populated; the nearby large cities of Mexico D.F. and Puebla are northwest and east of the volcano, respectively (Fig. 1).

Popocatepetl Stratovolcano

Popocatepetl is a dacitic-andesitic stratovolcano in the central-eastern sector of the Plio-Quaternary Trans-Mexican volcanic belt (TMVB); it forms the southern end of a north-south trending Quaternary volcanic range (Fig. 1). The TMVB extends east-west from the Pacific Ocean to the Gulf of Mexico, and its origin is linked to active plate subduction along the Middle America Trench. The volcanic chain that includes the volcanoes Tlaloc, Iztaccihuatl and Popocatepetl developed within a region characterized by intense Plio-Quaternary magmatic activity. This is manifested in extensive monogenetic cinder cone fields and tall, composite dacitic-andesitic stratovolcanoes, built on a region with thick crust (e.g., Urrutia Fucugauchi and Flores Ruiz, 1996; Wallace and Carmichael, 1999).

Popocatepetl is formed by two superposed volcanic structures: Popocatepetl volcano, with a conical shape truncated to the summit; and the older Nexpayantla volcano, with a remaining flank showing evidence of a long erosion period. Both are mostly constructed by lava flows intercalated with breccias and pyroclastic products. Large pyroclastic deposits (ash fall, ash flow and hot avalanches) are widely distributed around the Popocatepetl and constitute the basal cone. Composition of volcanic products ranges from mafic (basaltic andesites) to felsic rocks (rhyodacites); however andesites and dacites are more abundant. Glacial and gravity deposits occur in the Popocatepetl young units. Volcanic products are grouped into two formations: Nexpayantla Formation and Popocatepetl Formation, which are related to the two stages of construction of the structure (basal and recent cones respectively). The basal volcano formed by Nexpayantla Formation comprises rocks mostly of andesitic composition, starting with mafic lava flows, becoming felsic toward the upper part. Most differentiated rocks are rhyodacites, intercalated with volcanic breccias. An unconformity separates the sequences from the recent cone constituted by Popocatepetl Formation. This unit is composed of andesitic lavas and minor pumiceous breccias and tuff; toward the top it consists of porphydic andesites irregularly intercalated with unconsolidated pyroclastic deposits of mafic and felsic composition.

Popocatepetl has also experienced major cataclysmic eruptions; with the last Bezymiani-type or Mount Saint Helens-type event occurring 23 ka (Robin and Boudal, 1987; Siebe et al., 1996). Several major Plinian eruptions occurred after formation of the modern Popocatepetl cone, generating pyroclastic flows, lahars, and pumice + ash deposits. Explosive events represented by pyroclastic surges, pumice lapilli, and ash-fall deposits are documented for the past thousand years, including those of about 5000, 2100, 1350 and 1200-1100 yr ago (Siebe et al., 1996; Panfil et al., 1999). Large debris and lahar flows are common and constitute a major hazard; San Nicolas lahar traveled some 60 km down the flank some 1100-1300 yr BP (Gonzalez-Huesca et al., 1997). However, incomplete resolution of stratigraphic record does not yet allow definition of activity patterns between major and moderate events. Popocatepetl, activity between 1919 and 1927 (Waitz, 1921; Siebe et al.,

1996), was characterized by moderate eruptive events, formation of domes inside the summit crater, and ash plumes in historic times.

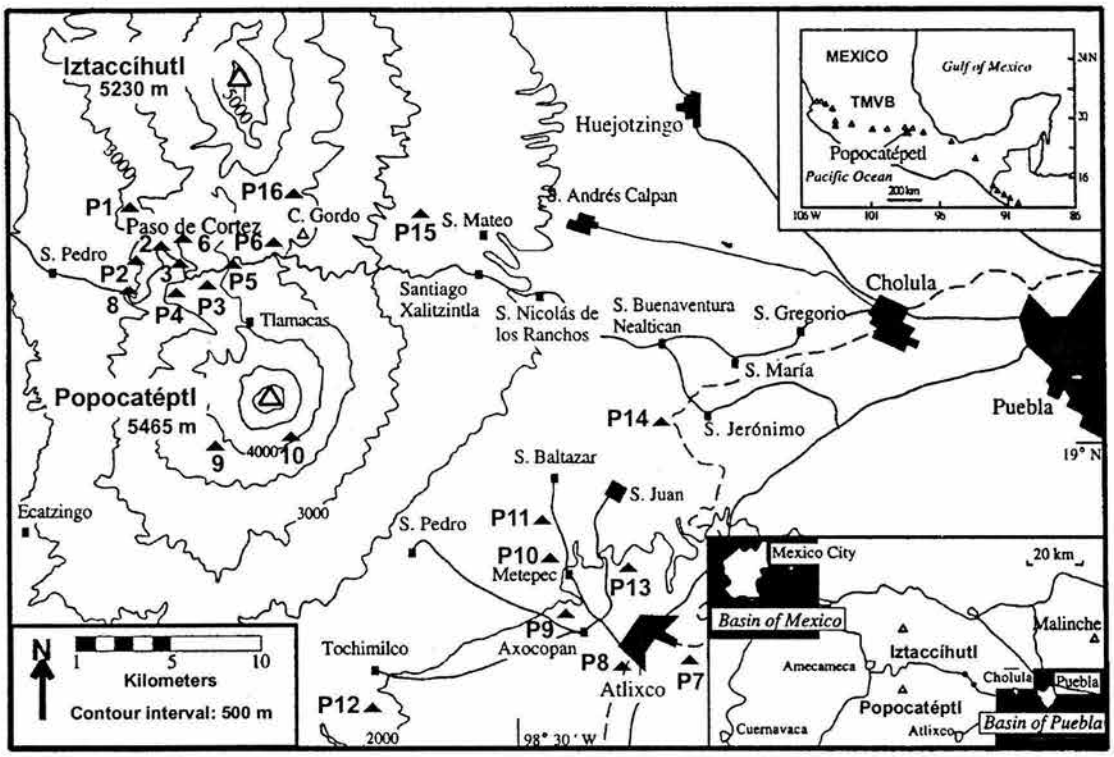

Fig. 1. Location of sampling sites (filled triangles) in the Popocatepetl stratovolcano, eastern sector of the Basin of Mexico. Popocatepetl forms the southern active end of the N-S trending volcanic range that also includes Iztaccihuatl stratovolcano. Sampling sites in this study are indicated by P and site number. Sites studied previously are simply indicated by a number (Carrasco-Nuñez et al., 1986). Popocatepetl lies at the active volcanic front of the E-W magmatic arc (Trans-Mexican volcanic belt) in the central-eastern sector of the arc (inset, upper right corner). The region is heavily populated, with the large cities of Mexico and Puebla also located nearby (inset, lower right corner). The base map adopted from Panfil et al. (1999).

Sample Descriptions and Geochemistry

For our study, paleomagnetic samples were collected with a portable gasoline-powered drill and oriented with magnetic compass. Nine units were sampled in the northern sector near the town of Tlamacas and seven on the southeastern flank sector near the towns of Tochimilco, Metepec, and S. Jeronimo in the Atlixco region (Fig. 1). A total of 140 oriented samples (paleomagnetism) and 32 representative block samples for geochemistry and petrology were collected from the lava flows. Paleomagnetic sites are referred as Popo, plus the site identification number, and petrography/geochemistry sites are referred as P and the site number. In Figure 1, sites previously studied by Carrasco-Nuñez et al. (1986) on the Popocatepetl stratovolcano are also plotted.

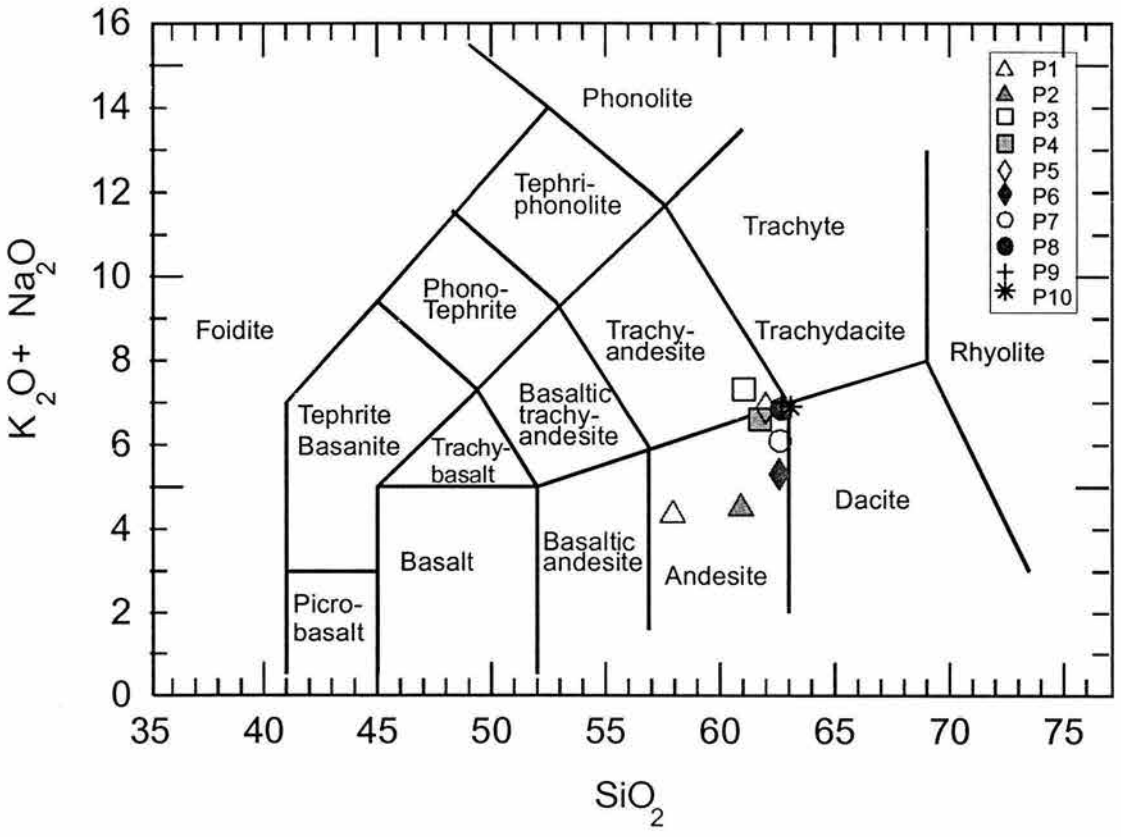

Fig. 2. $Na_2O + K_2O$ (wt %) plotted as a function of SiO_2 (Le Bas et al., 1986) for samples of the Popocatepetl stratovolcano (major-oxide data from Carrasco-Nuñez et al., 1986). Studied units classified mostly as andesites and some as trachyandesites in the silica versus total alkalies classification system for volcanic rocks.

Units studied mostly correspond to andesites and some trachyandesites (Fig. 2). Thin sections were prepared for representative samples from each unit. All samples are rich in plagioclase crystals and microcrystalline. Samples are olivine-bearing calc-alkaline and magnesian andesites (Fig. 3), with similar major-oxide and trace-element compositions; 57-63% SiO_2; > 6% MgO; low CaO, Al_2O_3 and FeO; and high Na_2O. Popocatepetl andesites are characterized by magnesian, Cr-spinel fosteritic olivine (e.g., Fig. 3), which has been taken as evidence of magma mixing with a mafic component still recognizable (e.g., Robin and Boudal, 1987). Chemical data for Popocatépetl units are plotted in the AFM (Alkalies-FeO-MgO) ternary diagram in Figure 4; samples fall all within the calc-alkaline field. Major-oxide chemical data are summarized in Table 1.

We determined the rare-earth-element (REE) patterns for five selected units, by induction-coupled plasma mass spectrometry (ICP-MS). For the analyses, 0.2 g of dried powder rock was digested with a mixture of concentrated acids (10 ml HF and 4 ml $HCLO_4$). The solution was evaporated to dryness and dissolved in 4 ml $HCLO_4$. After evaporation, the solution was made up to 50 ml with 1 % HNO_3.

The ICP mass spectrometer employed was a VG Elemental model PQ3. Detection limits are calculated as the concentration equivalent to three times the standard deviation of five replicates of the blank solution. For all elements, it is better than 50 ppt.

Calibration was performed with a 1, 10, 100 and 200 ppb multi-element standard solution (SPEX-high purity) and a blank solution of deionized water, all containing HNO_3 at 2 %. Matrix effects and instrumental drift were eliminated using In 115 (10 ppb) as internal standard. Validity of analytical procedure was evaluated on accuracy and precision tests by comparison of measured and reference values of andesite JA-2 (Govindaraju, 1987). All elements have precision better than 3% relative standard deviation. Data obtained for reference sample JA-2 agree with certified values.

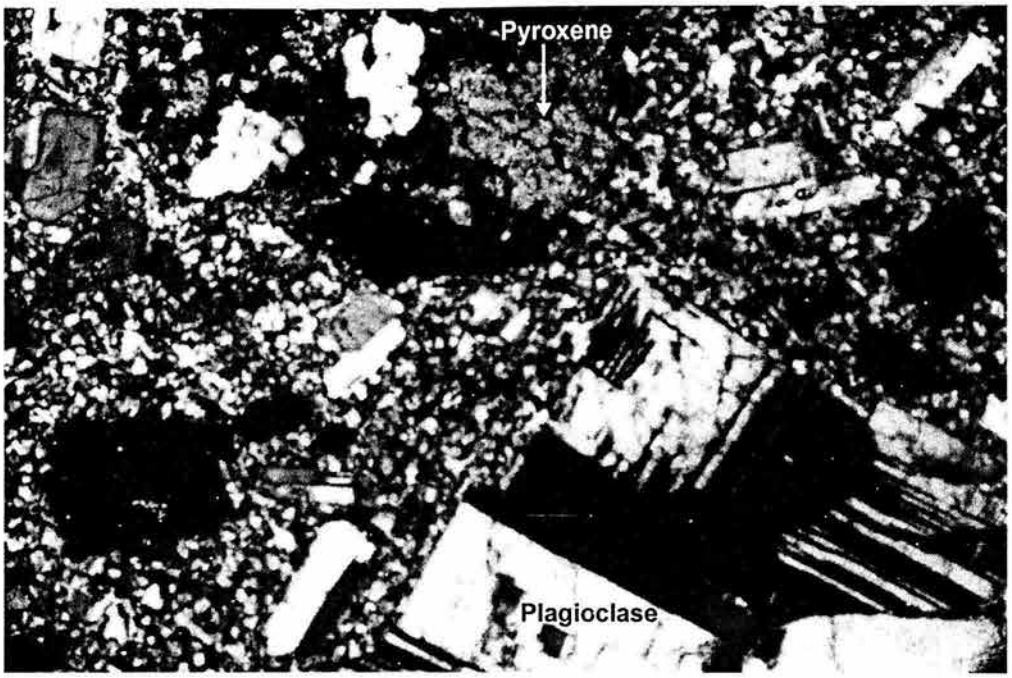

A)

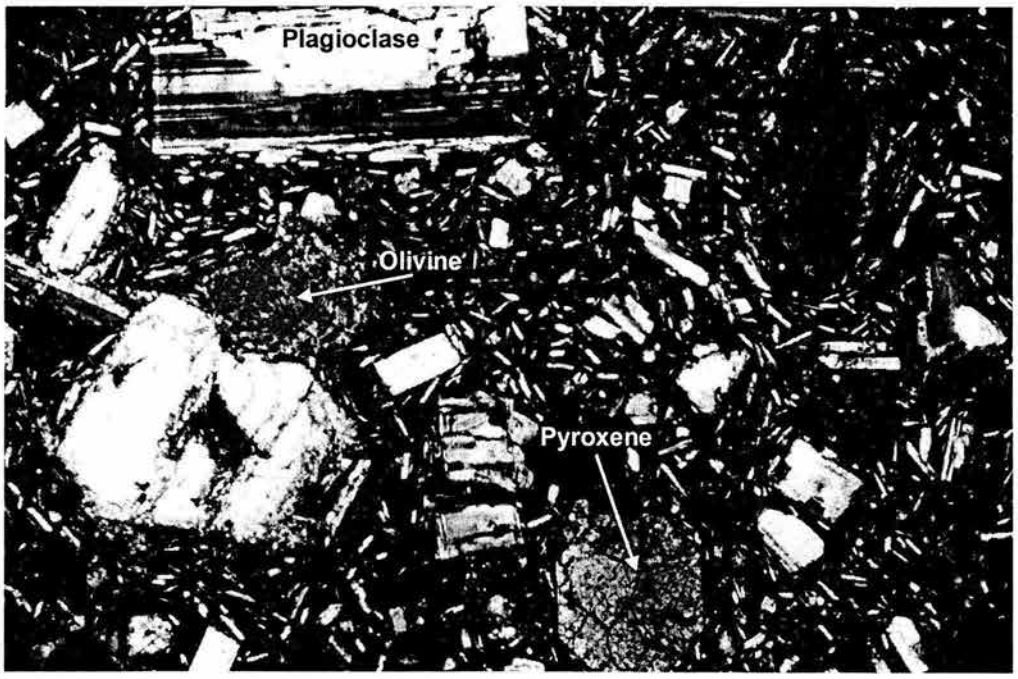

B)

Fig. 3. Examples of petrographic observations on thin sections from samples of site (A) Popo-7 and (B) Popo-10 (see Fig. 1 for site location). Popocatépetl andesites are characterized by abundant plagioclase crystals and the occurrence of magnesian, Cr-spinel fosteritic olivine.

REE, normalized to recommended chondrite reference values (Evensen et al., 1978), are shown in Figure 5. Samples from the different sectors in the volcano are characterized by relatively similar diagram trends (Fig. 1; P4 northern volcano sector, P7 near Atlixco, P10 and P11 near Metepec, and P15 near Santiago Xalitzintla and San Mateo).

Relative ages of the Popocatepetl and Nexpayantla volcanoes have been roughly estimated from geomorphology and glaciation features. Nexpayantla is deeply dissected and affected by glaciation (e.g., Heine, 1988). Paleomagnetic polarity measurements indicate that volcanic activity developed during the normal polarity Brunhes chron (Carrasco et al., 1986). Nixon (1989) proposed that volcanic activity in the Sierra Nevada range is probably not older than 1 Ma, and reported some dates for the neighboring Iztaccihuatl volcano of 200 Ka for lavas covering the Nexpayantla units.

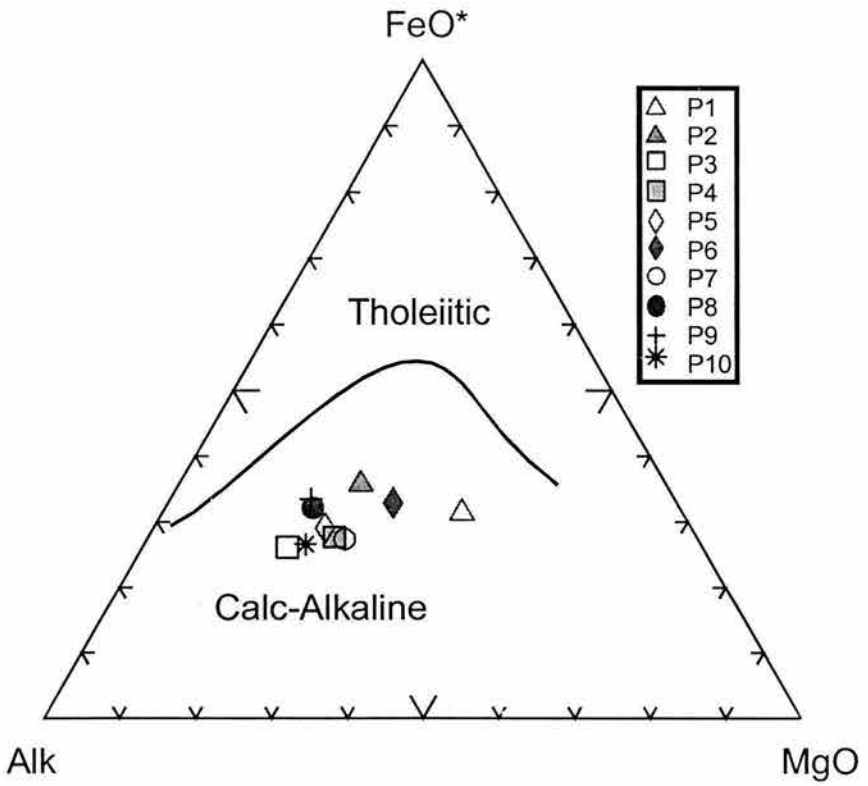

Fig. 4. Major-oxide chemical data for Popocatepetl units plotted in the AFM (Alkalies-FeO-MgO) ternary diagram. Fields for the tholeitic and calc-alkaline igneous rocks are shown. Popocatepetl samples fall all within the calc-alkaline field.

Table 1.
Summary of chemical data for flow units from Popocatepetl stratovolcano,
a) Major-oxides, and b) Rare Earth Elements

a) Major-Oxides.

	P1	P2	P3	P4	P5	P6	P7	P8	P9	P10
SiO_2	57.94	60.91	61.05	61.74	61.99	62.57	62.62	62.67	62.71	63.1
TiO_2	0.55	0.90	0.60	0.55	0.68	0.76	0.98	0.98	0.86	0.62
Al_2O_2	20.23	19.27	18.56	16.85	15.8	16.06	17.18	16.6	15.17	16.88
Fe_2O_3	1.30	1.04	0.16	0.92	0.33	1.88	0.20	1.38	2.49	1.08
FeO	3.49	3.04	3.34	2.99	3.84	2.94	3.39	3.31	2.63	2.53
MnO	0.08	0.06	0.08	0.06	0.09	0.45	0.56	0.06	0.06	0.05
MgO	5.87	2.67	2.55	3.38	3.21	4.18	3.39	2.74	2.70	2.80
CaO	4.98	5.16	5.89	6.47	6.40	5.51	5.56	5.24	5.43	5.28
Na_2O	3.63	3.63	4.83	4.70	4.90	3.90	4.35	4.96	5.00	4.95
P_2O_5	0.11	0.13	0.65	0.44	0.45	0.16	0.23	0.20	0.20	0.16

b) Rare Earth Elements.

	P4	P7	P10	P11	P15
La	21.62	20.92	13.62	14.17	14.59
Ce	51.93	48.27	33.12	34.07	34.93
Pr	5.66	5.66	3.75	3.85	3.96
Nd	24.31	25.09	16.80	17.18	17.60
Sm	5.13	4.53	4.23	3.80	3.91
Eu	1.61	1.44	1.14	1.15	1.18
Gd	5.06	4.03	3.94	3.83	3.84
Tb	0.66	0.35	0.43	0.42	0.43
Dy	3.89	1.81	3.35	3.13	3.29
Ho	0.58	0.30	0.51	0.47	0.48
Er	1.48	0.76	1.70	1.54	1.64
Tm	0.23	0.11	0.29	0.23	0.23
Lu	0.24	0.12	0.25	0.23	0.23

On this basis and considering the Neogene activity of Popocatepetl, Nexpayantla volcano is considered to be no older than ~780 ka and possibly no younger than 200 ka. Studies of Iztaccihuatl lava flows indicate dominant normal polarity, which has been assigned to the Brunhes chron (Urrutia-Fucugauchi, 1995).

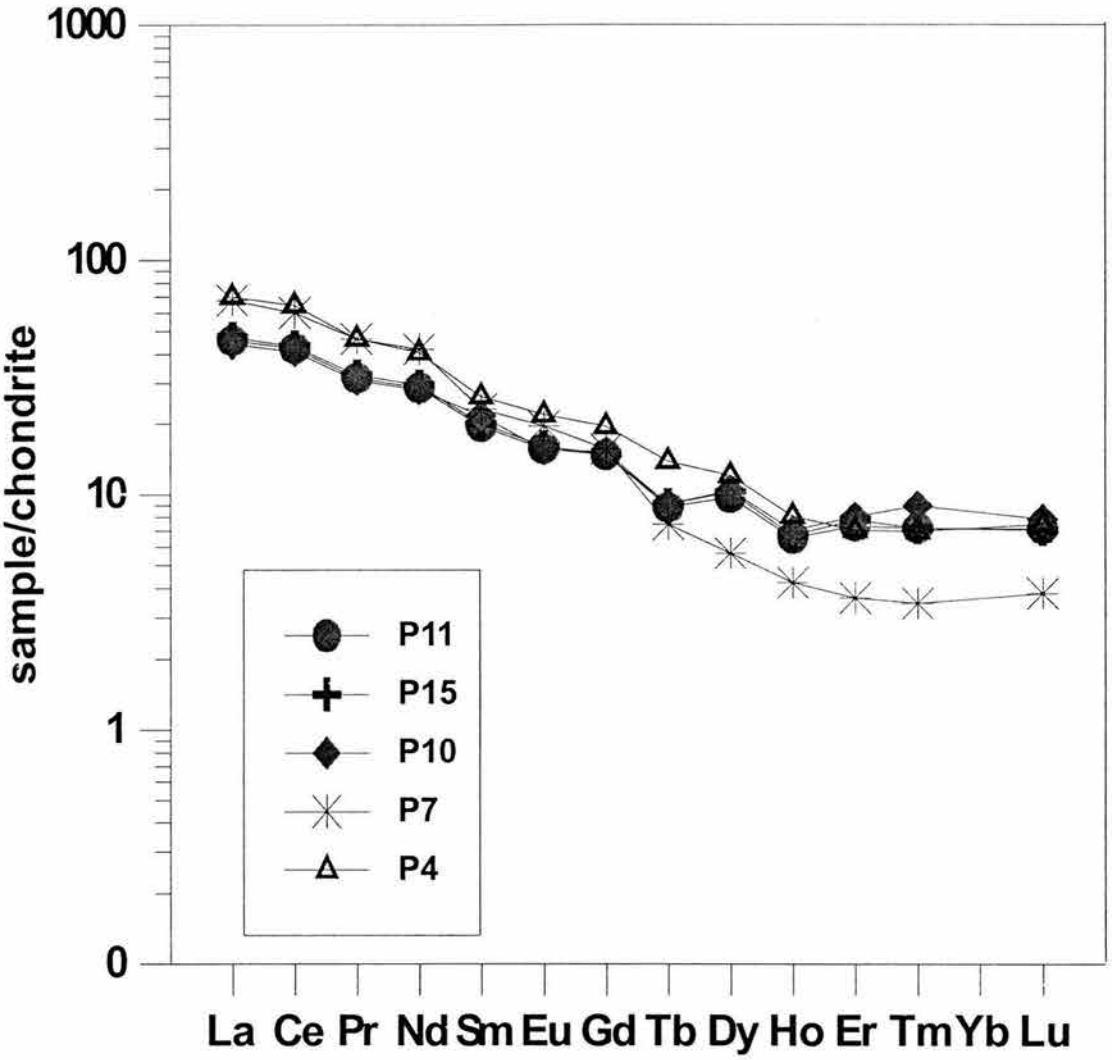

Fig. 5. Chondrite-normalized REE patterns for samples of the Popocatépetl stratovolcano. See Figure 1 for location of sampling sites in the northern, southern and eastern sectors of the stratovolcano.

Rock-Magnetic Experiments

In order to identify the magnetic carriers of the remanent magnetization, to obtain information about their paleomagnetic stability, and to assess the suitability of the studied samples for paleointensity studies, several rock-magnetic experiments were carried out (Figs. 6, 7, and 8). These experiments included: (1) continuous susceptibility measurements at low temperatures (from –190°C to room temperature); (2) continuous susceptibility measurements at high temperatures (from room temperature to 600°C); and (3) hysteresis measurements.

Low and high temperatures continuous susceptibility curves

Low-temperature variation of susceptibility (from about –190°C to room temperature) was recorded using a Highmore susceptibility bridge equipped with furnace in Mexico City laboratory (one sample per unit). Low-temperature variation of susceptibility down to liquid-nitrogen temperature was determined for volcanic rocks and synthetic analogs, and used to infer the characteristics of magnetic minerals and domain state (e.g., Radhakrishnamurty et al., 1981; Urrutia-Fucugauchi et al., 1984; Dunlop and Ozdemir, 1997).

Low-temperature susceptibility curves show a rather monotonic decrease from about -185°C to room temperature (Fig. 6; samples Popo-2 and Popo-15). The only exception is site Popo-9; this specimen yielded a poorly defined pick around –90°C that differs from the Verwey transition characteristic of pure magnetite. We attribute both behaviors to Ti-poor titanomagnetite. As showed by Ozdemir et al. (1993), the Verwey transition may be largely suppressed for the titanomagnetites with variable titanium content. Alternatively, similar behavior may also correspond to non-stoichiometric (partially oxidized) magnetite.

For the high-temperature susceptibility measurements, one sample from each site was heated to about 600°-650°C at a rate 20°C/min, then cooled at the same rate. The Curie temperature was determined by the Prévot et al. (1983) method. Almost all samples show the presence of a single magnetic/ferrimagnetic phase with Curie point compatible with relatively low-Ti titanomagnetite (Fig. 6). However, the cooling and heating curves are not perfectly reversible.

Reliable susceptibility versus temperature curves could not be obtained for some samples because of low initial susceptibility (e. g. Popo-7 and Popo-8).

Hysteresis measurements

Hysteresis measurements at room temperature were performed on all studied samples using the AGFM Micromag system in the paleomagnetic laboratory at Mexico City in fields up to 1.4 Tesla. The saturation remanent magnetization (M_r), the saturation magnetization (M_s) and coercitive force (H_c) were calculated after correction for the paramagnetic contribution. The coercivity of remanence (H_{cr}) was determined by applying progressively increasing backfield after saturation. Typical hysteresis plots are reported in Fig. 7A-7C. No potbellied or wasp-waisted behaviors were detected, which probably reflects very restricted ranges of the coercivities of magnetic phases. The only exception is site Popo-12 (Fig. 7B), which probably reflects the presence of ferromagnetic phases with different coercivities. Most probably this behavior is due to presence the mixture of (titano)magnetite and (titano)hematite with different coercivities (Tauxe et al., 1996). This hypothesis is supported by the IRM (isothermal remanent magnetization) acquisition curves which do not reach saturation with inductions of 0.3 T (Fig. 7E). The curve also shows an initial segment indicating a low coercivity mineral. The remaining IRM acquisition curves were found to be quite similar for the others samples. Saturation is reached in moderate fields (Fig. 7D-7F, bottom diagrams) of the order of 100-300 mT, which reveals that a spinel phase is the main mineral present. Based on the ratios of hysteresis parameters (Fig. 8), almost all samples fall in the pseudo-single-domain (PSD) grain-size region, probably indicating a mixture of multidomain (MD) and a significant amount of SD grains. If some superparamagnetic fraction also exists in these samples, the coercive force and saturation magnetization are somewhat lower or larger, respectively, than those ferrimagnetic fractions alone.

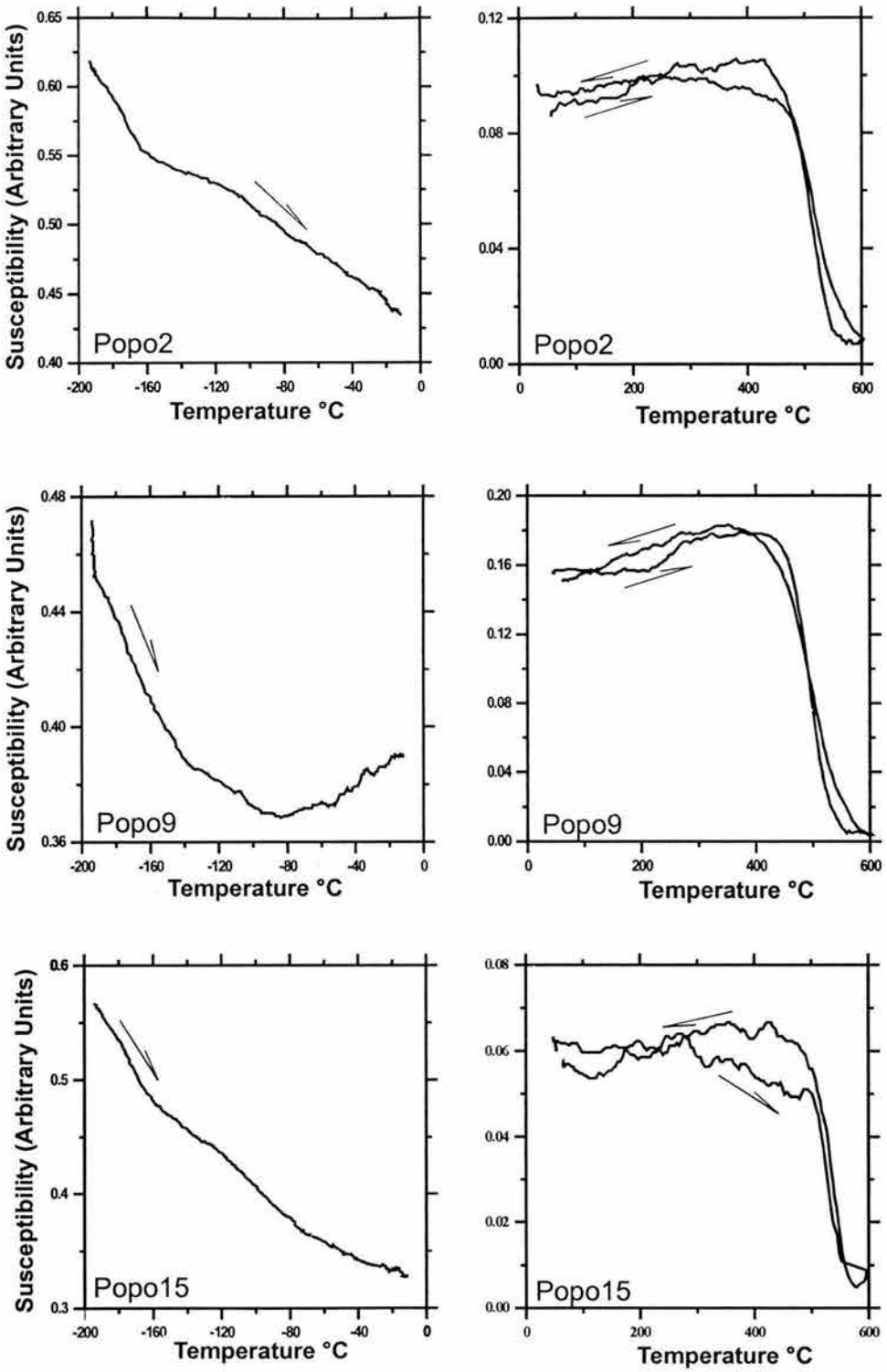

Fig. 6. Examples of temperature-dependent variation curves for samples from Popocatepetl stratovolcano. Diagrams on the left side correspond to low-temperature variation of susceptibility (from room temperature to liquid nitrogen temperature). Diagrams on the right correspond to high-temperature variation curves, to 600°C.

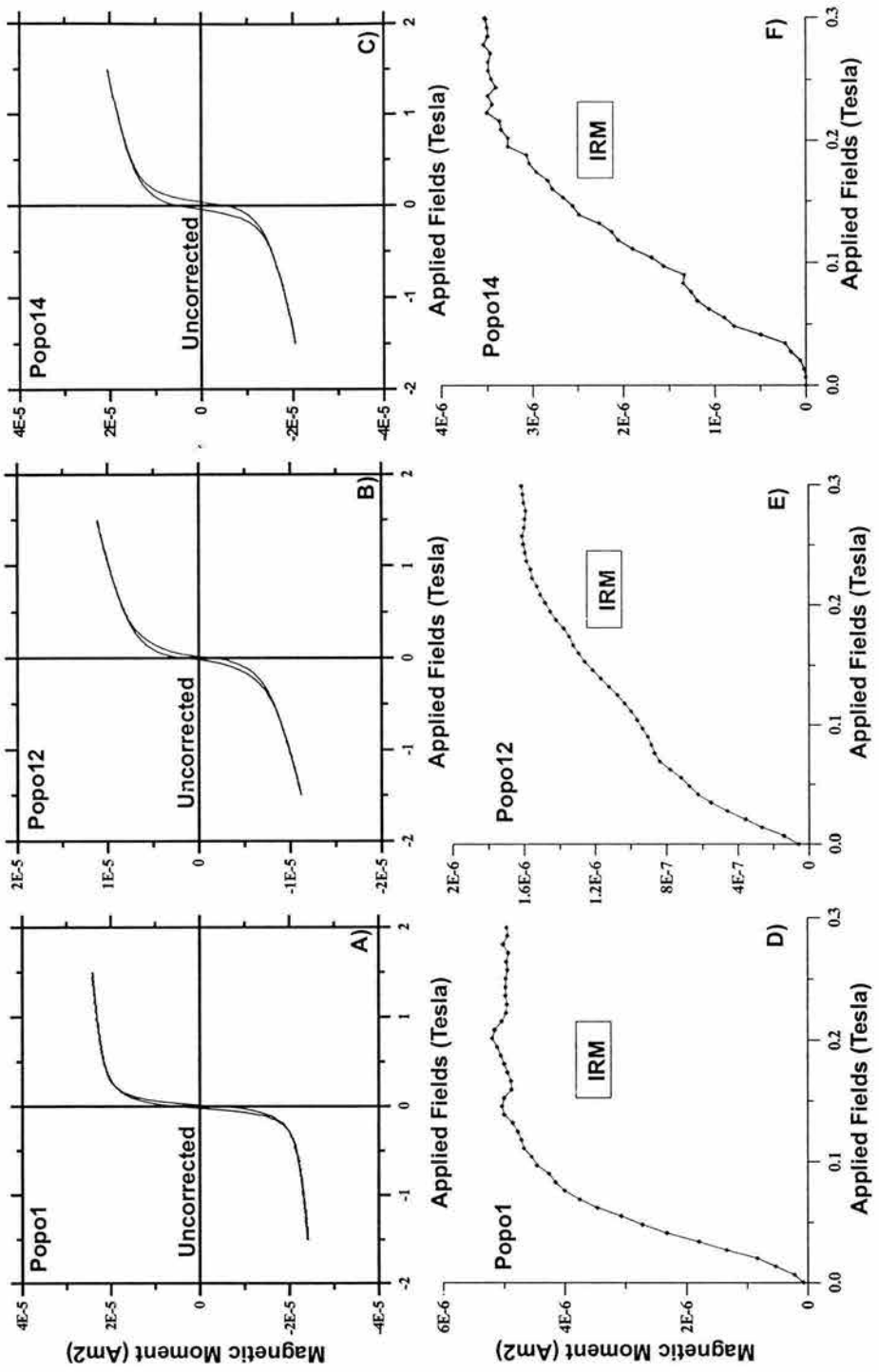

Fig. 7. A-C. Examples of hysteresis curves for samples of the Popocatepetl stratovolcano (top diagrams). Hysteresis curves have been determined in a MicroMag instrument, with maximum applied field to 1.4 Tesla. Loops shown have not been corrected for the diamagnetic/paramagnetic contribution. D-F. Examples of isothermal remanent magnetization (IRM) acquisition curves (bottom diagrams) for samples of Popocatepetl stratovolcano. Measurements were carried out in a home-made pulse magnetizer.

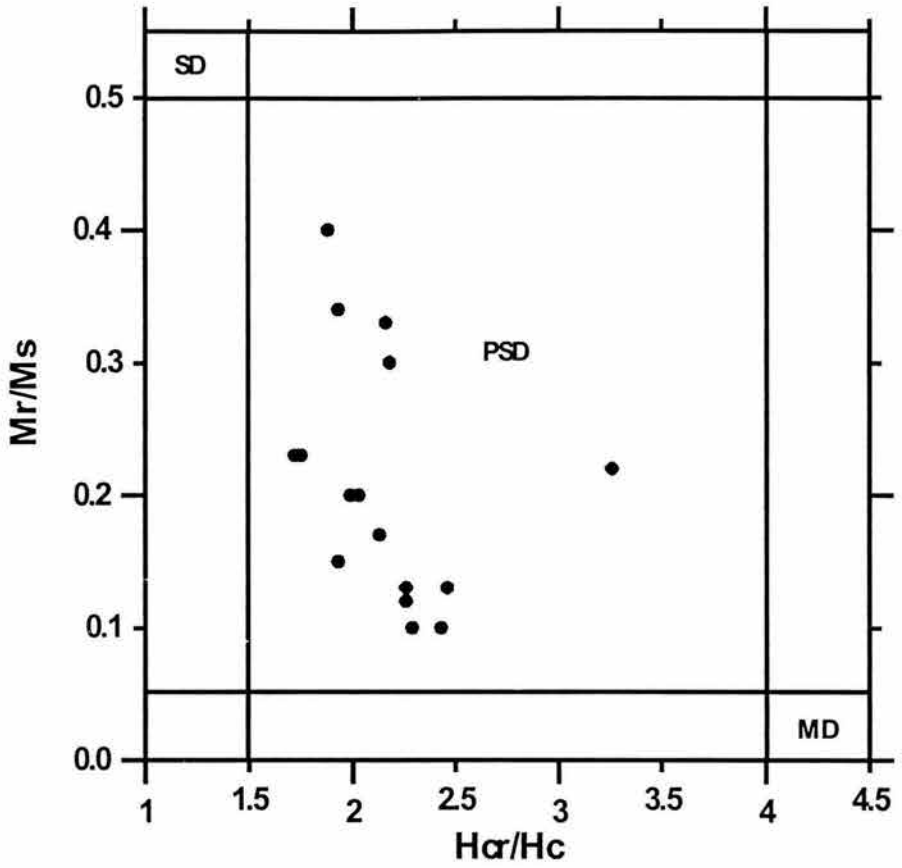

Fig. 8. Hysteresis parameter ratios for coercivity (Hcr/Hc) and remanence (Mr/Ms) plotted in a Day diagram (Day et al., 1977). Samples from the different units in Popocatepetl stratovolcano plot in the pseudo-single domain (PSD) field.

Paleodirectional Study

The remanent magnetization of samples from each unit was measured with a Molspin spinner magnetometer. Stepwise thermal (mainly) demagnetization up to 575° - 675°C using a non-inductive Schonstedt furnace to investigate the vectorial composition and stability of NRM. During thermal demagnetization, the low-field susceptibility at room temperature was measured after each step with a Bartington susceptibility meter (equipped with the laboratory dual-frequency sensor).

In most of studied units, only one remanence component was recognized (Fig. 9). Very small secondary components were easily removed applying 200°C or sometime 300°C (sample Popo-13-3Z). The greater part of remanent magnetization is removed at temperatures between 500°C and 550°C, which indicate low-Ti titanomagnetites as remanence carriers.

A characteristic magnetization direction (ChRM) was determined by the least-squares principal component analysis (PCA) method (Kirschvink, 1980), four to nine points being taken in the principal component analysis for the ChRM vector component determination. Magnetization directions were averaged, giving unit weight to lava flows; statistical parameters were calculated assuming a Fisherian distribution. Average unit ChRM directions are well determined (Table 2, Fig. 10), with α_{95} less than 12 degrees. One site (site Popo-2) was characterized by unusually high NRM intensity (more than several hundred A/m) and scattered NRM directions. Both factors may point to a strong lightning-produced magnetization overprint. These samples were rejected for further paleomagnetic statistical analysis.

Combining the paleomagnetic data for the lava flows in the Popocatepetl region, we obtain a mean paleodirection of I=35.4°, D=345.7°, k=21, α_{95}=8.5°, N=15 (Fig. 10). Four directional data were eliminated from the mean direction because these sites are characterized by erratic directions and high dispersions (Fig. 10-Table 2). All studied flows are characterized by normal polarity magnetization, which supports a maximum age within the Brunhes chron (<780 ka).

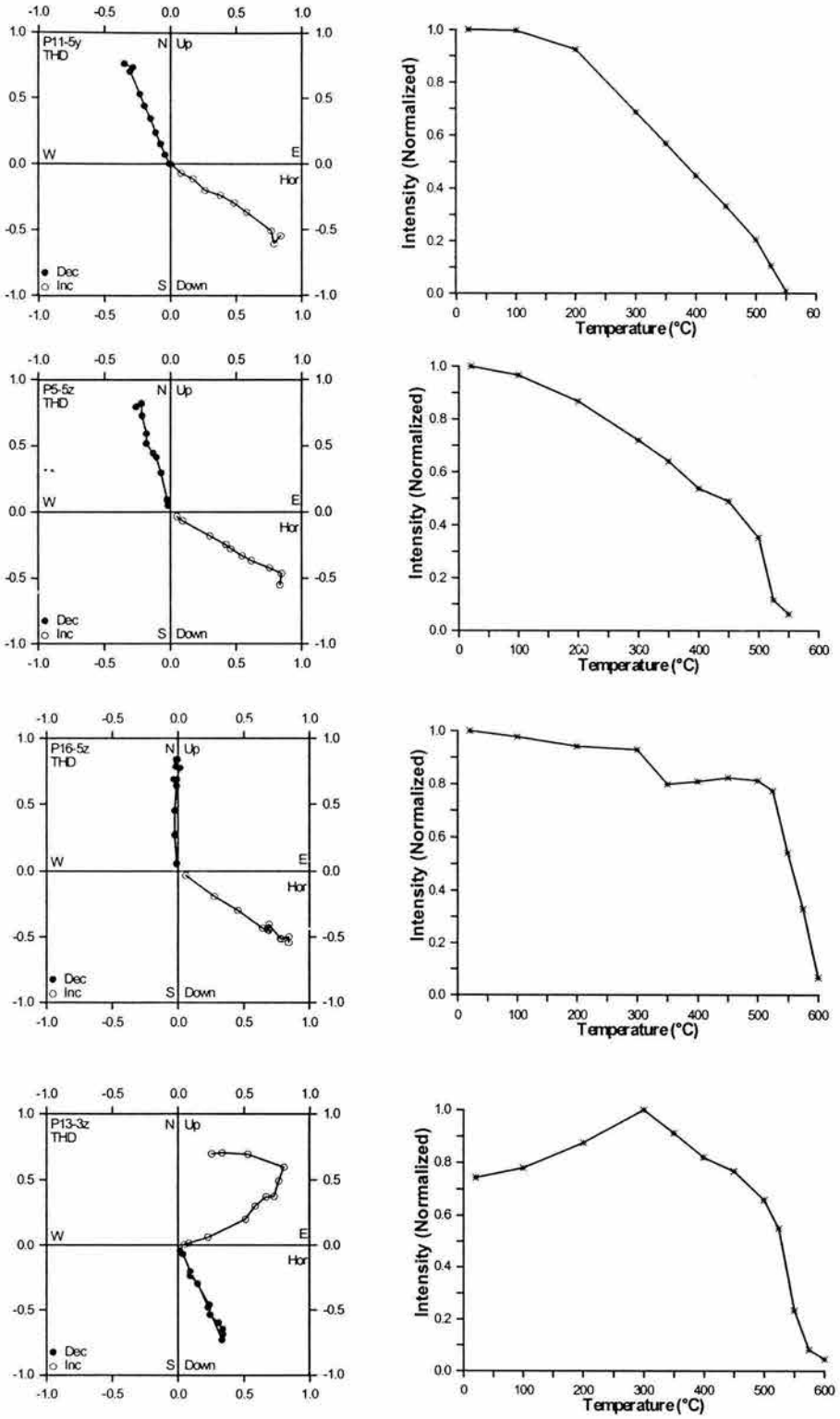

Fig. 9. Examples of thermal demagnetization data for samples of Popocatepetl stratovolcano. Diagrams on the left are vector plots (closed circles represent the horizontal component, open circles the vertical component). Diagrams on the right are normalized intensity plots as a function of temperature.

Table 2.
Summary of Paleomagnetic Data for Flow Units from Popocatepetl Stratovolcano

Site	Coordinates (°N)	(°W)	N	Dec.	Inc.	k	α95.	Lat.	Long.	Pol.
P1	19.08	98.66	9	3.5	35.9	229.3	3.4	86.6	336.9	N
P3	19.07	98.60	5	324.7	33.1	332.5	4.2	56.6	175.5	N
P5	19.05	98.62	4	350.9	32.6	182.9	6.8	81.3	164.2	N
P7	18.92	98.40	5	1.2	6.1	590.8	3.2	74.1	77.3	N
P8	18.90	98.43	5	332.4	53.6	122.2	6.9	61.1	209.0	N
P9*	18.93	98.47	4	290.8	13.0	56.8	12.3	21.8	171.2	N
P10	18.96	98.48	6	314.4	52.4	136.8	5.7	47.0	200.0	N
P11	18.96	98.48	7	347.5	37.6	148.2	5.0	78.1	183.8	N
P12*	18.88	98.57	4	46.5	51.6	107.3	8.9	46.3	324.2	N
P13	18.93	98.45	8	344.8	29.8	200.2	3.9	75.2	162.4	N
P14	19.00	98.42	9	348.3	48.9	79.8	5.8	74.8	219.3	N
P15	19.08	98.52	4	359.6	27.5	66.8	11.3	85.5	86.4	N
P16	19.07	98.60	8	2.3	26.6	164	4.3	84.5	57.4	N
Site			**N**	**Dec.**	**Inc.**	**K**	**α95.**	**Lat.**	**Long.**	**Pol.**
2*	19.05	98.64	5	315	5.75	10.9	24.2	43.1	186.0	N
3	19.04	98.63	6	331.7	46.2	119.2	6.1	62.8	194.4	N
6	19.06	98.63	4	332.2	29.9	83.3	10.1	63.3	173.4	N
8*	19.06	98.67	6	306.1	69.5	18.5	15.9	36.5	224.4	N
9	18.98	98.64	8	338	17.7	80.5	6.2	66.5	193.3	N
10	18.59	98.60	5	357.6	38.9	33	13.4	86.2	225.1	N

Mean directions: N=15; D=345.7; I=35.4; k=21; α95=8.5. Mean VGPs: N=15; Plat.=75.8; Plong.=188.6; K=25; A95=7.9. The source for sites 2-10 is Carrasco et al., 1986.
* Sites not included in calculation of overall mean direction (see text).

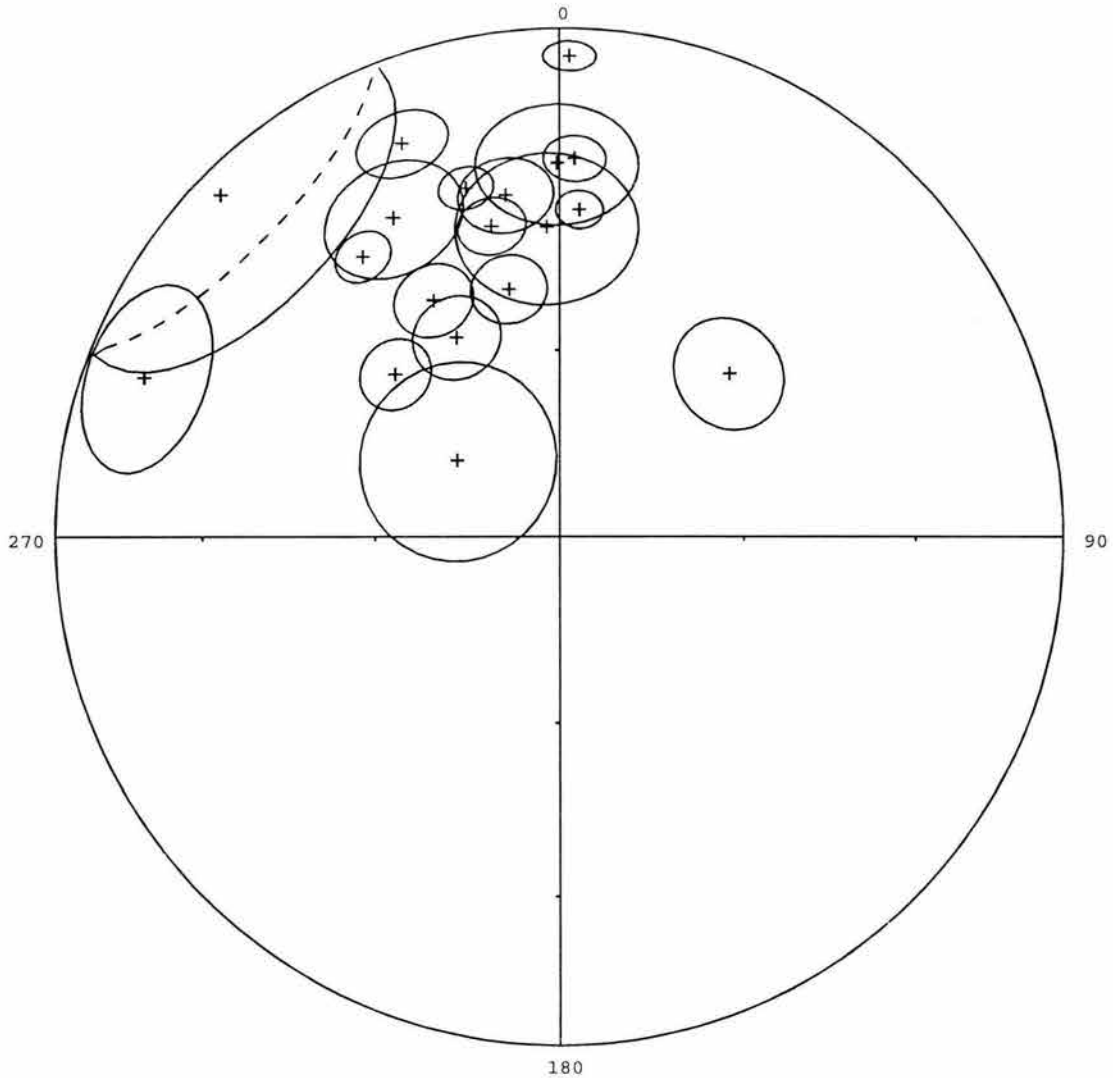

Fig. 10. Site mean directions (with the corresponding α_{95}) for Popocatepetl stratovolcano (Table 2), plotted in an equal-area stereographic projection. Magnetic polarity for all units is normal. The overall mean direction of selected sites is I = 35.4°, D = 345.7°, α_{95} = 8.5°, k = 21, N = 15.

Paleointensity Experiments

Paleointensity experiments were performed using the Thellier method (Thellier and Thellier, 1959) in its modified form (Coe et al., 1978). Heatings and coolings were performed in air and the laboratory field set to 30 microTesla. Eleven temperature steps were distributed between room temperature and 560°C. Temperature reproducibility between two steps was in general better than 2°C up to 350°C and better than 5°C above it. The pTRM/NRM (Goguitchaichvili et al., 1999a) were performed after every second step throughout the experiments.

Paleointensity data are reported on the Arai-Nagata (Nagata et al., 1963) plots; some typical examples are given in Figure 11. We only accepted determinations that fulfil the following criteria: (1) obtained from at least six NRM-TRM points corresponding to a NRM fraction larger than 1/3 (Table 3); (2) yielding quality factor (Coe, et al., 1978) of about 5 or more; and (3) with positive pTRM checks. The direction of NRM remaining at each step, obtained from the paleointensity experiments, are reasonably linear and point to the origin (Fig. 11). No deviation of NRM remaining directions towards the direction of applied laboratory field were observed. An exception was sample Popo-4, in which remaining direction shows a tendency to move towards the applied field. The apparent linearity observed in the corresponding NRM-TRM Arai-Nagata diagram has no geomagnetic significance (Goguitchaichvili et al., 1999b). A typical "concave-up" behavior was observed for sample Popo-3. Up to 500°C, important loss of NRM without any noticeable TRM acquisition and positive NRM-TRM checks is observed. This may correspond to irreversible motion of domain walls during the successive heating and cooling experiments (Levi, 1977). Alternatively, this behavior may result from irreversible variations of coercive force (Kosterov and Prévot, 1978) at low temperatures, and can be interpreted as transformation from a single-domain "metastable" state to multidomain state, which results in large NRM lost without any correlated pTRM acquisition.

Fourteen samples from four individual lava flows yielded acceptable paleointensity estimates (Table 3). For these samples the NRM fraction f used for determination ranges between 0.35 to 0.96, and the quality factor q varies from 3.4 to

46.9 (generally more than 6). The mean paleointensity values per flow range from 30.2 ± 7.3 to 46.9 ± 5.6 μT, and the corresponding Virtual Dipole Moments (VDM) range from 5.9 ± 0.9 to 9.2 ± 1.1 (10^{22} Am^2). Mean VDM obtained in this study is 7.2 ± 1.4 10^{22} Am^2, slightly lower than present-day value.

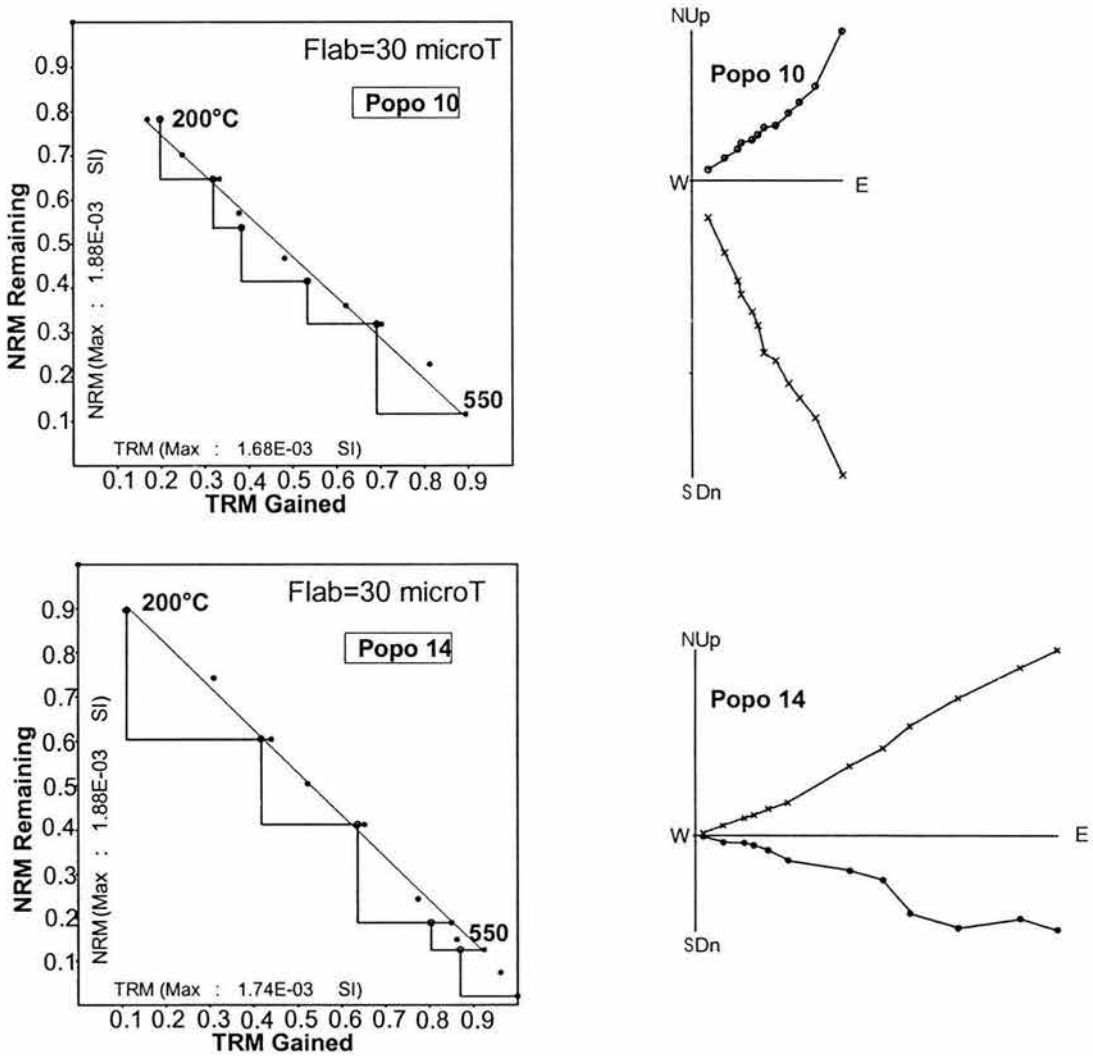

Fig. 11. Example of paleointensity determination data for a sample of site Popo-10 and Popo-14 from Popocatepetl stratovolcano. Diagrams on the left are the TRM-NRM Arai-Nagata plots; diagrams on the right are the corresponding vector thermal demagnetization plots.

Table 3

Site	*Specimen*	*Tmin-Tmax*	*N*	*f*	*g*	*q*	$F_E \pm \sigma(F_E)$	*VDM*	$F_E \pm$ *s.d.*	*VDMe*
P5	99P053A	400 - 560	7	0.75	0.76	15.4	38.4±1.4	8.78	**30.2 ± 7.3**	**6.9 ± 1.7**
	99P054A	400 - 560	7	0.66	0.76	8.4	27.8 ±1.8	6.36		
	99P055A	400 - 560	7	0.38	0.68	3.4	24.4 ± 4.4	5.58		
P9	99P092A	250 - 475	6	0.78	0.77	5.7	34.7 ± 5.3	7.02	**33.4 ± 3.6**	**6.8 ± 0.7**
	99P094A	200 - 540	9	0.88	0.84	16.1	29.3 ± 1.5	5.93		
	99P097B	250 - 475	6	0.61	0.79	6.5	36.1 ± 3.8	7.3		
P10	99P101A	200 - 540	9	0.59	0.85	6.1	35.8 ± 2.8	6.73	**31.2 ± 4.9**	**5.9 ± 0.9**
	99P102A	200 - 540	9	0.77	0.84	12.5	27.3 ± 1.7	5.14		
	99P106A	200 - 560	10	0.72	0.88	15.8	26.5 ± 1.1	4.99		
	99P108A	350 - 540	7	0.35	0.84	4.2	35.3 ± 2.6	6.64		
P14	99P142A	20 - 560	12	0.96	0.88	46.9	54.1 ± 0.9	10.6	**46.9 ± 5.6**	**9.2 ± 1.1**
	99P144A	200 - 540	9	0.62	0.87	10.7	42.8 ± 2.2	8.39		
	99P145A	200 - 540	9	0.66	0.86	10.4	42.1 ± 2.3	8.25		
	99P149A	200 - 560	10	0.83	0.88	24.4	48.9 ± 1.9	9.58		

Summary of Paleointensity Data for Volcanic Units of Popocatepetl Stratovolcano

Discussion

Rock-magnetic experiments reveal that remanence is carried in most volcanic units by Ti-poor titanomagnetites, resulting from oxy-exsolution during flow cooling. Unblocking temperature spectra and relatively high coercivities point to "small" pseudo-single domain magnetic grains for these (titano)magnetites. Single-component, linear demagnetization plots were detected in most cases. All studied sites yield normal polarity magnetization, which support an interpreted maximum age within the Brunhes chron, younger than 780 ka. Evidence of a strong lightning-produced magnetization overprint was detected for one site.

Combining the paleomagnetic data available for the lava flows of Popocatepetl stratovolcano (Table 2), we obtain a mean paleodirection with I=35.4°, D=345.7°, k=21, α_{95}=8.5°, N=15, which deviates counterclockwise from the present-day field direction. The cause for this declination discordance is not clear, because of the young age of the volcanic units and the concordant paleomagnetic directions observed in the nearby Iztaccihuatl stratovolcano. Individual flow mean paleomagnetic directions show high angular dispersion and some deviation from a Fisherian distribution (Fig. 10). Further studies of the volcanic units may help in determining any possible local structural or tectonic deformation in this part of the basin of Mexico.

The western boundary of the basin of Mexico is formed by the Sierra de las Cruces volcanic range. K-Ar dating studies in lava flows range from 3.71 Ma to 390 ka (Mora-Alvarez et al., 1991; Osete et al., 2000). K-Ar dates and magnetic polarity stratigraphy document an apparent southward migration of activity (with mean rates of 16 m/ka between 3.6 and 1.8 Ma and up to 40 m/ka during the Gauss chron). The mean direction determined is I = 30.6°, D = 350.7°, k = 30, α_{95} = 5.3°, N = 25. This direction deviates to the west of the expected direction, which may reflect a small tectonic rotation of the Sierra de las Cruces area in Plio-Quaternary times (Osete et al., 2000). In that study, it was also observed that the mean paleomagnetic directions for the northern and southern sectors of the volcanic range present different declinations but similar inclinations. Although they are statistically undifferentiated, there is a 9° difference between the oldest sector (D = 345.3°, ~3.7–2.8 Ma) and the younger section (D = 354.6°, ~2–0.7 Ma). Along the eastern limit of the Basin of Mexico, volcanic activity has similarly migrated southwards over time, and the active Popocatepetl lies south of the volcanic range. Southern migration of magmatic activity (i.e., towards the trench) characterizes the TMVB, suggesting a relationship with plate subduction and tectonics in southern and central Mexico. Further studies of volcanic units within and around the Basin of Mexico are required to illuminate the tectonic evolution of the basin.

Twenty-five samples were selected for Thellier palaeointensity experiments because of their stable remanent magnetization and reasonably reversible continuous thermomagnetic curves. Fourteen samples from four individual lava flows, yielded reliable paleointensity estimates with the flow-mean virtual dipole moments ranging

from 5.9 to 9.2 x 10^{22} Am^2 (Table 3). Results are of high technical quality and comparable to other paleointensity data recently obtained on younger lava flows. The NRM fractions used for paleointensity determination range from 35 to 96% and the quality factors vary between 3.4 and 46.9, being normally greater than 6. Mean VDM obtained in this study is 7.2 ± 0.4 x 10^{22} Am^2, which is slightly lower than present-day value (which is about 8 x10^{22} Am^2).

Relatively few Quaternary paleointensity determinations are available for comparison in the region of central Mexico. Alva-Valdivia et al. (2001) presented paleointensity results for volcanic units in Los Tuxtlas field, eastern Mexico. K-Ar dating indicates that units studied range from 2.2 Ma to 800 ka. VDM values range from 6.4 to 9.1 x 10^{22} Am^2. A mean VDM value, based on data from the Los Tuxtlas field and other coeval data, is 6.4 x 10^{22} Am^2, some 20% lower than the present-day value but within the range estimated for the past 5 Ma (Juarez and Tauxe, 2000). Morales et al. (2001) have recently reported paleointensity data for lava flows from the nearby Chichinautzin monogenetic volcanic field (southern part of the Basin of Mexico). The volcanic flows studied span the interval of about 390 to 2 ka (latest Pleistocene and Holocene). The virtual dipole moment values are higher, with a mean value of 11.8 ± 2.6 x 10^{22} Am^2. The flow unit paleointensities in that study vary from 25.9 to 61.4 μT, with a mean value of 49.7 ± 13.6 μT. The high values agree with other studies and paleointensity compilations that indicate high paleointensity at about 2000 years ago. The average paleointensity for the past 50 ka estimated from the Montpellier paleointensity database is around 6.5 ± 3.3 x 10^{22} Am^2 (ftp://ftp.dstu.univ-montp2.fr/pub/paleointb); see also the compilation by Perrin and Shcherbakov (1997) and Perrin et al. (1998). The mean value obtained in this study for the Popocatépetl stratovolcano units of 7.2 ± 0.4 x 10^{22} Am^2 is slightly higher than the mean value for the past 50 k.y., but is of the same order of magnitude as the average field for the 300 ka to 5 Ma interval (Perrin and Shcherbakov, 1997; Juarez and Tauxe, 2000).

Acknowledgments

We thank E. Hernandez for assistance with the ICP-MS analyses, and M. Espinosa for field and laboratory assistance in the paleomagnetic study. Useful comments and assistance with the Popocatépetl volcano project were provided by Dr. A. Kosterov. The Secretaria de Relaciones Exteriores, Mexico provided a student scholarship (Gennaro Conte). We acknowledge partial support for this project from CONACYT grant J32727-T and DGAPA-UNAM project IN-116201.

References

Alva-Valdivia, L., Goguitchaichvili, A., Urrutia-Fucugauchi, J., Further constraints for the Plio-Pleistocene geomagnetic field strength: New results from the Los Tuxtlas volcanic field (Mexico). *Earth Planets Space*, 53, 873-881, 2001.

Arciniega-Ceballos, A., Chouet, B., Dawson, P., Very long-period signals associated with vulcanian explosions at Popocatepetl volcano, Mexico. *Geophys. Res. Lett.*, 26, 3013-3016, 1999.

Arciniega-Ceballos, A., Chouet, B., Dawson, P., Long-period events and tremor at Popocatepetl volcano (1994-2000) and their broadband characteristics. *Bull. Volcanol.*, 65, 124-135, 2000.

Boudal, C., Robin, C., Relation entre dynamismes eruptifs et realimentation magmatiques d'origin profonde au Popocatepetl. *Canadian J. Earth Sci.*, 25, 955-971, 1987.

Carrasco-Nuñez, G., Silva, L., Delgado-Granados, H., Urrutia-Fucugauchi, J., 1986. Geologia y paleomagnetismo del Popocatepetl. Comunicaciones Tecnicas Publ. Ser. Inv. Inst. Geofis., UNAM, 33, 1986.

Coe, R., Gromme, S., Mankinen, E.A., Geomagnetic paleointensity from radiocarbon-dated flows on Hawaii and the question of the pacific nondipole low. *J. Geophys. Res.*, 83, 1740-1756, 1978.

Day, R., Fuller, M., Schmidt, V.A., Hysteresis properties of titanomagnetites: grain size and compositional dependence. *Phys. Earth Planet. Inter.*, 13, 260-267, 1977.

Dunlop, D.J., Ozdemir, O., Rock-Magnetism, Fundamentals and Frontiers. *Cambridge University Press*, 573 pp, 1997.

Evensen, N.M., Hamilton, P.J., O Nions, R.K., Rare earth abundances in chondritic meteorites. *Geochim. Cosmochim. Acta*, 42, 1190-1212, 1978.

Goguitchaichvili, A., Prevot, M., Camps, P., No evidence for strong fields during the R3-N3 Icelendic geomagnetic reversals. *Earth Planet. Sci. Lett.*, 167, 15-34, 1999a.

Goguitchaichvili, A., Prevot, M., Dautria, J.M., Bacia, M., Thermo-detrital and crystalline magnetizations in an Icelandic hyaloclastite. *J. Geophys. Res.*, 104, 29,219-29,239, 1999b.

Goguitchaichvili, A., Prevot, M., Camps, P., Urrutia-Fucugauchi, J., On the features of the geodynamo following reversals or excursions by absolute geomagnetic paleointensity data. *Phys. Earth Planet. Inter.*, 124, 81-93, 2001.

Gonzalez-Huesca, A., Delgado-Granados, H., Urrutia-Fucugauchi, J., The San Nicolas lahar at Popocatepetl volcano (Mexico): A case study of a glacier-melt related debris flow triggered by a blast at the outset of a Plinian eruption. *Proc. IAVCEI Assembly*, Puerto Vallarta, p. 94, 1997.

Govindaraju, K., Compilation of working values and sample description for 272 geostandards. Geostandard Newsletter, 13, 1-113, 1987.

Heine, K., Late Quaternary glacial chronology of the Mexican volcanoes. *Die Geowissenschaften*, 6/7, 197-205, 1988.

Juarez, T., Tauxe, L., The intensity of the time averaged geomagnetic field the last 5 Myr. Earth Planet. Sci. Lett., 175, 169-180, 2000.

Kirschvink, J.L., The least-square line and plane and analysis of palaeomagnetic data. *Geophys. J. R. Astr.* Soc., 62, 699-718, 1980.

Kosterov, A., Prevot, M., Possible mechanisms causing failure of Thellier paleointensity experiments: results of rock-magnetic study of the Lesotho basalts, South Africa. *Geophys. J. Int.*, 134, 554-572, 1999.

Levi, S., The effect of magnetite particle size on paleointensity determination of the geomagnetic field. *Phys. Earth Planet. Inter.*, 13, 245-259, 1977.

Mora-Alvarez, G., Caballero, C., Urrutia-Fucugauchi, J., Uchiumi, S., Southward migration of volcanic activity in the Sierra de las Cruces, basin of México? A preliminary K-Ar dating and paleomagnetic study. *Geofis. Int.*, 30, 61-70, 1991.

Morales, J., Goguitchaichvili, A., Urrutia-Fucugauchi, J., A rock-magnetic and paleointensity study of some Mexican volcanic lava flows during the Latest Pleistocene to the Holocene. *Earth Planets Space*, 893-902, 2001.

Nagata, T., Arai, Y., Momose, K., Secular variation of the geomagnetic total force during the last 5000 years. *J. Geophys. Res.*, 68, 5277-5281, 1963.

Nixon, G.T., The geology of Iztaccihuatl volcano and adjacent areas of the Sierra Nevada and Valley of Mexico. *Geol. Soc. Am. Sp. Pap.*, 219, 58 pp, 1989.

Osete, M.L., Ruiz-Martinez, V.C., Caballero, C., Galindo, C., Urrutia-Fucugauchi, J., Tarling, D.H., Southward migration of continental volcanic activity in the Sierra de las Cruces, Mexico: palaeomagnetic and radiometric evidence. *Tectonophysics*, 318, 201-215, 2000.

Ozdemir, O., Dunlop, D.J., Muskowitz, M., The effect of oxidation on the Verwey transition in magnetite. *Geophys. Res. Lett.*, 20, 1671-1674, 1993.

Panfil, M.S., Gardner, T.W., Hirth, K.G., Late Holocene stratigraphy of the Tetimpa archaeological sites, northeast flank of Popocatepetl volcano, central Mexico. *Geol. Soc. Am. Bull.*, 111, 204-218, 1999.

Perrin, M., Shcherbakov, V.P., Paleointensity of the Earth magnetic field for the past 400 My: evidence for a dipole structure during the Mesozoic low. *J. Geomag. Geoelectr.*, 49, 601-614, 1997.

Perrin, M., E. Schnepp, V. Shcherbakov, Paleointensity database updated. *EOS* 79, 198, 1998.

Prevot, M., Mankinen, R.S., Gromme, S., Lecaille, A., High paleointensit of the geomagnetic field from thermomagnetic studies on rift valley pillow basalts from the middle Atlantic ridge. *J. Geiophys. Res.*, 88, 2316-2326, 1983.

Radhakrishnamurty, C., Likhite, S.D., Deutsch, R., Murthy, G.S., On the complex magnetic behaviour of titanomagnetites. *Phys. Earth Planet. Inter.*, 30, 281-290, 1981.

Robin, C., Le Volcán Popocatépetl (Mexique): structure, evolution pétrologique et risques. *Bull. Volcanol.*, 47, 1-23, 1984.

Robin, C., Boudal, C., A gigantic Bezymiani-type event at the beginning of modern volcan Popocatepetl. *J. Volcanol. Geoth. Res.*, 31, 115-130, 1987.

Siebe, C., Abrahms, M., Macias, J.L., Obenholzner, J., Repeated volcanic disasters in prehispanic time at Popocatepetl, central Mexico: past key to the future? *Geology*, 24, 399-402, 1996.

Tauxe L., Mullender T.A.T., Pick T. (1996) Pot-bellies, wasp-waists and superparamagnetismo in magnetic hysteresis. *Journal of Geophysical Research,* V. 95, pp. 12337-12350.

Thellier, E., Thellier, O., Sur l'intensité du champ magnétique terrestre dáns le passé historique et géologique. *Ann. Geophys.*, 15, 285-376, 1959.

Urrutia-Fucugauchi, J., Constraints on Brunhes low-latitude paleosecular variation – Iztaccihuatl stratovolcano, basin of Mexico. *Geofis. Int.*, 34, 253-262, 1995.

Urrutia-Fucugauchi, J., Flores Ruiz, J.H., Bouguer gravity anomalies and regional crustal structure in central Mexico. Int. Geol. Rev., 38, 176-194, 1996.

Urrutia-Fucugauchi, J., Radhakrishnamurty, C., Negendank, J.F.W., Magnetic properties of a columnar basalt from central Mexico. *Geophys. Res. Lett.*, 11, 832-835, 1984.

Wallace, P.J., Carmichael, I.S.E., Quaternary volcanism near the Valley of Mexico: implications for subduction zone magmatism and the effects of crustal thickness variations on primitive magma compositions. *Contrib. Mineral. Petrol.*, 135, 291-314, 1999.

Waitz, P., Popocatepetl again in activity. *Am. J. Sci.*, 5th Ser., 1, 81-85, 1921.

Paleomagnetism of Michoacan-Guanajuato Volcanic Field, Central Mexico: Implications for the Paleosecular Variation of the Earth's Magnetic Field at Low Latitudes

G. Conte[1], J. Urrutia-Fucugauchi[1], A. Goguitchaichvili[1]

[1] Laboratorio de Paleomagnetismo y Geofisica Nuclear, Instituto de Geofisica, Universidad Nacional Autonoma de Mexico, Ciudad Universitaria, 04510 México D.F., MEXICO

Submitted: Physics of the Earth and Planetary Interiors.

Abstract

We report detailed rock-magnetic, paleomagnetic and paleointensity studies of 24 Plio-Quaternary volcanic units from the Michoacan-Guanjuato volcanic field (MGVF). The MGVF belongs to Trans-Mexican volcanic belt (TMVB) and is formed by over 1000 volcanic centers (almost 90% of them are cinder cones). Rock magnetic experiments show that remanence is carried in most of cases by Ti-poor titanomagnetites, resulting from oxy-exsolution of original titanomagnetite during flow cooling. Unblocking temperature spectra and high coercivities point to "small" pseudo-single domain magnetic grains for the titanomagnetites. Single component, linear demagnetization plots were observed in most cases. Seven sites yield reverse polarity magnetization while fifteen volcanoes are normally magnetized. The mean paleodirection obtained in this study is I=28.4°, D=357.9°, k=21, α_{95}=7.3°, with a mean paleomagnetic pole position P_{lat}=85.7°, P_{long}=104.5°, K=27, α_{95}=6.4°. Site-mean directions are undistinguishable from the expected Plio-Quaternary paleodirections, as derived from reference poles for the North American polar wander curve and previously reported paleodirections for TMVB. Absolute paleointensities obtained from twelve samples from two sites gave values close to the present geomagnetic field strength. The combination of new results obtained in this study with all currently available paleomagnetic data from central Mexico yield S_F=13.0 with S_U=14.5 and S_L=11.8 (statistical parameters to estimate the dispersion of virtual geomagnetic poles) for the last 70,000 years, which are in good agreement with the latitude-dependent PSV model of McFadden (1988, 1991) for the last 5 Ma.

Key Words: *Paleomagnetism, Geomagnetic Secular Variation, Quaternary, Central Mexico*

Introduction

Detailed knowledge of the full vectorial variation of the geomagnetic field is important to obtain information on the geodynamo. Variations of Earth's magnetic field which are manifested slowly through the years are called paleosecular variations (PSV) and are known from direct instrumental measurements since the 16th century, when observatory records initiated. Direct observations show that the direction and magnitude of the non-dipolar field is irregularly distributed over the Earth's surface; variation of the field is larger in the southern hemisphere than in the northern hemisphere, and completely lacking in the central Pacific Ocean region (Doell and Cox, 1972). In order to extend the knowledge of the paleosecular variation over time scales larger than observatory records two potential datasets may be used: paleomagnetic records obtained from sedimentary and volcanic rocks of known age. Sediments can provide semi-continuous records of magnetic field variation, but problems with remanence acquisition mechanism and diagenetic process may affect the signal. Data obtained from lavas, while providing spot readings, are not subject to the controversies over reliability that make interpretation of sedimentary data so difficult (Tauxe, 1993; Dunlop and Özdemir, 1997; Love, 2000). Moreover, volcanic data can yield, in some cases, absolute intensities, while sedimentary data can only give relative intensity variation.

A simple method to estimate the PSV comes from calculation of the angular standard deviation (ASD) of virtual geomagnetic poles (VGPs) for a given locality. This method is widely used because there are several models of combination of dipole and non-dipole components that predict the ASD characteristic of PSV with latitude (McFadden et al., 1988, 1991). Doell and Cox (1971) and later McWilliams et al. (1982) observed, in the zone of the Pacific Ocean around the Hawaii islands, a low angular dispersion of the VGPs during the past 800 ka or more, and proposed the presence of a low non-dipole field in the central Pacific. Later, Doell and Cox (1972) observed that this low non-dipole field correlates with that calculated from the International Geomagnetic Reference Field (IGRF) for 1945 for the western and central parts of Mexico, and suggested that the low non-dipole field anomaly of central Pacific extended to this region (including the Trans-Mexican volcanic belt).

The U.S.-Japan Paleomagnetic Cooperation Program in Micronesia (1975) supported this conclusion and considered that a global belt of low average angular dispersion encircles the Earth between 0° and 40° north. Steele (1985) and Herrero-Bervera et al. (1986) tested this conclusion for recent part of Brunhes chron. They investigated the PSV for central Mexico from recent volcanic rocks and concluded than the ASD was in agreement with the value predicted from PSV model and that Mexico was not part of low non-dipole field. Bohnel et al. (1990) revised this conclusion and found the PSV for central Mexico lower than the PSV models, similar to value for Hawaii and that the difference with the study of Herrero-Bervera et al. (1986) was due to the selection criteria applied to the data set (Urrutia-Fucugauchi, 1997).

However, low ASD estimates may occur when paleomagnetic data set cover a short interval, when VGPs data are not part of Fisherian distributions at 95% probability level, when additional dispersion sources such as tectonic effects or geomagnetic excursions are present (McFadden, 1980), or for different cut-off angle selection procedures.

In the present study, we have studied in detail 24 monogenetic volcanic centers of the Michoacan-Guanajuato volcanic field erupted between 2.27 Ma to present according to the available radiometric ages. In addition, we re-examined previously published data and a new updated paleomagnetic database for central Mexico is presented. The principal objective of this study is to estimate the paleosecular variation of geomagnetic field for the region.

Geological Setting and Sampling

The Michoacan-Guanajuato volcanic field is located in the west-central part of the Trans-Mexican volcanic belt. The TMVB is related to the subduction of the Cocos and Rivera plates beneath the southwestern margin of the North American plate. The basal units of the TMVB are late Miocene, and in the western sector cover rocks of the Oligocene to early Miocene Sierra Madre Occidental silicious volcanic province. TMVB is a 20-150 km wide, 1,000 km long and about 2,000 m high volcanic plateau, which roughly extends from the coast of the Pacific to the Gulf of Mexico; it includes high stratovolcanoes (e.g. Popocatépetl, Colima, Pico de

Orizaba), shield volcanoes (e.g., Cerro Paracho, Cerro Culiacan, Cerro Yahuarato) monogenetic cinder cones (e.g., Paricutin and Jorullo) and silicic calderas. Unlike typical trench-arc systems, the TMVB is not parallel to the Middle America Trench (MAT), but forms an angle of about 20° (Molnar and Sykes, 1969; Urrutia-Fucugauchi and Castillo, 1977) (Figure 1). From the geochemical studies, the TMVB is a province of both calc-alkaline and alkaline composition, which accounts for the occurrence of dacitic, andesitic, and basaltic rocks (Aguilar-Vargas and Verma, 1987). The construction of andesitic centers in the western part of the TMVB that lie above the subducted portion of the Rivera plate started between 0.6 and 0.2 Ma (Nixon et al., 1987). However, in the central and eastern parts of the arc, where the Cocos plate is subducting, andesite-dacite volcanoes began considerably earlier, at approximately 1.7 Ma (Nixon et al., 1987). In addition to the TMVB products, volcanic rocks in central Mexico includes those eastern alkaline province of Oligocene to Quaternary age, andesitic and rhyolitic ignimbrites of Sierra Madre Occidental of Oligocene to Miocene age, and Californian province (Demant and Robin, 1975) (Figure 1).

The western portion of the TMVB can be subdivided into three rift systems: 1) Tepic-Zacoalco graben trending NW-SE 2) Colima graben which has an N-S orientation and 3) the Chapala rift trending E-W (Figure 1). The Michoacán-Guanajuato Volcanic Field is localized to the east of the Chapala Lake, which marks the axis of the Chapala rift. The geographic boundaries of the Michoacan volcanic zone are delineated by the 18°45' and 20°15' parallels and the 100°25' and 100°45' meridians. The MGVF, with an area of 40,000 km^2, contains over 1,000 small-size monogenetic volcanoes including: cinder cones (90%), maars, tuff rings, lava domes, and lava flows with hidden vents; most centers are calc-alkaline, but alkaline and transitional rocks are also found (Hasenaka, 1994; Hasenaka et al., 1994).

Cinder cone lavas have a wide compositional range from 47 to 65% SiO_2, calc-alkaline to alkaline, among wich cal-alkaline olivine basalt or olivine basaltic andesite; most of them (75%) are distributed in an area between 200 km and 300 km of distance from the MAT (Figure 2) (Hasenaka 1990, Hasenaka, 1994; Hasenaka and Carmichael, 1985). The median cinder cone has a height of 90 m, a basal

diameter of 800 m, a crater diameter of 230 m, and a volume of 0.021 km^3 (Hasenaka and Carmichael, 1985). In general, cinder and lava cones are active for a short period of time, of a few months to tens years and rarely the activity restarts. Two cinder cones were born in historic times; the Paricutín in 1943-1952 (Luhr and Simikin, 1993) and the Jorullo in 1759-1774 (Luhr and Carmichael, 1985).

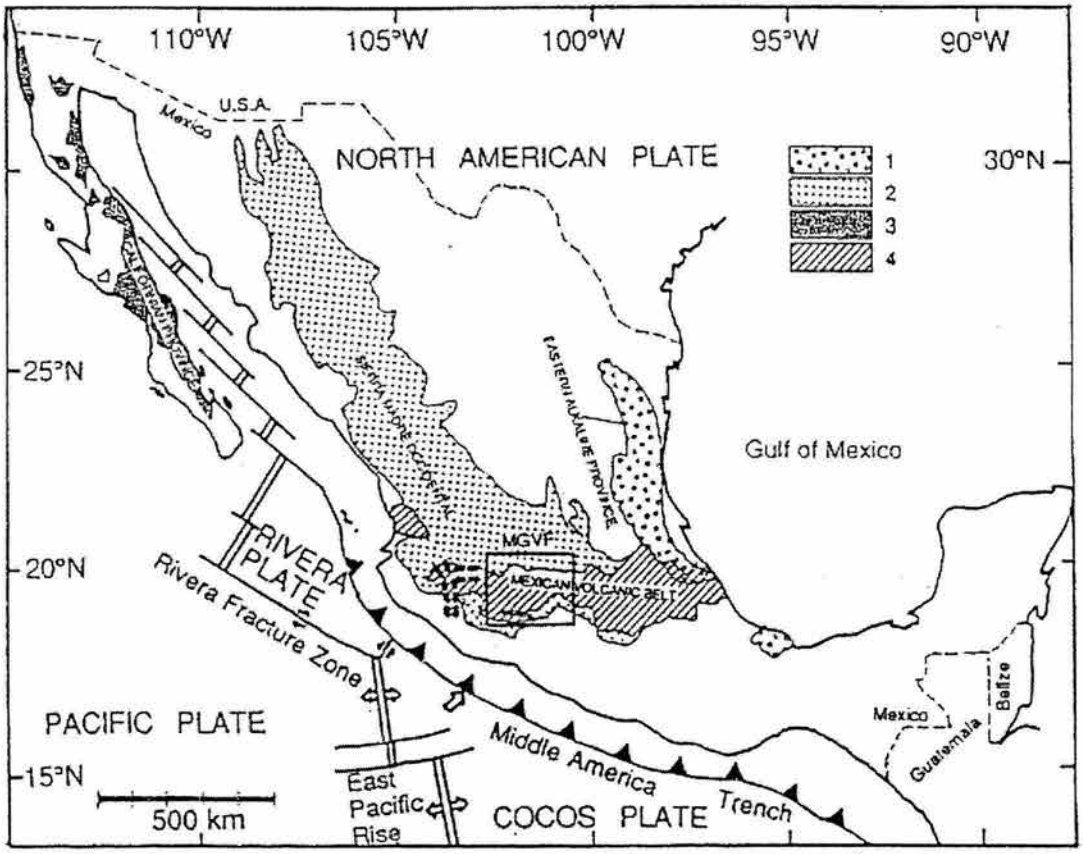

Fig. 1 Main volcanic provinces of Mexico: 1) Eastern Alkaline Province; 2) Sierra Madre Occidental; 3) Baja Californian Province; 4). Trans-Mexican volcanic belt. Inset of the MGVF is shown as a rectangle. (adapted from Ban et al., 1992)

In addition to the small monogenetic volcanoes, there are about 300 medium-sized volcanos that have mainly erupted calc-alkaline andesites with the majority of lavas falling in the SiO_2 range between of the 55% to 61% (Hasenaka, 1994). This medium-sized volcanoes represent principally Icelandic-type (Ban et al., 1992). These shield volcanoes, were built during an essentially continuous discharge from a central vent, and thus are also monogenetic volcanoes (Ban et al., 1992).

Geomorphologically the lava flows associated to medium-sized volcanoes are older than those from cinder cones, thus they are possible precursors to the small-sized volcanoes (Hasenaka, 1994).

Six cinder cones have been dated by the ^{14}C method yielding an age between 3,800-29,000 yr BP, and other 71 cones seem to correspond to the same time interval (probably within the last 40,000 yr BP) judging from the degree of erosion. These young volcanoes occur mostly in the southern half of the volcanic field (Hasenaka and Carmichael, 1985, 1987). Ban et al. (1992) have dated eight medium-sized shield volcanoes and one stratovolcano, reporting ages between 0.06 Ma and 2.27 Ma, while Nixon et al. (1987) have dated other three shield volcanoes (0.87-2.60 Ma).

Both the small and medium sized volcanic centers have a similar distribution in space. However the medium-sized centers are more frequent in the northern part of the MGVF than small-sized cones, while the cinder cones in the north are older (>40,000 years) than those in the south, suggesting a southern migration of the eruptive activity. This migration has occurred in the last 1 Ma, probably in response to changes in plate motions (Ban et al., 1992)

The MGVF is ideal to extract information on the secular variation of the geomagnetic field, because the life of the monogenetic volcanoes is of few years to 20 years, therefore each of them presents little dispersion of the direction of the geomagnetic field. Our sampling strategy was largely conditioned by previous studies over area, since we tried to sample only the volcanoes with available radiometric dates (Figure 3). The names of the studied volcanoes and ages are listed in Table 1. We note that for six volcanic centers only relative ages can be estimated roughly based on paleomagnetic directions and their location within MGVF. Cerro Cainjuata, Cerro Urujuato and Cerro Gordo, yielded normal paleodirections (see below) suggesting that "probably" were formed during Bruhnes chron. Moreover the first two are situated in south of the TMVB and then are considered <40,000 years (see Ban et al., 1992), while Cerro Gordo situated in northern is probably between 40 ka to 0.78 Ma. El Fresno and Cerro Grande both yielded reversed paleodirections and suggested that they probably are formed during Matuyama chron. The new radiometric (K-Ar) date of one of these volcanic centers (El Estribo volcano), yielded

an age 25±4 ka (Hervé Guillou, personal communication 2003) (Stéphane Scaillet and Hervé Guillou, 2004).

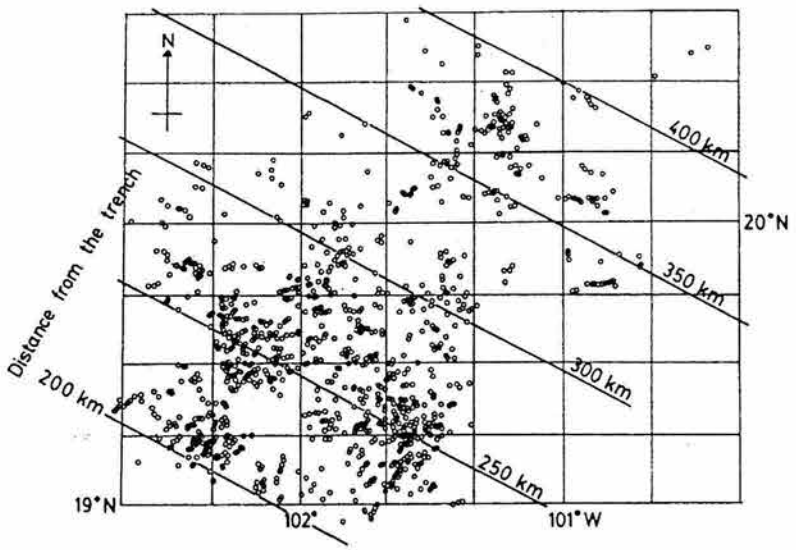

Fig. 2 Distribution of small-sized monogenetic volcanoes (circles) in the Michoacán-Guanajuato volcanic field. The majority of cinder cones (75%) are distributed between 200 km and 300 km of distance from Middle America Trench (adapted from Hasenaka and Carmichael, 1985).

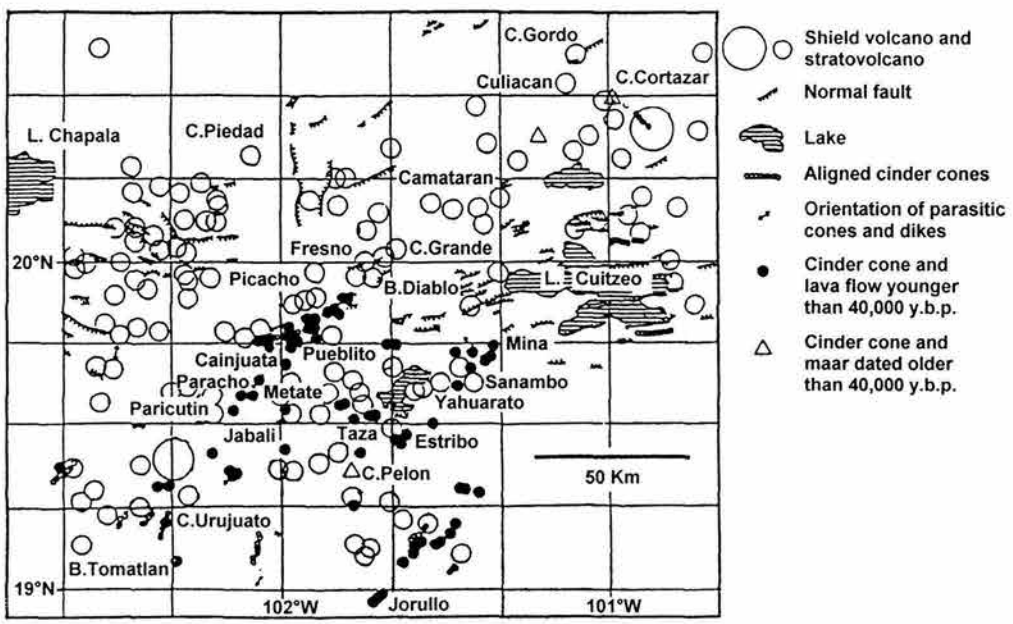

Fig. 3 Schematic map showing the location of the volcanoes sampled on Michocán-Guanajuato Volcanic field (base map adapted from Ban et al., 1992).

Table 1

Site	*Coordinates* (°N)	(°W)	*Age*	*n/N*	*Dec.(°)*	*Inc.(°)*	*K*	α_{95}(°)	*Plat.*	*Plog.*	*Pol.*	*Ref. Age*
19-Paricutin*	19.53	102.25	1943-1945 AD	7/9	47.3	27.5	7.3	70	63.4	322.9	N	2
24-El Jorullo	19.00	101.75	1759-1774 AD	7/8	354.7	58.8	4.7	165	68.9	246.9	N	2
21-El Jabalí	19.42	102.13	3.83±0.15 Ka	6/10	349.5	26.1	2.2	898	78.4	140.1	N	2
18-El Metate	19.57	102.02	4.7±0.2 Ka	8/11	16.1	24.6	1.9	816	73.2	8.9	N	2
15-La Taza	19.53	101.69	8.43±0.33 Ka	10/10	336.6	30.3	4.2	134	67.6	163.7	N	2
11-La Mina	19.70	101.40	17.17±0.43 Ka	8/8	345.5	4.6	2.2	633	67.5	119.6	N	2
14-El Estribo*	19.52	101.66	25±4 Ka	5/7	303.9	29.6	5.9	170	36.7	173.9	N	4
8-El Pueblito	19.82	101.92	29±3.3 Ka	8/9	21.6	33.7	3.2	306	69.6	348.4	N	2
16-Cerro Cainjuata	19.66	102.03	< 40 Ka	11/11	6.8	40.6	2.5	346	82.7	317.4	N	4
22-Cerro Urujuato	19.00	102.20	< 40 Ka	13/13	337.5	16.5	2.1	403	65.8	144.9	N	4
2-Cerro Gordo	20.40	100.97	>40 Ka (Brunhes)	8/12	5.3	33.0	5.9	88	84.4	13.6	N	4
17-Cerro Paracho	19.62	102.07	60±10 Ka	8/10	15.7	23.3	3.8	211	73.2	11.9	N	1
7-El Picacho	19.82	101.95	170±30 Ka	9/10	349.5	17.3	4.4	140	75.0	122.4	N	1
20-El Pelon	19.30	101.92	370±50 Ka	7/11	347.8	24.2	7.7	63	76.5	140.4	N	2
23-Buenavista Tomatlan	19.14	102.55	540±80 Ka	12/12	2.61	17.2	2.5	292	79.3	63.4	N	1
13-Yahuarato	19.62	101.57	540±70 Ka	6/10	183.5	-29.4	2.2	950	-84.9	217.2	R	1
12-Cerro Sanambo	19.63	101.44	870±50 Ka	12/12	181.3	-23.0	3.3	177	-82.3	248.9	R	3
4-Cerro Camataran*	20.19	101.52	1.17±0.14 Ma	5/13	164.9	-38.1	22.3	13	-75.9	355.9	R	1
5-Cerro Grande	20.10	101.59	>40 Ka (Matuyama)	10/12	200.8	-42.3	5.3	83	-70.3	151.8	R	4
10-El Fresno	19.94	101.77	>40 Ka (Matuyama)	8/11	182.9	-3.6	2.7	430	-71.6	248.7	R	4
6-Cerro Grande La Piedad	20.33	102.10	1.60±0.10 Ma	9/11	165.9	-45.1	4.7	122	-75.6	16.5	R	3
9-Brinco del Diablo	19.91	101.75	1.88±0.24 Ma	11/12	348.3	26.9	1.7	722	77.5	143.3	N	1
3-Cerro Culiacán	20.33	101.01	2.10±0.24 Ma	9/10	170.7	-35.6	6.6	62	-80.6	346.6	R	1
1-Cerro Grande Cortazar*	20.40	100.88	2.27±0.27 Ma	/	/	/	/	/	/	/	/	1
Mean			0-2.10 Ma	20	357.9	28.4	7.3	21	85.7	104.5		

Site mean paleodirections of cleaned remanence and corresponding VGP positions for MGVF volcanics. N: number of treated samples, n: number of specimens used for calculation, Dec: Declination, Inc: Inclination, k and α_{95}: precision parameter and radius of 95% confidence cone of Fisher statistics, Plat/Plong: Latitude/Longitude of VGP position. Sites are listed in stratigraphic order.
* Sites not included in calculation of overall mean direction.

1: Ban et al., (1992)
2: Hasenaka and Carmichael (1985)
3: Nixon et al., (1987)
4: This study

Rock Magnetic Properties

Rock magnetic measurements were carried out to identify the magnetic minerals present and potential responsible for remanent magnetization and to obtain information about their paleomagnetic stability. These experiments included: a) Continuous measurement of susceptibility vs T curves, b) IRM (isothermal remanent magnetization) acquisition experiments, and c) Hysteresis measurements.

Susceptibility vs Temperature

These experiments were carried out using a Bartington susceptibility meter MS-2 equipped with a furnace. Curie points were determined using Prevot et al.'s (1983) method. One sample per site was heated up to 600°C at a rate 10°C/min, and then cooled at the same rate (Figure 4). In most of cases the samples show the presence of a single magnetic/ferrimagnetic phase with Curie temperature (Tc) between 530-580°C, compatible with the low-Ti titanomagnetite. We note that in some cases, the cooling and heating curves are not perfectly reversible (sample M203). Few samples show two different thermomagnetic phases during heating (sample M25). The lower Curie point ranges between 250-350°C, and the higher one is about 550-580°C. The cooling curve of this sample shows only a single phase, compatible with magnetite. This behavior can be explained by transformation of titanomaghemite into magnetite during heating (Özdemir et al., 1993). In a single case (sample M97), the curve yields evidence of two ferrimagnetic phases during heating and cooling. Both Ti-rich and Ti-poor titanomagnetites seem to co-exist in this lava flow.

Hysteresis measurements

Hysteresis measurements at room temperature were carried out on all studied samples using the AGFM 'Micromag' system in fields up to 1.4 Tesla. The hysteresis parameters (saturation remanent magnetization M_r, saturation magnetization M_s, and coercive force H_c) were calculated after correction for the paramagnetic contribution. Coercivity of remanent (H_{cr}) was determined by applying a progressively increasing back-field after saturation. Near the origin no potbellied and wasp-waisted behaviors (Tauxe et al., 1996) were detected, which probably reflects very restricted range of the grains coercivities (Figue 5).

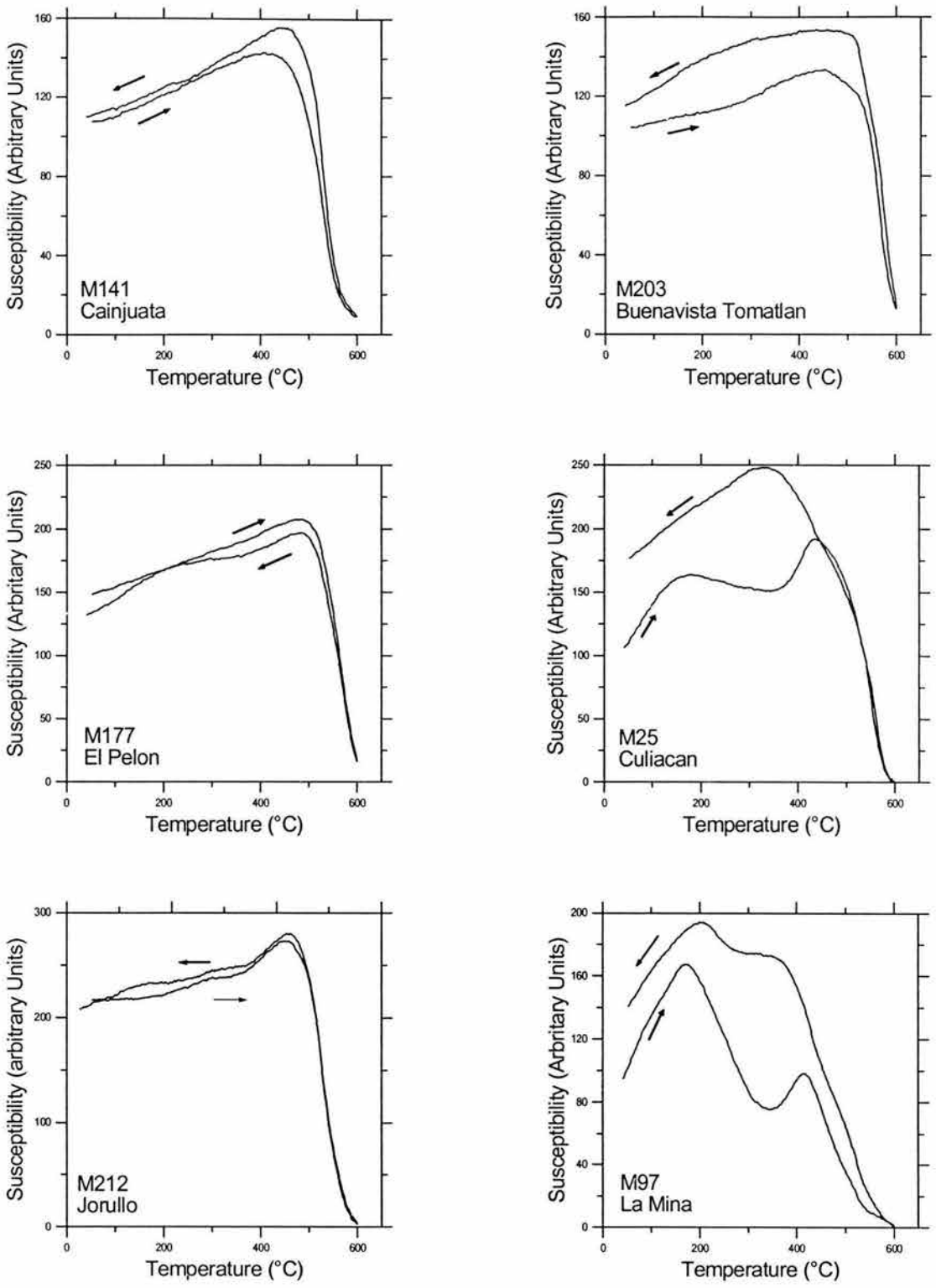

Fig. 4 Susceptibility vs. temperature (in air) curves of representative samples. Arrows indicate the heating and cooling curves.

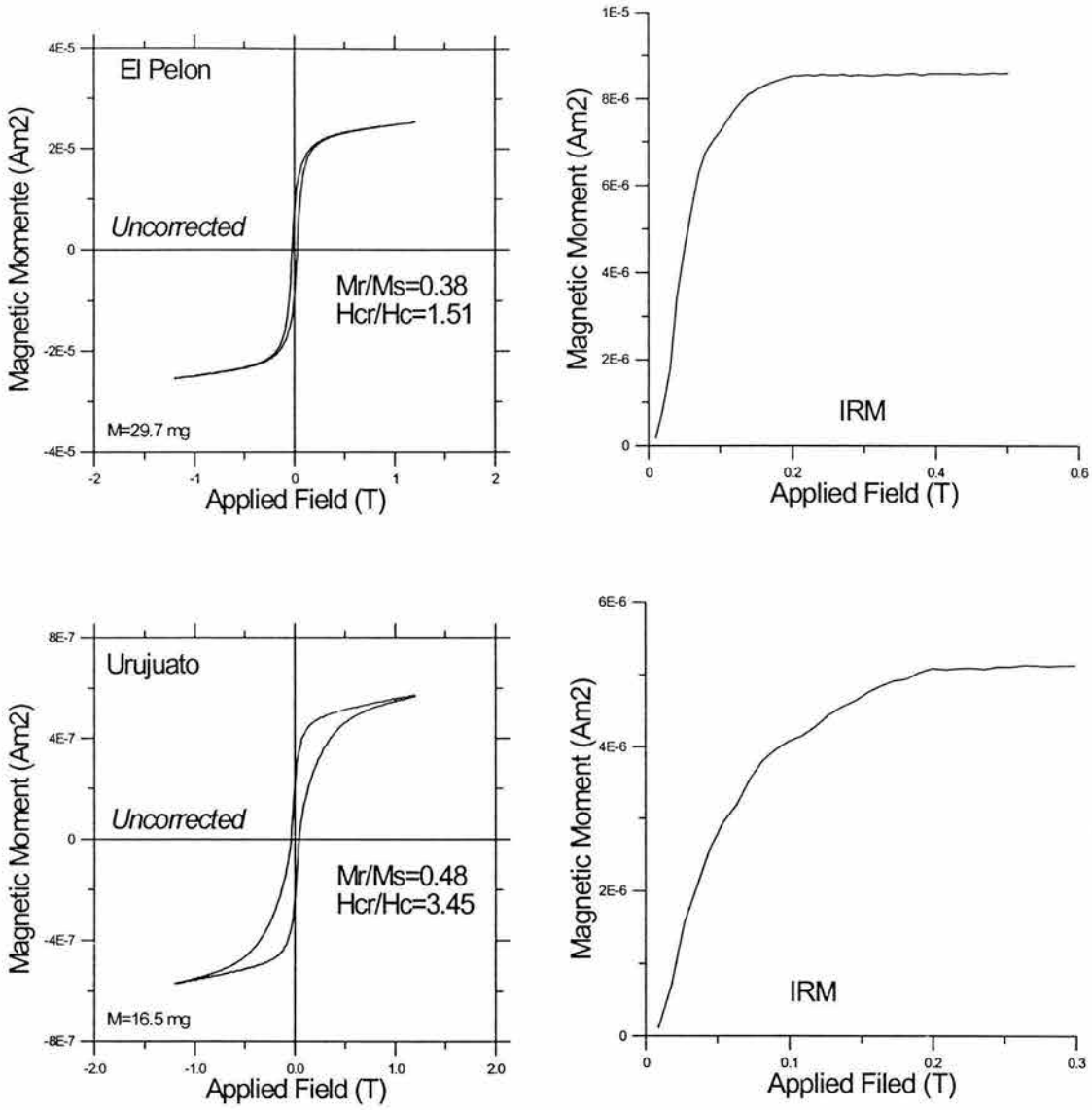

Fig. 5 Typical example of hysteresis loop (uncorrected) and associated IRM acquisition curves (see also text for further explanation).

Only exception is site Urujuato (M22) that shows typical wasp-waisted behavior. Most probably this behavior is due to presence of dominantly single domain (SD) and superparamagnetic grains (SP) (Tauxe et al., 1996). IRM (Isothermal Remanent Magnetization) intensity curve indicate, that the saturation is reached in low/moderate fields of the order of 100-200 mT (e.g. El Plon). This suggests that a spinel phase

(titano)magnetite and/or (titano)maghemite is the main remanence carrier. Judging from the ratios of the hysteresis parameters (H_{cr} / H_c ranges between 1.02 and 3.45 and M_r / M_s varies from 0.13 to 0.58), it seems that all samples fall in the pseudo-single-domain (PSD) grain size region (Day et al., 1977), probably indicating a mixture of multidomain (MD) and a significant amount of SD grains (Figure 6).

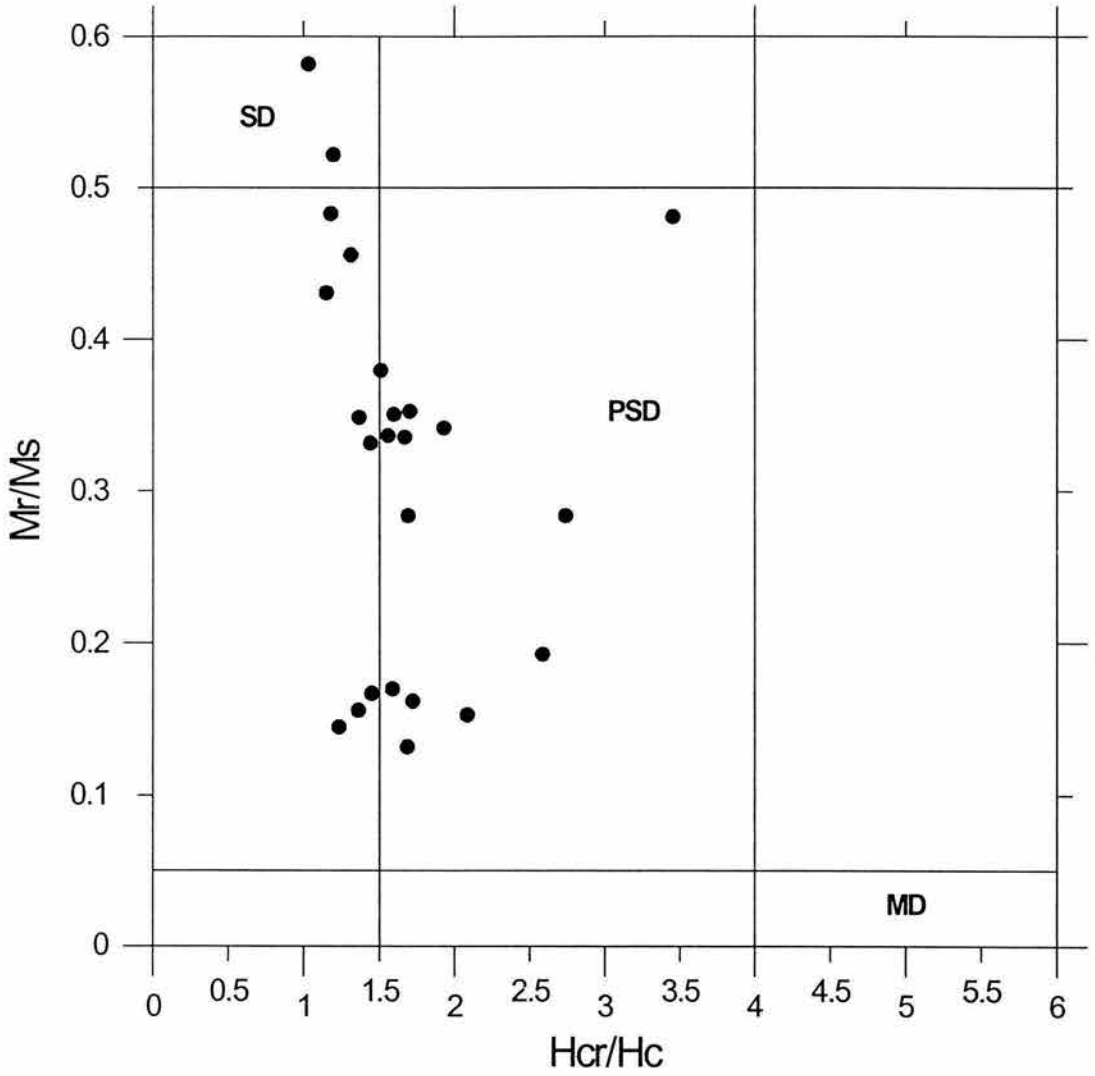

Fig. 6 Day plot (Day et al., 1977) with the hysteresis parameters ratios.

Paleodirections

Laboratory procedures

The intensity and direction of natural remanent magnetization (NRM), of 6 to10 samples from each unit, were measured with a JR-5A spinner magnetometer (sensitivity~10^{-9} Am^2). Both alternating field (AF) demagnetization up to 100 mT peak fields using a *Molspin* AF-demagnetizer, and stepwise thermal demagnetization up 575-675°C using a non-inductive Schonstedt furnace were carried out to investigate the vectorial composition and stability of NRM.

Demagnetizations

In total, 240 specimens were subjected to magnetic cleaning. In general, a single stable paleomagnetic component was recognized (Figure 7). A small secondary component, which is probably a viscous overprint, is sometimes present and easily removed by heating to 200-300° C or applying 10-20 mT. Few samples (e.g. El Pelon in Figure 7) show evidence for strong secondary magnetizations, which was removed about 500°C. Most of the remanent magnetization is removed at temperature below 520°C, this temperature indicate, once again, that low-Ti titanomagnetites is the main remanence carrier. The median destructive fields (MDF) range between (30-40 mT) pointing to small PSD grains as remanence carriers (Dunlop and Özdemir, 1997).

Results

The characteristic remanent magnetization (ChRM) was determined by the least-squares principal component analysis (PCA) method (Kirschvink, 1980), 4 to 9 points being taken for this determination. The obtained directions were averaged and statistical parameters calculated assuming a Fisher distribution (Fisher, 1953). Results for all 24 sites are summarized in Table 1. Seven sites yielded reverse polarity magnetizations and 16 sites are of normal magnetization (Figure 8). One site (Cerro Grande de Cortazar) was characterized by high NRM intensity (more that several hundred A/m) and scattered NRM direction probably due to the lightning. All samples from this site were excluded from further paleomagnetic analysis.

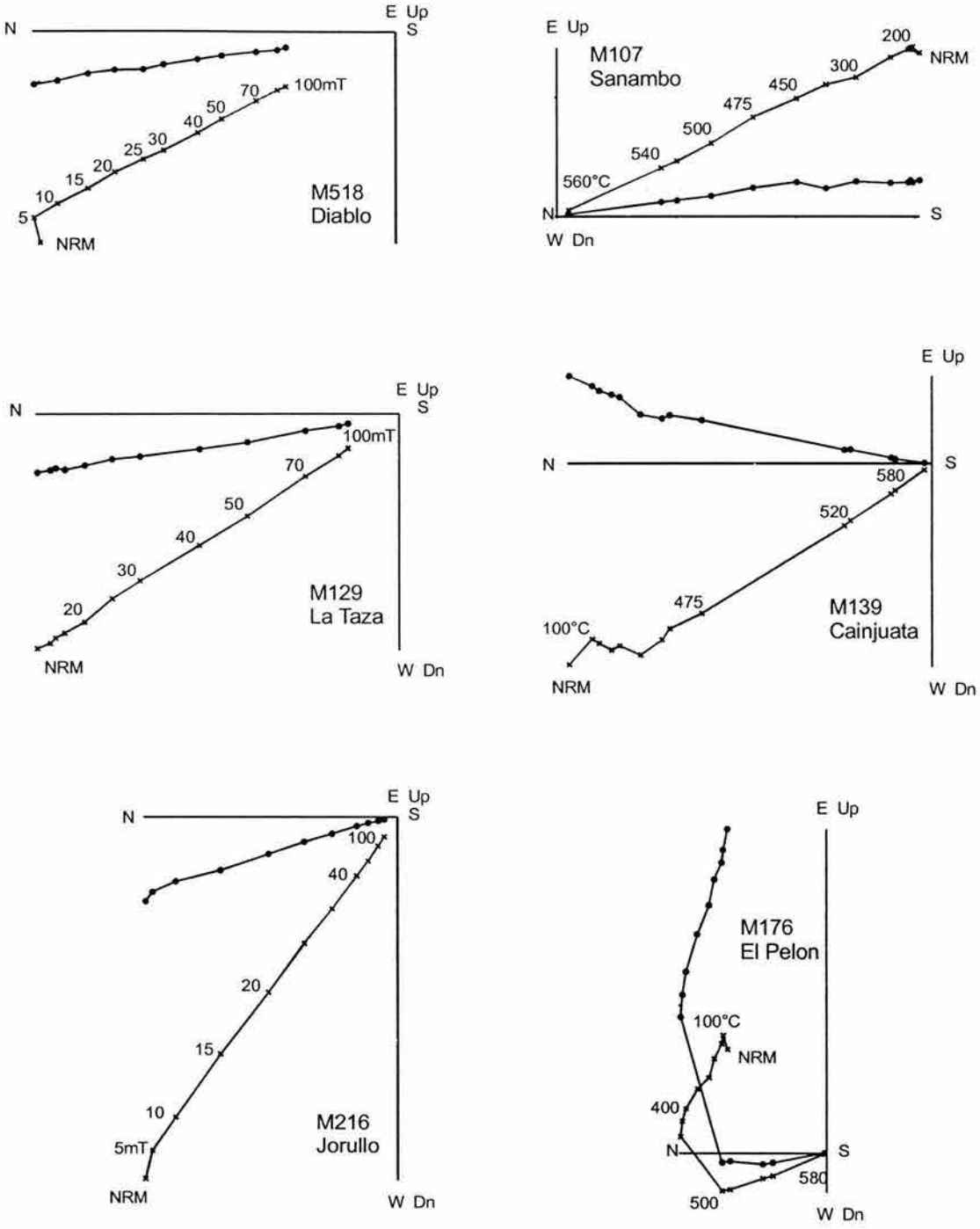

Fig. 7 Orthogonal vector plots of stepwise thermal or alternating field demagnetization of representative samples (stratigraphic coordinates). The numbers refer either to the temperatures in °C or to peak alternating fields in mT. o - projections into the horizontal plane, x – projections into the vertical plane.

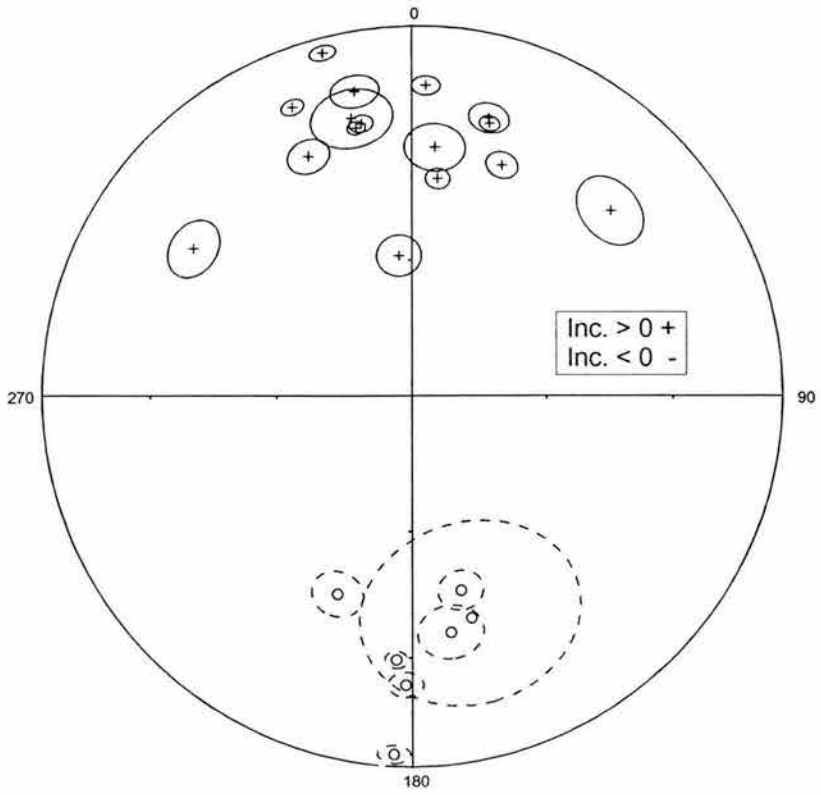

Fig 8 Equal area projection of site-mean paleodirections.

Paleointensity Determinations

Thellier Experiments

The Thellier method (Thellier and Thellier, 1959) in its modified form (Coe, 1967; Coe et al., 1978) was used in this study. This technique involves heating samples twice at each temperature step: once in a zero magnetic field to remove a portion of NRM and once in a laboratory field to determine the partial thermoremanence (pTRM) gained. The ratio of NRM lost to pTRM gained is proportional to the ancient field. This technique was used in present study to determine absolute geomagnetic paleointensity. Heating and cooling cycles were carried out using a MDT80 furnace, and the laboratory field was set to 30 microTesla. Thirteen temperature steps were distributed between room temperature and 580°C. During the experiment five control heatings (so-called "pTRM" checks) were performed to check for thermal alteration (Coe et al., 1978).

Results

Altogether forty-eight samples from six sites (volcanoes) were pre-selected for Thellier paleointensity experiment because of stable one component magnetization accompanied by relatively high MDF values, elevated blocking temperature, and reasonably reversible k-T curve. Some typical Arai-Nagata curves (Nagata et al., 1963) are shown Figures 9 and 10, and the results are given in Table 2. The criteria that we used for individual paleointensity determination are basically similar to those reported by Conte et al. (2004) and can be described as follows. We only accepted determinations that fulfill the following criteria: (1) obtained from at least six NRM-TRM points corresponding to a NRM fraction larger than 1/3, (2) yielding quality factor (Coe et al., 1978) of about 5 or more, and (3) with positive 'pTRM' checks i.e. the deviation of "pTRM" checks was less that 15% (Table 2).

Finally only twelve samples, from two volcanoes, yield reliable paleointensity estimates. For these samples the fraction f of NRM used for paleointensity determination ranges between (0.66-0.99) and the quality factor q from (12.3-61.4) generally greater than 5. Moreover, the NRM end points, obtained from the Thellier experiments at each step, are reasonably linear and point to the origin (Figures 9-10, right side); no deviation of the direction NRM left toward the applied laboratory field was observed. The remaining samples were rejected because they show typical "concave-up" behavior (Dunlop and Özdemir, 1997).

Main Results and Discussion

We consider the characteristic paleomagnetic directions determined in this study to be of primary origin. This is supported by the observation of normal and reversed polarities. In addition, thermomagnetic curves show that the remanence is carried in most cases by Ti-poor titanomagnetite, resulting from oxi-exsolution of original titanomagnetite during the initial flow cooling, which most probably indicates thermoremanent origin of a primary magnetization. Moreover, distributed unblocking temperature spectra and relatively high coercivity point to 'small' pseudo-single domain magnetic structure grains as responsible for remanent magnetization. Single-component, linear demagnetization plots were observed in most cases.

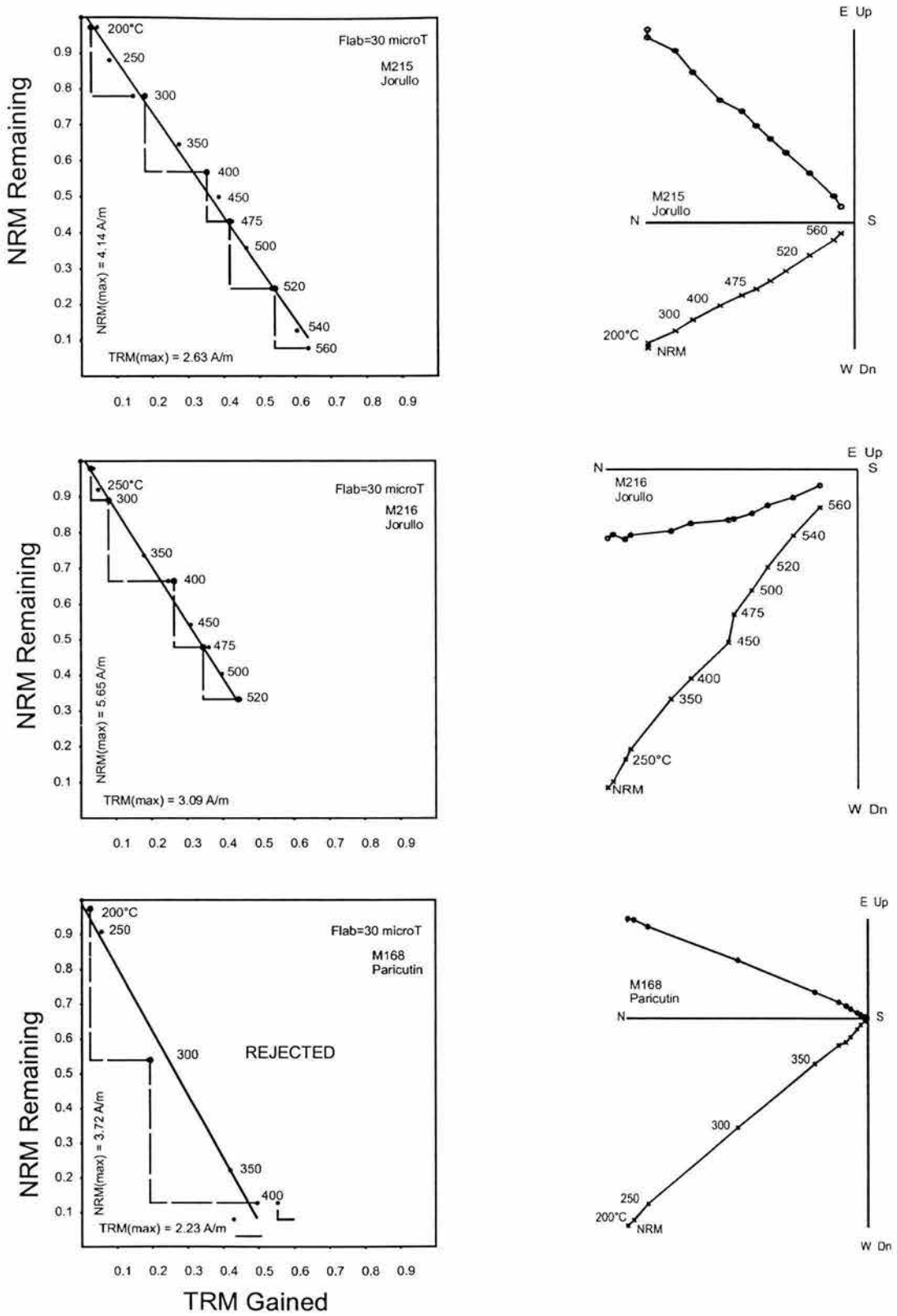

Fig. 9 The representative NRM-TRM plots and associated orthogonal diagrams from MGVF samples. In the orthogonal diagrams we used the same notations as in figure 7.

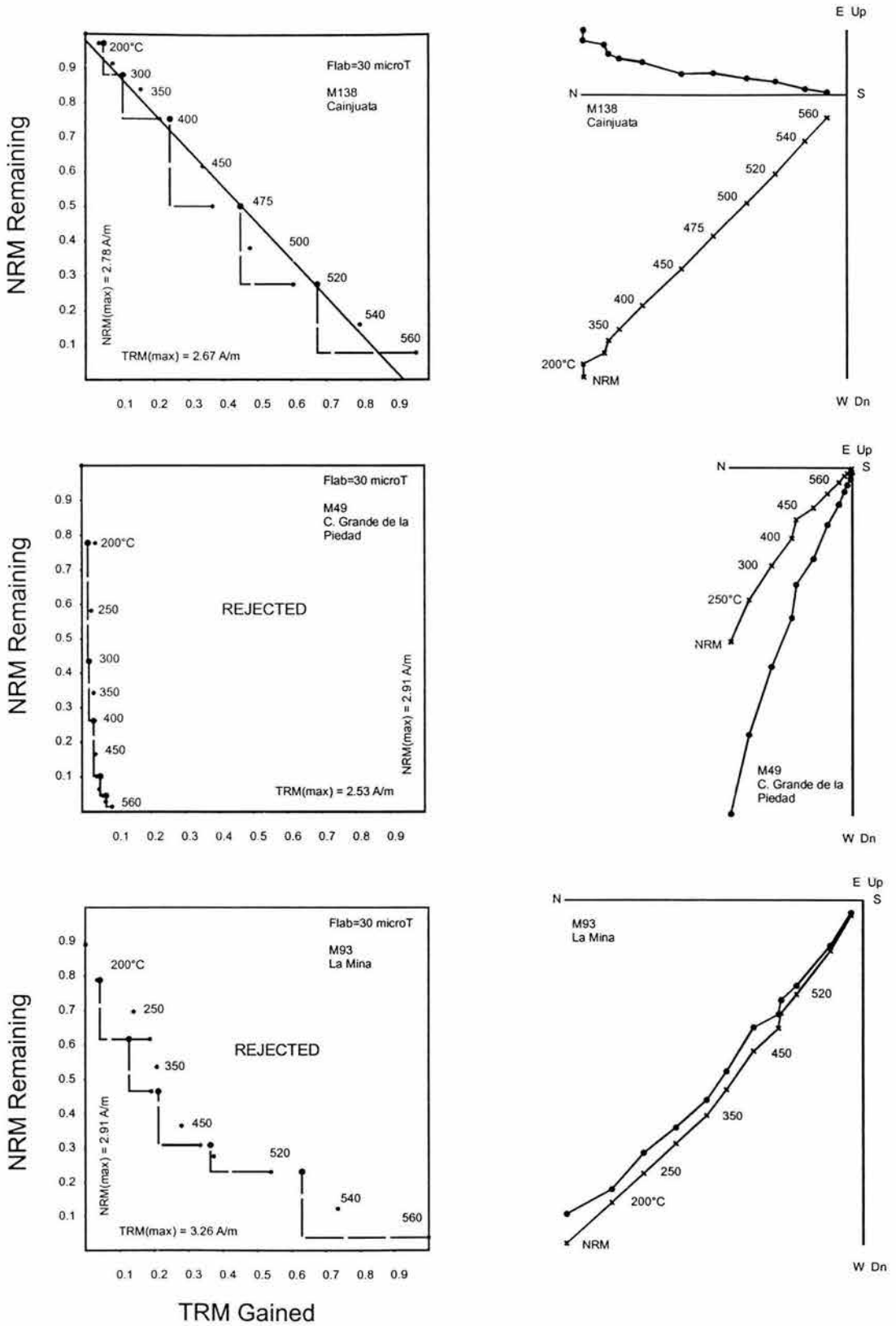

Fig. 10 The representative NRM-TRM plots and associated orthogonal diagrams from MGVF samples. In the orthogonal diagrams we used the same notations as in figure 7.

Table 2

Site	Sample	*N'*	T_{min}-T_{max}	*f*	*g*	*q*	$F_E \pm \sigma(F_E)$	*VDM*	*VDMe*
			°C				(μT)	$10^{22}Am^2$	$10^{22}Am^2$
Jorullo	M211	12	20-560	0.88	0.88	35.20	47.4 ± 1.0	8.56	***8.1 ± 1.1***
1759-1754	M213	11	20-560	0.89	0.87	59.35	52.0 ± 0.6	8.63	
	M214	11	20-560	0.89	0.88	23.36	57.5 ± 1.9	9.63	
	M215	12	20-560	0.90	0.90	28.08	43.2 ± 1.2	6.35	
	M216	10	20-520	0.66	0.86	28.60	45.1 ± 0.9	8.18	
	M218	12	20-560	0.96	0.77	61.34	43.0 ± 0.5	7.06	
Cainjuata	M138	12	20-560	0.99	0.89	15.43	31.7 ± 1.8	6.64	***7.3 ± 0.6***
< 40 Kyr	M139	12	20-560	0.94	0.88	15.94	29.7 ± 1.5	6.66	
	M140	12	20-560	0.89	0.86	15.94	37.7 ± 1.8	8.2	
	M141	12	20-560	0.97	0.88	18.11	37.5 ± 1.7	7.78	
	M142	10	20-560	0.91	0.82	12.25	35.9 ± 2.2	7.59	
	M143	10	20-560	0.96	0.84	12.30	33.8 ± 2.2	7.00	

Paleointensity results from MGVF volcanic units, n is the number of NRM-TRM points used for palaeointensity determination, Tmin-Tmax is the temperature interval used, *f*, *g* and *q* are the fraction of extrapolated NRM used, the gap factor and the quality factor (Coe et al., 1978) respectively. F_E is the paleointensity estimate for an individual specimen, and $\sigma(F_E)$ is its standard error; VDM and VDMe are individual and average virtual dipole moments.

The mean paleodirection obtained in this study is I=28.4°, D=357.9°, k=21, α_{95}=7.3°, N=20, which corresponds to the mean paleomagnetic pole position P_{lat}=85.7°, P_{long}=104.5°, K=27, α_{95}=6.4° (Table 1). These directions are practically undistinguishable from the expected Plio-Quaternary paleodirections, as derived from reference poles for the North American polar wander curve (Besse and Courtillot, 1991) and in agreement with previously reported directions from TMVB Tuxtla volcanics (Alva-Valdivia et al., 2001; Morales et al., 2001; Herrero-Bervera et al., 1986). The palaeosecular variation curve of our results, together with all currently available paleomagnetic data from central Mexico for the last 70,000 years are shown in Figure 11 (Urrutia and del Pozzo, 1993; Gonzalez et al., 1997; Morales et al., 2001; Bohnel and Molina, 2002).

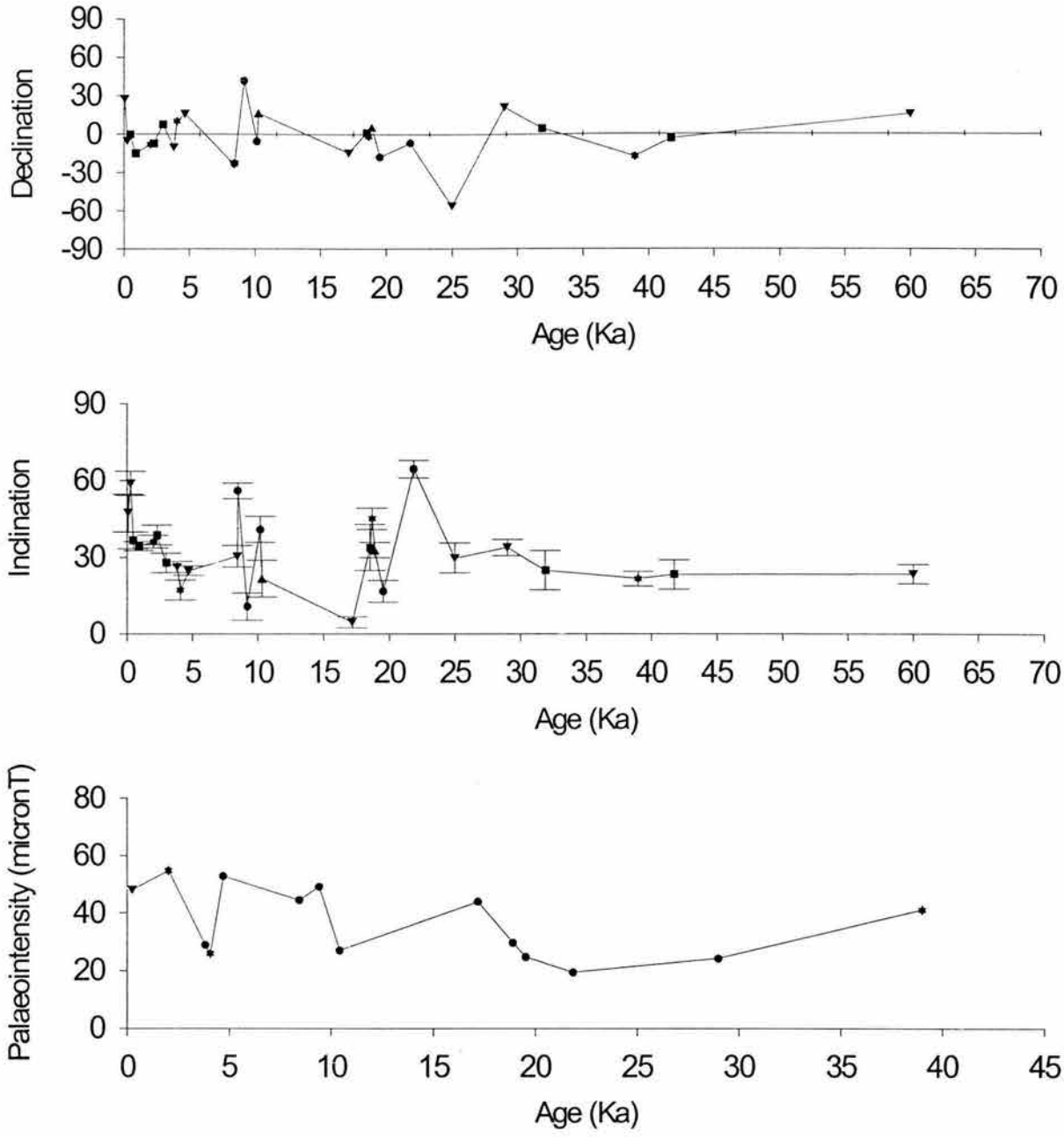

Fig. 11 Palaeosecular variation for Central Mexico determined for the last 70,000 years, by lava flows from the Trans-Mexican Volcanic Belt. Data set: (▼) This Study, (■) Bohnel and Molina 2002, (✱) Morales et al. 2001, (●) Gonzalez et al. 1997, (▲) Urrutia and del Pozzo 1993.

Absolute paleointensities, obtained from only two sites (twelve samples), yielded the values close to the present geomagnetic field strength (Table 2). The Thellier and Thellier (1959) method of geomagnetic absolute intensity determination, which is

considered the most reliable one, imposes many restrictions on the choice of samples that can be used for a successful determination (Kosterov and Prévot, 1998). The almost 75 percent failure rate that we find in our study is not exceptional for a Thellier paleointensity study, if correct pre-selection of suitable samples and strict analysis of the obtained data are made. Although our results are not numerous, some credit should be given because of good technical quality determination, attested by the reasonably high Coe et al's quality factors. However, there are not enough data to discuss VDM variation trough time.

Seven sites yielded reverse polarity and 16 sites are normally magnetized. Site Cerro Grande Cortazar (Table 1) is characterized by high NRM intensity (several hundred A/m) and scattered direction probably due to the lightning. All samples from this site were rejected for further paleomagnetic analysis. An interesting feature of the geomagnetic record obtained from MGVF is that lava flow Brinco del Diablo, dated as 1.88±0.24 Ma yielded well-defined normal paleodirections, which probably corresponds to worldwide observable Olduvai geomagnetic event within globally reverse Matuyama chron (Cande and Kent, 1995). Sites Buenavista Tomatlan and Yahuarato (Table 1) both gave similar radiometric dates (540±80 ka and 540±70 ka respectively) but paleodirections are of normal and reverse polarity, respectively. Age uncertainties and possible problems related to rather old K-Ar dating technique make difficult to affirm whether these findings are sustained by true geomagnetic phenomena. It may be speculated however that site Yahuarato records the ^{40}Ar-^{39}Ar dated Big Lost event (incremental heating age of 580.2±7.8 ka after Singer et al., 2002). Sites El Fresno and Cerro Grande both yielded fully reversed paleodirections. On the basis of field observations, these units are older than 40 ka (Table 1). In absence of absolute dating, it is not clear whether they are formed during Matuyama chron or correspond to short duration geomagnetic events within Brunhes chron.

A simple way to estimate the PSV is to calculate the angular standard deviation ASD of virtual geomagnetic pole for a given locality (McFadden et al., 1988, 1991). The classic formula $S_F^2 = S_T^2 - S_W^2 / n$ was used for estimating paleosecular variation in this study where, here, S_T is the total angular dispersion

$S_T = \left[(1/N-1)\sum_{i=1}^{N}\delta i^2\right]^{1/2}$ (Cox, 1969), N the number of sites used in the calculation, δ_i the angular distance of the *i*th virtual geomagnetic pole from the axial dipole, S_W the within site dispersion and, *n* the average number of sample per site.

Using the new data obtained in this study, we obtained S_F =15.4 with S_U =19.6 and S_L =12.7 (upper and lower limits respectively). The ASD is higher that that predicted by the latitude-dependent variation model of McFadden et al. (1988, 1991) for the last 5 Ma (Figure 12, Table 4). Table 3 lists all currently available data from volcanic rocks of central Mexico. For the selection of data, we use the paleolatitude of 60° as a cut-off angle to separate the paleosecular variation of intermediate geomagnetic regime, and rejecting the data with $\alpha_{95} > 15°$. Data S6 and M-15 present similar mean dates but their uncertainties are different, thus they both were considered.

Table 3

Site	N	Inc.	Dec.	K	a95	Plat.	Plog.	Ref.	Age	Number
IZTA-78	7	28.3	1.3	243.2	3.9	85.9	64.3	1	B	1
IZTA-79	4	31.8	13.8	96.1	9.4	76.8	357.5	1	B	2
IZTA-80*	7	33.7	354.6	13	17.4	84.9	166.6	1	B	3
IZTA-82	8	39.8	356.1	178	4.2	84.9	217.4	1	B	4
IZTA-84	7	-8	355.5	70.5	7.2	66.6	93.3	1	B	5
IZTA-133	6	25.5	10.2	207.5	4.7	78.7	20.2	1	B	6
IZTA-10	6	28.5	7.4	199.3	4.8	82	19.2	1	B	7
IZTA-11	7	23.5	3.6	168.4	4.7	82.4	54.3	1	B	8
IZTA-13	7	31.5	355.9	569.1	2.5	85.6	145.9	1	B	9
IZTA-14*	7	45.7	10.9	10.6	19.4	77.1	310.9	1	B	10
IZTA-16	7	38.6	13.4	31.2	11	77.1	337.3	1	B	11
IZTA-18	7	52.9	17.3	65.6	7.5	68.8	305.4	1	B	12
IZTA-19	7	51	20.6	31.7	10.9	67.5	313.6	1	B	13
IZTA-20	7	60.8	22.7	158.4	4.8	60.1	297.3	1	B	14
IZTA-21	7	32.1	352.4	131.7	5.3	82.6	160.8	1	B	15
IZTA-23	7	24.6	0.3	43.8	9.2	83.9	79.3	1	B	16
IZTA-24	7	21.3	355.3	82.4	6.7	80.8	112.3	1	B	17
IZTA-25*	6	61.5	27	327.6	3.7	57.2	300	1	B	18
IZTA-26	7	24.4	331.9	29.3	11.3	62.3	163.2	1	B	19
IZTA-27	6	30	354	79.6	7.6	83.6	146.1	1	B	20
IZTA-29	7	38.1	7.4	72.6	7.1	82.7	331.6	1	B	21
IZTA-30	7	31.9	356.6	79.4	6.8	86.3	144.6	1	B	22
IZTA-31	7	35.9	3.8	64.3	7.6	86.3	337.3	1	B	23
IZTA-32	7	30	356.7	43.2	9.3	85.7	129.9	1	B	24
CHI-6	17	34.3	358	301	2.1	88	202.7	2	A	25
CHI-8	9	27.1	7.2	51	7.3	83.1	2.6	2	A	26
CHI-9	8	27.1	4.5	115	5.2	83.5	321.1	2	A	27
CHI-10	9	34.9	6	118	4.8	84.3	10.4	2	A	28
CHI-13	8	38.9	355.1	114	5.2	84.7	158.5	2	A	29
CHI-15	7	33.6	356.1	62	7.7	86.2	202.3	2	A	30
JU*	7	22.4	323.2	289	3.5	53.8	164.5	2	A	31

XA	5	22.1	343.8	242	4.9	72.6	146.9	2	A	32
P-2	8	25.7	3	62	7.1	83.6	287.5	2	A	33
MOE-5	8	38.3	346.5	114	5.2	77.1	183.8	2	A	34
MOE-10	6	34.9	356.9	92	7	87.1	172	2	A	35
MOE-34	7	41.8	352.8	489	2.7	81.7	208.3	2	A	36
CHII-15	11	36.3	345.7	347	2.5	76.5	177.5	2	A	37
CHI-1	8	26.7	357.6	73	6.5	84.5	253.9	2	A	38
CHI-2	14	12.9	6.1	205	2.8	76.2	304.9	2	A	39
CHI-3	12	46.6	330.3	577	1.8	61.5	165.4	2	A	40
CHI-4	9	11.6	342.6	160	4.1	68.6	224.9	2	A	41
CHI-5	11	18.6	345.5	118	4.2	72.9	221.4	2	A	42
OZ	4	23.1	352.8	412	4.5	80.1	125.9	2	A	43
ACO	7	32.6	357.6	82	6.7	87.3	138.5	2	A	44
MOE-28	7	33.4	358.5	253	3.8	88.2	132	2	A	45
CHI-11	12	36.1	16.1	230	2.9	74.8	14.6	2	A	46
TEU-1	7	17.1	338.7	200	4.2	66.9	147.2	2	A	47
TEU-2	5	22.4	358.2	95	7.8	82.3	93.8	2	A	48
MOE-8	6	23.9	352	219	4.5	79.7	130	2	A	49
MOE-36	7	36.1	346.6	101	6	77.4	176.9	2	A	50
MOE-24	3	21.4	7.8	192	8.9	78.9	36.8	2	A	51
MOC-55	7	18	352.7	76	7	77.8	117.1	2	A	52
MOC-56	7	35.5	358.3	153	4.9	88.3	186	2	A	53
MOE-1	8	24.1	353.3	118	5.1	80.6	125.3	2	A	54
MOE-4	5	21.5	23.8	67	9.4	65.6	7.1	2	A	55
MOE-7	9	23.7	353.3	39	8.3	80.5	124.3	2	A	56
MOE-9	7	17.3	10	36	10.3	75.7	36.9	2	A	57
MOE-11	7	27.3	341.8	22	13.1	71.9	157.8	2	A	58
MOE-12	4	17.4	9.3	58	12.2	76.2	38.9	2	A	59
MOE-13	7	17.3	355.7	24	12.6	78.7	102.9	2	A	60
MOE-14	7	24.7	6.7	104	6	80.9	34.9	2	A	61
MOE-15	8	38.8	354.9	429	2.7	84.6	199.3	2	A	62
MOE-23	8	38.5	1	259	3.5	87.5	282.9	2	A	63
MOE-25	5	15.4	352.6	95	7.9	76.4	113.7	2	A	64
MOE-27	10	17.6	1.9	26	9.6	79.5	70.5	2	A	65
MOE-30	5	6.1	14.3	50	11	68.5	38.5	2	A	66
MOE-31	8	25.3	16.2	37	9.2	73.3	9.8	2	A	67
MOE-32	7	19.1	2	25	12.4	80.2	69.1	2	A	68
MOE-37	8	47.8	338.4	31	10.1	68.2	200.7	2	A	69
MOE-38*	6	12.2	46.4	59	8.8	43	0.8	2	A	70
MOE-39*	6	7.9	217.8	22	16.5	46.1	18.9	2	A	71
MOE-41	7	32.8	348.9	61	7.8	79.4	164.3	2	A	72
MOE-43	6	35.2	2.8	33	11.9	87.4	349.7	2	A	73
MOE-44	8	35.1	9.7	77	6.4	80.9	349.44	2	A	74
MOE-45*	5	18.3	5.9	24	15.6	78.5	50.3	2	A	75
CHI-12	13	15.9	6.4	21	9.2	77.4	309.6	2	A	76
C/3	7	21.6	16.8	71	7.2	72.0	14.4	3	A	77
M/6	6	32.8	6.0	513	3.0	84.2	3.1	3	A	78
IZTA-1	6	35.8	354.9	223	4.1	85.1	180.5	4	B	79
IZTA-3	7	38.7	347	502	2.7	77.5	186.1	4	B	80
IZTA-7	7	29.5	15.7	169	4.7	74.7	1.5	4	B	81
R-8	4	/	/	81	10.3	76.1	20.1	5	A	82
R-13	5	/	/	36	12.9	78.3	232.2	5	A	83
R-14	6	/	/	246	4.3	80.3	74.5	5	A	84
J-1	6	/	/	150	5.5	80.2	204.5	5	A	85
J-2	6	/	/	206	4.7	79.7	219.1	5	A	86
J-3	6	/	/	69	8.1	83.2	203.4	5	A	87
J-4	8	/	/	329	3.7	75.3	24.8	5	A	88
J-7	6	/	/	29	10.5	85.6	202.8	5	A	89
J-10	6	/	/	28	12.8	81.8	133.3	5	A	90
J-11	7	/	/	24	12.6	81.6	25.2	5	A	91
J-12	6	/	/	43	10.3	83.5	343.0	5	A	92
R-3	6	/	/	38	11.0	68.8	148.5	5	A	93
R-9	7	/	/	586	2.5	63.7	150.9	5	A	94
S5	7	64.4	353.3	318	3.4	62.2	250.5	6	A	95
S6	6	55.9	337.4	463	3.1	63.7	216.3	6	A	96
S7	6	16.6	342.6	255	4.2	70	140.6	6	A	97
S11	7	40.8	354.6	139	5.1	83.4	211.9	6	A	98
M2*	3	10.7	42.2	540	5.3	46.6	1.4	6	A	99
JB	8	17	10.4	198	3.9	75.6	35.2	7	A	100
JD	8	10.8	13.8	353	3	70.9	34.4	7	A	101

JE	8	23.1	4	277	3.3	82	51.7	7	A	102
JH	8	21.5	342.7	371	2.9	71.6	148.3	7	A	103
JJ	13	33	352.8	498	1.9	83.1	163.7	7	A	104
JL	10	45	358.8	131	4.2	82.4	152.9	7	A	105
JM	13	36	352	269	2.5	82.4	179.6	7	A	106
Ceb	7	36.6	360	361	3.2	89.23	75.5	8	A	107
Tox	26	34.4	345	248	1.8	75.83	173.56	8	A	108
Tet	8	38.6	352.6	201	3.9	82.56	194.15	8	A	109
Jal	8	27.8	7.8	218	3.8	81.1	25.07	8	A	110
Col	23	33.7	1.4	12	9	88.45	17.64	8	A	111
Pri	7	24.8	4.7	63	7.7	81.13	45.37	8	A	112
Joy	3	23.2	356.6	450	5.8	81.82	107.08	8	A	113
P1	9	35.9	3.5	229	3.4	86.6	336.9	9	B	114
P3*	5	33.1	324.7	333	4.2	56.6	175.5	9	B	115
P5	4	32.6	350.9	183	6.8	81.3	164.2	9	B	116
P7	5	6.1	1.2	591	3.2	74.1	77.3	9	B	117
P8	5	53.6	332.4	122	6.9	61.1	209	9	B	118
P10*	6	52.4	314.4	137	5.7	47	200	9	B	119
P11	7	37.6	347.5	148	5	78.1	183.8	9	B	120
P13	8	29.8	344.8	200	3.9	75.2	162.4	9	B	121
P14	9	48.9	348.3	80	5.8	74.8	219.3	9	B	122
P15	4	27.5	359.6	67	11.3	85.5	86.4	9	B	123
P16	8	26.6	2.3	164	4.3	84.5	57.4	9	B	124
3	6	46.2	331.7	119	6.1	62.8	194.4	9	B	125
6	4	30.0	332.2	83	10.1	63.3	173.4	9	B	126
9	8	17.8	338	81	6.2	66.5	193.3	9	B	127
10	5	38.9	357.6	33	13.4	86.2	225.1	9	B	128
M-2	8	33.03	5.33	88	5.9	84.43	13.55	10	B	129
M-3	9	35.62	350.69	62	6.6	80.59	166.64	10	C	130
M-4*	5	38.05	344.93	13	22.3	75.87	175.94	10	C	131
M-5	10	42.3	20.76	83	5.3	70.32	331.77	10	C	132
M-6	9	45.07	345.88	122	4.7	75.62	196.51	10	C	133
M-7	9	17.32	349.47	140	4.4	75.04	122.44	10	B	134
M-8	8	33.68	21.59	306	3.2	69.57	348.36	10	A	135
M-9	11	29.64	348.3	722	1.7	77.48	143.25	10	C	136
M-10	8	3.62	2.99	430	2.7	71.64	68.71	10	C	137
M-11	8	4.75	345.45	633	2.2	67.52	119.63	10	A	138
M-12	12	23.02	1.32	177	3.3	82.26	68.93	10	B	139
M-13	6	29.41	3.5	950	2.2	84.88	37.2	10	B	140
M-14*	5	29.64	303.95	170	5.9	36.71	173.95	10	A	141
M-15	10	30.27	336.65	134	4.2	67.56	163.71	10	A	142
M-16	11	40.63	6.81	346	2.5	82.73	317.44	10	A	143
M-17	8	23.3	15.7	211	3.8	73.17	11.92	10	A	144
M-18	8	24.62	16.11	816	1.9	73.17	8.87	10	A	145
M-19*	7	47.27	27.51	70	7.3	63.41	322.93	10	A	146
M-20	7	24.2	347.77	63	7.7	76.51	140.44	10	B	147
M-21	6	26.07	349.47	898	2.2	78.43	140.11	10	A	148
M-22	13	16.45	337.53	403	2.1	65.77	144.92	10	A	149
M-23	12	17.18	2.61	292	2.5	79.34	63.37	10	B	150
M-24	7	58.82	354.73	165	4.7	68.94	246.89	10	A	151

Summary of paleomagnetic data from volcanic rocks of Central Mexico.
* Data not include in PSV analysis.
1, Steel 1985
2, Bohnel et al. 1990
3, Urrutia and Martin del Pozzo 1993
4, Urrutia 1995
5, Urrutia 1997
6, Gonzalez et al. 1997
7, Morales et al. 2001
8, Bohnel and Molina 2002
9, Conte el al. 2004
10, This Study
A, < 70,000
B, 70 Ka-0,78 Ma
C, > 0,78 Ma

Combination of our data with selected previously published results from TMVB yield S_F=13.0 with S_U=14.5 and S_L=11.8, which is in good agreement with the model (McFadden et al., 1988, 1991); thus this data set does not support the hypothesis that central Pacific low non-dipole region might extend westwards into central Mexico as suggested by Doell and Cox (1971) for the Brunhes chron. Tanaka and Kono (1991) and Mankinen and Champion (1993) have also obtained data supporting the existence of a significant non-dipole field at central Pacific region. McEllhinny and McFadden (1997) have re-examined the old data from Hawaii and Tahiti and used a new statistical method to account of those flows that have repeatedly sampled the same geomagnetic field vector. They concluded that the amplitude of the secular variation is consistent with values from other worldwide-scattered sites, not supporting the hypothesis of the Pacific low non-dipole field.

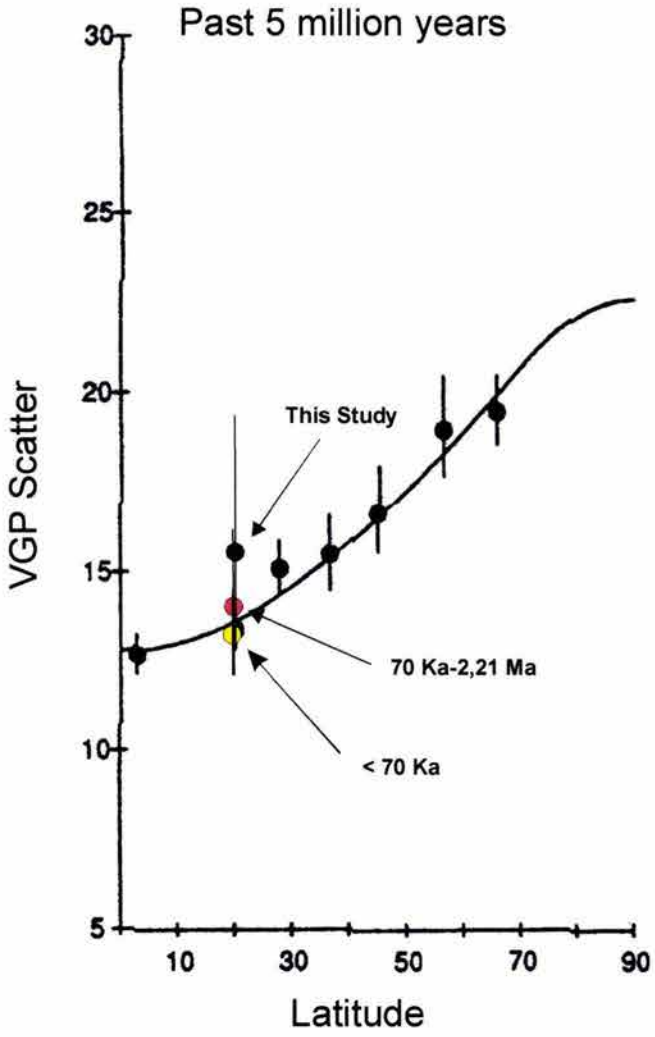

Fig. 12 Paleosecular variation of lavas (PSVL) for the last 5 Ma. (Adopted from McFadden et al., 1988 and 1991).

Table 4

	Age	*N*	*Plat.*	*Plog.*	$A_{95}(^{\circ})$	*K*	S_f	S_u	S_l
Steel 1986	76,000-580,000	24	86.9	333.2	5.5	29.6	14.2	17.6	11.9
Herrero-Bervera et al. 1986	0-580,000	45	86.4	133.0	3.5	35.7	13.9	16.1	12.1
Bohnel et al., 1990 (Rev. Herrero et al.1986 + new data)	Brunhes, 70% < 40,000	74	88.3	72.4	3.3	26.6	15.4	17.4	13.8
Bohnel et al. 1990-Sel. M	Brunhes, 70% < 40,000	68	87.9	95.1	2.6	43.7	11.7	13.2	10.5
Urrutia 1997 (Rev. Bohnel et al. 1990 + new data)	Brunhes	84	88.4	111.5	2.6	36	12.9	14.4	11.7
Urrutia 1997-Sel M	Brunhes	81	87.8	106.5	2.4	43	11.6	13.0	10.5
Urrutia 1997-Sel V	Brunhes	79	88.1	90.8	2.3	47	11.1	12.5	10.0
This Study	**< 2,10 Ma**	**20**	**85.7**	**104.7**	**6.4**	**27.0**	**15.4**	**19.6**	**12.7**
All published data + this study	**< 70,000**	**90**	**87.1**	**131.0**	**2.5**	**35.8**	**13.0**	**14.5**	**11.8**
All published data + this study	**70 Ka-2,1 Ma**	**48**	**87.8**	**157.7**	**3.7**	**32.7**	**13.8**	**16.0**	**12.1**

Angular dispersion of the VGPs from Central Mexico.
Sel. M-Selection McFadden, 1980
Sel. V-Selection Vandamme 1994

Acknowledgements

We thank Prof. Herve Guillou for the K/Ar studies of the Michoacan-Guanajuato volcanic field. Economic support for this project has been provided UNAM-DGAPA grant n° 116201 and 100403.

References

Aguilar-Vargas and Verma, 1987. Composicion quimica (elementos mayores) de los magmas en el Cinturon Volcanico Mexicano. *Geofisica Internacional*, V. 26, pp. 195-272.

Alva-Valdivia L. and Urrutia-Fucugauchi J. (1996). Shallow paleomagnetic inclination in the historic 1943-1948 lava flow in the Paricutin Volcano, Mexico. *EOS, Trans Am. Geophys. Un.* 77 (46), *Fall Mtng. Suppl.*, F155.

Alva-Valdivia L., Goguitchaichvili A., Urrutia-Fucugauchi J., and Morales. (2001). Further constraints for the Pliocene geomagnetic field strangth: New results from the Los Tuxtla volcanic field (Mexico). *Earth Planets Space*, V. 53, pp. 873-881.

Ban M., Hasenaka T., Delgado-Granados H. and Takaoka N., 1992. K-Ar ages of lavas from shield volcanoes in the Michoacan-Guanajuato volcanic field, Mexico. *Geofisica International*, V. 31, pp. 467-473.

Besse J. and Courtillot V. (1991). Revised and Synthetic Apparent Polar Wander Paths of the African, Eurasian, North American and Indian Plates, and True Polar Wander Since 200 Ma. *Journal of Geophys. Research*, V. 96, pp.4029-4050.

Bohnel H., Molina-Garzia R. (2002). Secular variation in Mexico during the last 40,000 years. *Phys. Earth Planet. Inter.*, V. 133, pp. 99-109.

Bohnel H., Urrutia-Fucugauchi J., and Herrero-Bervera. (1990). Paleomagnetic data from central Mexico and their use for paleosecular variation studies. *Phys. Earth Planet. Inter.*, V. 64, pp. 224-236.

Campos Enriquez J. J., Campos Enriquez J. O., and Urrutia-Fucugauchi J. (1991). Variación secular reciente y cartas de los elementos del campo geomagnético en Mexico. *Geofisica Internacional*, V. 30, n. 2, pp. 107-116.

Cande S. C., and Kent D. V. (1995). Revised calibration of the geomagnetic polarity time scale for the Late Cretaceous and Cenozoic. *J. Geophys. Res.*, V. 100, pp. 6093-6095.

Coe R. (1967). The determination of paleo intensities of the Earth's field with emphasis on mechanism which could cause non-ideal behavior in Thellier's method. *Journal of Geomagn. and Geolectr.*, V. 19, pp. 157-179.

Coe R., Gromme S. and, Mankinen E. A. (1978). Geomagnetic paleointensity from radiocarbon-dated lava flows on Hawaii and the question of the Pacific non-dipole Low. *Journal of Geophysical Research,* V. 83, pp. 1740-1756.

Conte G., Urrutia-Fucugauchi J., Goguitchaichvili A., Soler-Arechalde A. M., Morton-Bermea O., and Incoronato A. (2004). Paleomagnetic study of lavas from the Popocatepetl Volcanic Region, Central Mexico. *International Geology Review,* V. 46, pp. 210-225

Cox A. (1969). Confidence limits for the precision parameter k. *Geophys. J. R. astr. Soc.* V. 18, pp. 545-549.

Day R., Fuller M., and Schmidt, V. A. (1977). Hysteresis properties of titanomagnetites: Grain size and compositional dependence. *Physics of the Earth and Planetary Interiors*, V. 13, pp. 260-267.

Demant A. and Robin C., 1975. Las fases del Volcanismo en Mexico; una síntesis en relación con la evolución geodinamica desde el Cretácico. *Revista Inst. Geol.* UNAM, 75 (1), pp.70-83.

Doell R., and Cox A. (1971). Pacific geomagnetic secular variation. *Science,* V. 71, pp. 248-254.

Doell R., and Cox A. (1972). The Pacific geomagnetic secular variation anomaly and the question of lateral uniformity in the lower mantle, in The Nature of the Solid Earth, edited by *E. C. Robertson, McGraw-Hill*, New York, pp. 245-284.

Dunlop D. J., and Ozdemir O. (1997). Rock-magnetism Fundamentals and frontiers. *Cambridge, UK, Cambridge University Press*, pp. 573.

Fisher, R. A., (1953). Dispersion on the sphere. *Proc. R. Soc. Lond. Ser.* A 217, pp. 295-305.

Goguitchaichvili A., Alva-Valdivia L., Rosasa-Elguera J., Urrutia-Fucugauchi J., Gonzalez J., Morale J., Solé J. (2002). An integrated paleomagnetic study of

Rio Grande de Santiago volcanic succession (tras-Mexican volcanic belt): revisited. *Phys. Earth Planet. Inter.* V. 130, pp. 175-194.

Goguitchaichvili A., Camps P., and Urrutia-Fucugauchi J. (2001). On the features of the geodynamo following reversals and excursions: By absolute geomagnetic intensity data. *Phys. Earth Planet. Inter.* V. 124, pp. 81-93.

Goguitchaichvili A., Chauvin A., Roperch P., Prevot M., Vergra M., Moreno H. (2000). Paleomagnetism of the Miocene Farellones formation in Chile. *Geophys. Journal Int.* 140, pp. 357-374.

Goguitchaichvili A., Prevot M., and Camps P. (1999) No evidence for strong fields during R3-N3 Icelandic geomagnetic reversals. *Earth Planet. Sci. Lett.* V. 167, pp. 15-34.

Gonzalez S., Sherwood G., Bohnel H., and Schnepp E. (1997). Paleosecular variation in Central Mexico over last 30,000 years: the record from lavas. *Geophys. J. Int.* V. 130, pp. 201-219.

Hasenaka and Carmichael, 1985. A compilation of location, size, and geomorphological parameters of volcanoes of the Michoacan-Guanajuato volcanic field, central Mexico. *Geofisica Internacional*, 24-4: pp.577-607.

Hasenaka and Carmichael, 1987. The cinder cones of Michoacan-Guanajuato, central Mexico: petrology and chemistry. *J. Petrol.,* V. 28: pp. 241-269.

Hasenaka T. (1994). Size, distribution, and magma output rate for shield volcanoes of the Michoacan-Guanajuato volcanic field, Central Mexico. *J. Volcanol. Geotherm. Res.,* V. 63, pp. 13-31.

Hasenaka T., Masao Ban and Hugo Delgado Granados (1994). Contrasting volcanism in the Michoacan-Guanajuato Volcanic Field, central México: Shield volcanoes vs. cinder cones. *Geofisica Internaciónal,* V. 33, (1), pp. 125-138.

Herrero-Bervera E., Urrutia-Fucugauchi J., Martin del Pozzo A., Bohnel H., and Guerrero J. (1986). Normal amplitude Brunhes paleosecular variation at low-latitudes: A paleomagnetic record from the Trans-Mexican Volcani Belt. *Geophysical Research Letters,* V. 13 (13), pp. 1442-1445.

Juarez M. T., Tauxe L., Gee J. S., Pick T. (1998). The intensity of the Earth's magnetic field over the past 160 million years. *Nature 394*, pp. 878-881.

Kirschvink, J. L., (1980). The least-squares line and plane and the analysis of palaeomagnetic data. *Geophys. J. R. Astr. Soc.* 62, pp. 699-718.

Kosterov A. and Prévot M. (1998). Possible mechanisms causing failure of Thellier paleointensity experiments: results of rock-magnetic study of the Lesotho basalt, Southern Africa. *Geophysical Journal International.* V. 134, pp. 554-572.

Love J. J. (2000). Palaeomagnetic secular variation as a function of intensity. *Philos. T. Roy. Soc.,* V. 358, pp. 1191-1223.

Luhr J. F. and Siminik T. (1993). Paricutin. The volcano born in a Mexican cornfield. *Geoscience Press, Inc.*, Arizona, USA, pp. 427.

Luhr J. F. and Carmichael S. E. (1985). Jorullo Volcano, Michoacan, Mexico (1759-1774): The earliest stage of fractionation in calc-alkaline magmas. *Contrb. Mineral Petrol.*, Vol. 90, pp. 142-161.

Mankinen E. A., and Champion D. E. (1993). Latest Pleistocene and Holocene geomagnetic intensity on Hawaii. *J. Geophys. Res.,* V. 262, pp. 412-423.

McEllhinny M. W., McFadden P. L., and Merrill R. (1996). The myth of the Pacific dipole window. *Earth Planet Sci. Lett.,* V. 143, pp. 13-22.

McEllhinny M.W., and McFadden P.L. (1997). Paleosecular variation over the past 5 Myr based on a new generalized database. *Geophys. J. Int.,* V. 131, pp. 240-252.

McFadden P. L. (1980). Determination of the angle in a Fisher distribution which will be exceeded with a given probability. *Geophysic. J. R. astr. Soc.* V. 60, pp. 391-396.

McFadden P., Merrill T., McElhinny W. (1988). Dipole/Quadrupole Family Modeling of Paleosecular Variation. *Journal of Geophysical Research*, V. 93 (B10), pp. 11,583-11,588.

McFadden P.L., Merrill R., McEllhinny M. W., and Lee S. (1991). Reversals of the Earth's magnetic field and temporal variations of the dynamo families. *J. Geophys. Res.,* V. 96, pp 3923-3933.

McWilliams M., Holcomb R., and Champion D. (1982). Geomagnetic secular variation from ^{14}C dated lava flows on Hawaii and the question of the Pacific non-dipole low. *Phil. Trans. R. Soc. Lond.*, A, V. 306, pp. 211-222.

Molnar P. and Sykes L. R., 1969. Tectonics of the Caribean and Middle America regions from focal mechanisms and seismicity, *G. S. A. Bulletin,* 80, pp. 1639-1684.

Morales J., Goguitchaichvili A., Alva-Valdiva L., Gratton N., Urrutia-Fucugauchi J., Rosas-Elguera J., and Soler-Arechalde A. (2003). An attempt to determine the microwave paleointensity on historic Paricutin volcano lava flows, Central Mexico. *Geofisica Internacional,* V. 42, (1), pp. 95-100.

Morales J., Goguitchaichvili A., and Urrutia-Fucugauchi J. (2001). A rock-magnetic and paleointensity study of some Mexican volcanic lava flows during the Latest Pleistocene to the Holocene. *Earth Planet. Space* V. 53, pp. 839-902.

Nagata T., Fisher R. M., Momose K. (1963). Secular variation of the geomagnetic total force during the last 5000 years. *Journal of Geophysical Research,* V. 68, pp. 5277-5281.

Nixon G. T., Demant A., Armstrong R. L. and Harakal J. E. (1987). K-Ar and Geologic Data Bearing on the Age and Evolution of the Trans-Mexican Volcanic Belt. *Geofisica Internacional,* V. 26-1, pp. 109-158.

Özdemir O., Dunlop D. J., and, Muskowitz M. (1993). The effect of oxidation on the Wervey transition in magnetite. *Geophysical Research Letters,* V.20, pp. 1671-1674.

Prévot M., Mankinen R. S., Gromme S., and Leccaille A. (1983). High paleointensity of the geomagnetic field from thermomagnetic studies on rift valley pillow basalts from the middle Atlantic ridge. *Journal of Geophysical Research*, V.88, pp. 2316-2326.

Riisager J., Perrin M., Riisarger P., and Ruffet G. (2000) Paleomagnetism, paleointensity and geochronology of Miocene basalts and baked sediments from Velay Oriental, French Massif Central. *Journal Geophys. Res.* V. 105, pp. 883-896.

Riisarger P., Riisarger J., Abrahamsen N., and Waagstein R. (2002). Thellier paleointensity experiments on Faroes flood basalts: Technical aspects and geomagnetic implications. *Phys. Earth Planet. Inter.,* V. 113, pp. 91-100.

Selkin P. A., Tauxe L. (2000). Long-term variations in palaeontensity. *Philos. Trans. R. Soc. London* A 358, pp. 1065-1088.

Steele K. W. (1985). Paleomagnetic constraints on the volcanic history of Iztaccihuatl. *Geofisica Internacional,* V. 24 (1), pp. 159-167.

Stéphane S. and Guillou H. (2004). A critical evaluation of young (near-zero) K-Ar ages. *Eartn and Planetary Science Letters*, V. 229, pp.265-275.

Tanaka H., and Kono M. (1991). Preliminary results and reliability studies on historical and radiocarbon dated Hawaiian lavas. *J. Geomag. Geoelectr.,* V. 43, pp. 375-388.

Tauxe L. (1993). Sedimentary records of relative paleointensities: Theory and Practise. *Rev. Geophys.,* V. 31, pp. 319-354.

Tauxe L., Mullender T.A.T., Pick T. (1996) Pot-bellies, wasp-waists and superparamagnetismo in magnetic hysteresis. *Journal of Geophysical Research,* V. 95, pp. 12337-12350.

Thellier E. and Thellier O. (1959). Sur l'intensite de champ magnetique terrestre dans le passe historique et geologique. *Ann. Geophys,*. V. 15, pp. 285-376.

U.S.-Japan Paleomagnetic Cooperation Program in Micronesia (1975). Paleosecular variation of lavas from the Marianas in the Western Pacific Ocean. *Journal Geomag. Geolectr.,* V. 27, pp. 57-66.

Urrutia-Fucugauchi J. and Martin del Pozzo A. (1993). Implicaciones de los datos paleomagneticos sobre la edad de la Sierra de Chichinautzin, cuenca de Mexico. *Geofisica Internacional*, V. 32, pp. 523-533.

Urrutia-Fucugauchi J. (1995). Constraints on Brunhes low-latitude paleosecular variation-Iztaccíhuatl stratovolcano, basin of Mexico. *Geofisica Internacional,* V. 34 (3), pp. 253-262.

Urrutia-Fucugauchi J. (1997). Comments on "A new method to determine paleosecular variation" by D. vandamme. *Phys. Earth Planet. Inter.,* V. 102, pp. 295-300.

Urrutia-Fucugauchi J. and Campos-Enriquez O. (1993). Geomagnetic secular variation in Central Mexico since 1923 AD and comparison with 1945-1990 IGRF models. *Journal Geomagn. Geoelectr.,* V. 45, pp. 243-249.

Urrutia-Fucugauchi J., and G. L. del Castillo, (1977). Un modelo del Eje Volcanico Mexicano. *Bol. Soc. Geol. Mexicana,* V. 38, pp. 18-28.

Vandamme D. (1994). A new method to determine paleosecular variation. *Phys. Earth Planet. Inter,.* V. 85, pp. 131-142.

Zijderveld, J. D. A.. (1967). A. C. demagnetization of rocks: analysis of results, in Methods in Palaeomagnetism. E*ds Colinson, D. W., Creer, K. M. & Runcorn, S. K., Elsevier, Amsterdam.* pp. 254-286.

Erroneous Results from Historic Lavas: A Microwave Paleointensity Analysis of Paricutin Volcano, Mexico

A. Goguitchaichvili, Gennaro Conte, J. Urrutia-Fucugauchi, L. Alva-Valdivia, J. Morales.

Laboratorio de Paleomagnetismo y Geofisica Nuclear, Instituto de Geofisica, UNAM, Ciudad Universitaria, 04510 México DF, MÉXICO.

Submitted in: Geofisica Internacional.

Abstract

We report a microwave paleointensity study of historic lavas from Paricutin volcano, erupted during the period between 1943 and 1948. Most samples are characterized by uni-vectorial orthogonal plots. Rock-magnetic and microscopy studies indicate pseudo-single-domain titanomagnetites as the remanence carriers. The microwave paleointensity technique was applied to selected samples using both Kono and Ueno (1977) and Coe et al. (1978) variants of the Thellier method. The samples yielded technically high quality paleointensity results, though show high within-flow dispersion and are significantly different from the expected value of 45μT. This is also seen in results using the Thellier method (Urrutia-Fucugauchi et al., 2004). Explanations for this behaviour are explored, with reference to other historic lava studies. The technically high quality of the results suggest there is no criteria that can distinguish between correct and erroneous paleointensity data.

Introduction

The determination of the absolute strength of the geomagnetic field is important for understanding the processes in the core that generate the field and the processes by which the field reverses polarity. Reliable absolute palaeointensities are generally much more difficult to obtain than directional data, because only certain igneous rocks which satisfy specific magnetic criteria (e.g. Kosterov & Prévot, 1998) are considered useful for paleointensity determination.

The intensity of a paleofield may be estimated by comparing the intensity of the thermoremanent magnetization (TRM) acquired by a volcanic rock at the time of cooling with the strength of a laboratory TRM produced by a known field (Koenisberger, 1938). However, heating of the magnetic remanence carriers above their maximum blocking temperatures may alter initial magnetic mineralogy and may invalidate the original TRM and laboratory TRM ratio. Thellier and Thellier (1959) devised a method to study partial TRM (pTRM), obtained from parts of the blocking/unblocking temperature spectra unaffected by magneto-mineralogical alteration. However, for the majority of natural rocks, alteration may occur at low

temperatures, which can impede an accurate determination of paleointensity (Calvo et al., 2002).

A TRM is formed when heat, in the form of phonons, is sufficient to generate spin waves (magnons) within the individual magnetic domains (Walton et al., 1993). These spin waves allow magnetization to reverse, and during cooling the magnetization becomes fixed with a statistical bias towards the ambient magnetic field direction. Alternatively, spin waves can be generated within magnetic grains by direct microwave excitation (e.g. Shaw et al., 1996). The TRM formed by this method is almost identical to the one formed by heating (Hill et al., 2002), except only the magnetic system is heated and cooled in a few seconds (and not the matrix). As this microwave TRM (T_MRM) does not involve bulk sample heating (Walton et al., 1993), this technique is ideal for determining palaeointensities.

It is pertinent to study the paleomagnetic behaviour of historic lava flows, as the geomagnetic field at time of extrusion is known. In this study, we report a microscopic, rock-magnetic and microwave paleointensity investigation of the historic lava flows of Paricutin volcano, Mexico, during the period between 1943 and 1948. These lava flows are well exposed and appear fresh. Absolute intensity values obtained were compared to the data from the Teoloyucan Geomagnetic Observatory, located north of Mexico City, 320 km East of Paricutin volcano (Figure 1).

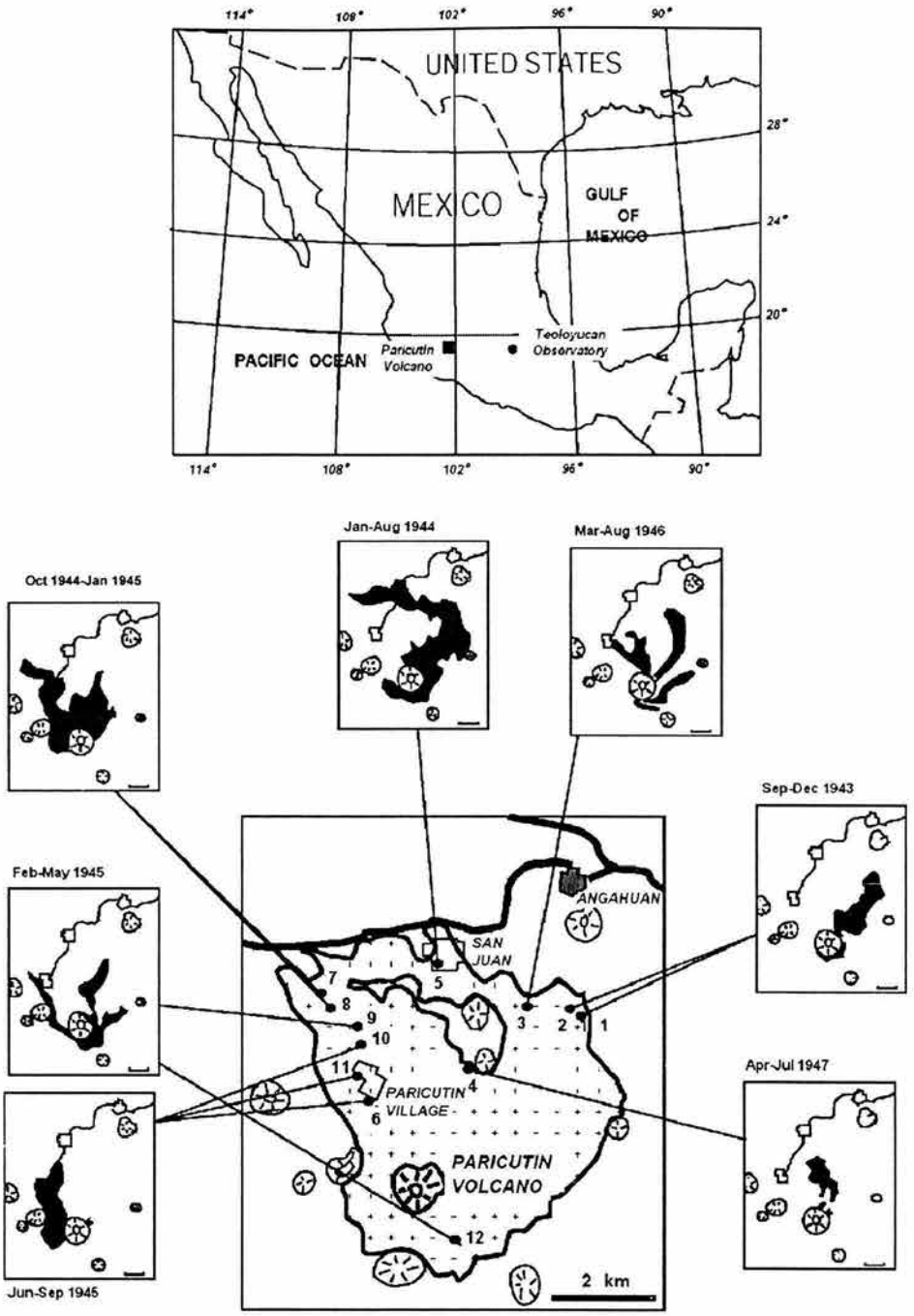

Fig. 1 Location of Paricutin volcano and Teoloyucan Geomagnetic Observatory. Schematic map of the Paricutin volcano, its lava field (shaded area) and location of paleomagnetic sampling sites (numbered dots). The distribution of sites in terms of lava eruptive episodes is shown in the small maps, with dates of the episode and the aerial extension of lavas (maps adopted from Luhr and Simkin, 1993). Each site corresponds to one individual lava flow.

Sampling Details

One of the best-documented cases of volcano formation is the 1943-1952 eruption of Paricutin in central Mexico (Figure 1). Paricutin Volcano first erupted on February 20, 1943 near San Juan Parangaricutiro village, Michoacan State, Mexico (Ordoñez, 1943). This is in the Michoacan-Guanajuato volcanic field, characterized by numerous cinder cones and medium-sized shield volcanoes.

Both formation and growth of Paricutin volcano have been extensively discussed by Fries, (1953), Segerstrom, (1965), Luhr & Simkin, (1993) amongst others. Volcanism continued from 1943 through to 1952 (Figure 1). The composition and petrography of erupted material changed from olivine-bearing basaltic andesites in 1943 to orthopyroxene-bearing andesites at the end of 1952 (Wilcox, 1954). One hundred and two oriented standard paleomagnetic cores from 12 flows were collected from seven different lava effusion episodes, which cover the interval between September-December 1943 and March-August 1946 (Figure 1). Samples were distributed throughout each flow both horizontally and vertically in order to minimize effects of block tilting and lightning strikes. Cores were obtained with a gasoline-powered portable drill, and oriented with both magnetic and sun compasses.

Rock Magnetic Experiments

To identify the magnetic remanence carriers and to obtain information about their paleomagnetic stability, rock-magnetic experiments were performed. These experiments include reflected light microscopy, measurements of susceptibility curves, hysteresis combined with IRM (isothermal remanent magnetization) experiments and alternating field (AF) demagnetisation of the natural remanent magnetization (NRM)

Microscopy Observations

A study of the opaque mineralogy was conducted with an optical microscope using polished sections and oil immersion. In general, the studied samples exhibit two generations of Fe-Ti oxides (Figure 2a). 'Skeletal' titanomagnetites are abundant in most of the studied lavas indicating fast cooling (e.g. sample P-25). However, it is

hard to observe any textural characteristics. In other cases, typical titanomagnetite-ilmenite intergrowths (Haggerty, 1976) were detected (e.g. sample P-72). Theoretically, the NRM carried by these grains may be a TRM, as this paragenesis typically develops at temperatures higher than the Curie point of magnetite (~ 578°C).

Continuous Susceptibility Measurements

Continuous susceptibility measurements were performed on one sample per flow using a Bartington MS2 system. Samples were heated up to ~625°C at a rate 20°C/min and cooled at the same rate. We note that in some cases, the cooling and heating curves are not perfectly reversible. Curie temperatures were determined by the Prévot et al. (1983) method. In general, the curves show the presence of a single magnetic/ferrimagnetic phase with Curie point 570°C compatible with relatively low-Ti titanomagnetites (Figure 2b). This agrees with the microscopic observations.

Hysteresis Experiments

Room temperature hysteresis measurements were performed on all samples using the AGFM 'Micromag' apparatus at the paleomagnetic laboratory in Mexico City, with applied fields up to 1 Tesla. Saturation remanent magnetization (M_r), saturation magnetization (M_s) and coercive force (H_c) were calculated after correction for paramagnetic contribution (Figure 2c). Coercivity of remanence (H_{cr}) was determined by applying a progressively increasing backfield IRM after saturation. No potbellied or wasp-waisted behavior (Tauxe et al., 1996) was detected, reflecting restricted ranges of magnetic mineral coercivities. From the ratios of hysteresis parameters, all samples plot in the pseudo-single domain (PSD) grain size region (Day et al., 1977). Corresponding IRM acquisition curves (not shown) were found to be similar for all samples. Saturation is reached in moderate fields of the order of 150-200 mT, suggesting spinels, probably titanomagnetites, as remanence carriers.

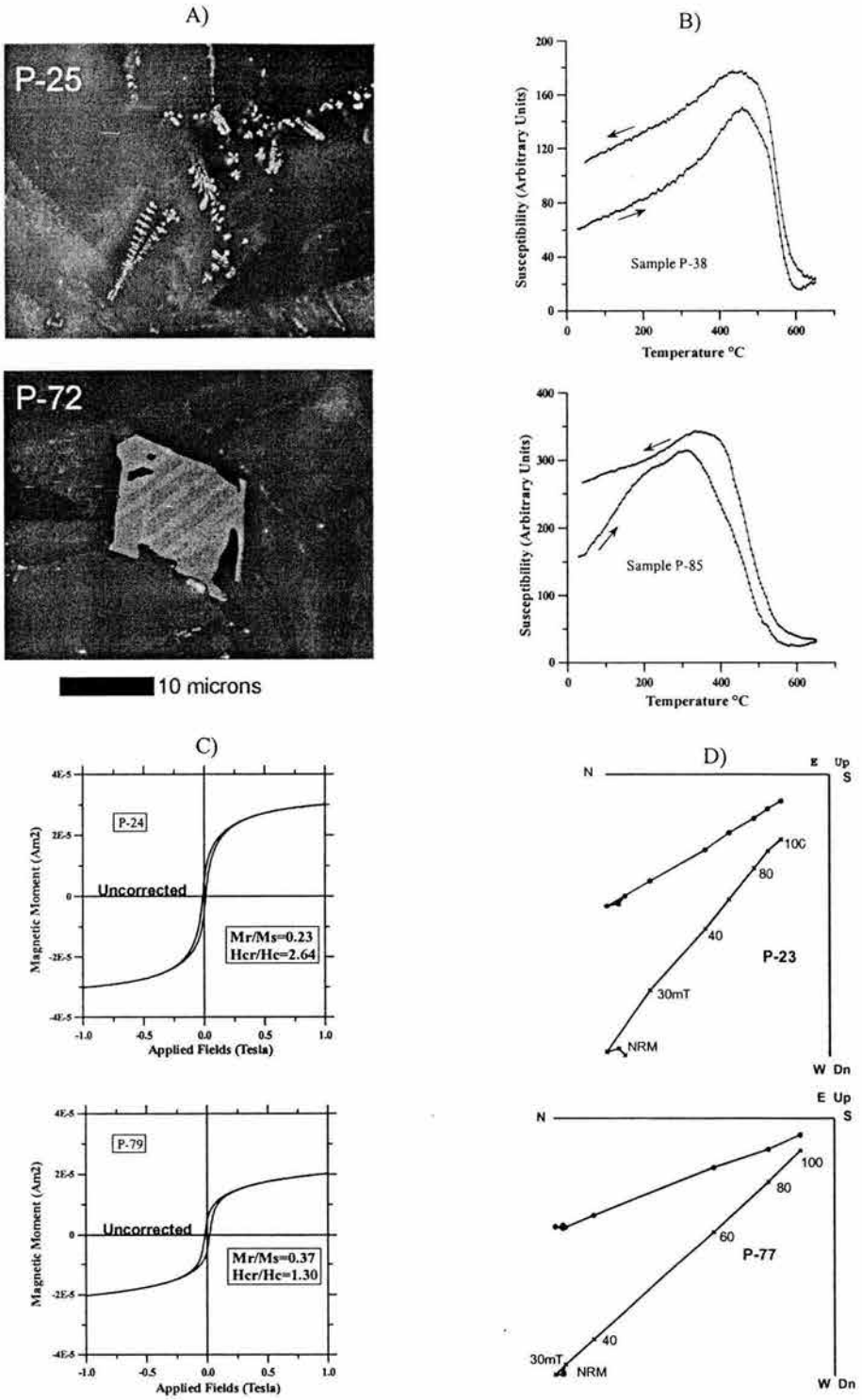

Fig. 2 A) Representative photomicrographs of the opaque minerals; B) Representative susceptibility versus temperature curves. The arrows indicate the heating and cooling curves; C) Examples of hysteresis loops (uncorrected for paramagnetic component) of sample chips; D) Orthogonal vector plots of stepwise AF demagnetization (stratigraphic coordinates). Numbers refer to peak alternating fields in mT. o – projections into the horizontal plane, x – projections into the vertical plane.

AF demagnetization

Remanence measurements were made using a JR6 (AGICO) spinner magnetometer. Stepwise AF demagnetization used a Molspin AF demagnetizer, providing fields up to 100 mT. Most samples show single component magnetization (Figure 2d). A generally small secondary component, probably of viscous origin, is sometimes present but easily removed. The median destructive fields (MDF) range mostly from 35 to 50 mT, suggesting small pseudo-single domain grains as remanent magnetization carriers (Dunlop and Özdemir, 1996). The overall-mean direction estimated for all flows is: Dec=1.8°, Inc=37.5°, k=26, α_{95}=8.7°, N=12 (Urrutia-Fucugauchi et al., 2004).

Rock magnetic summary

From the results of all the above experiments, the majority of the samples exhibit a single component thermal remanence that is carried by low-Ti titanomagnetites, of a grain size in the pseudo-single domain range.

Microwave Paleointensity Experiments

Two sets of experiments were carried out at the Geomagnetism Laboratory, University of Liverpool. The first method used, detailed by Hill and Shaw (1999), is a variant of the stepwise Thellier method (Kono and Ueno, 1977), in which a microwave thermoremanence (T_MRM) is induced perpendicular to the primary NRM direction, so that only a single microwave application is required for each power step (Figure 3a). This eliminates the need for accurate reproducibility of microwave power absorbed by the sample. This method was performed on 21 samples (Figure 3a). 13 sister samples were subjected to the double 'heating' modified Thellier type (Coe, 1967) procedure (Figure 3b), with demagnetisation and remagnetisation steps performed in a zero and an arbitrarily oriented applied field, respectively. The latter method included the addition of pT_MRM checks.

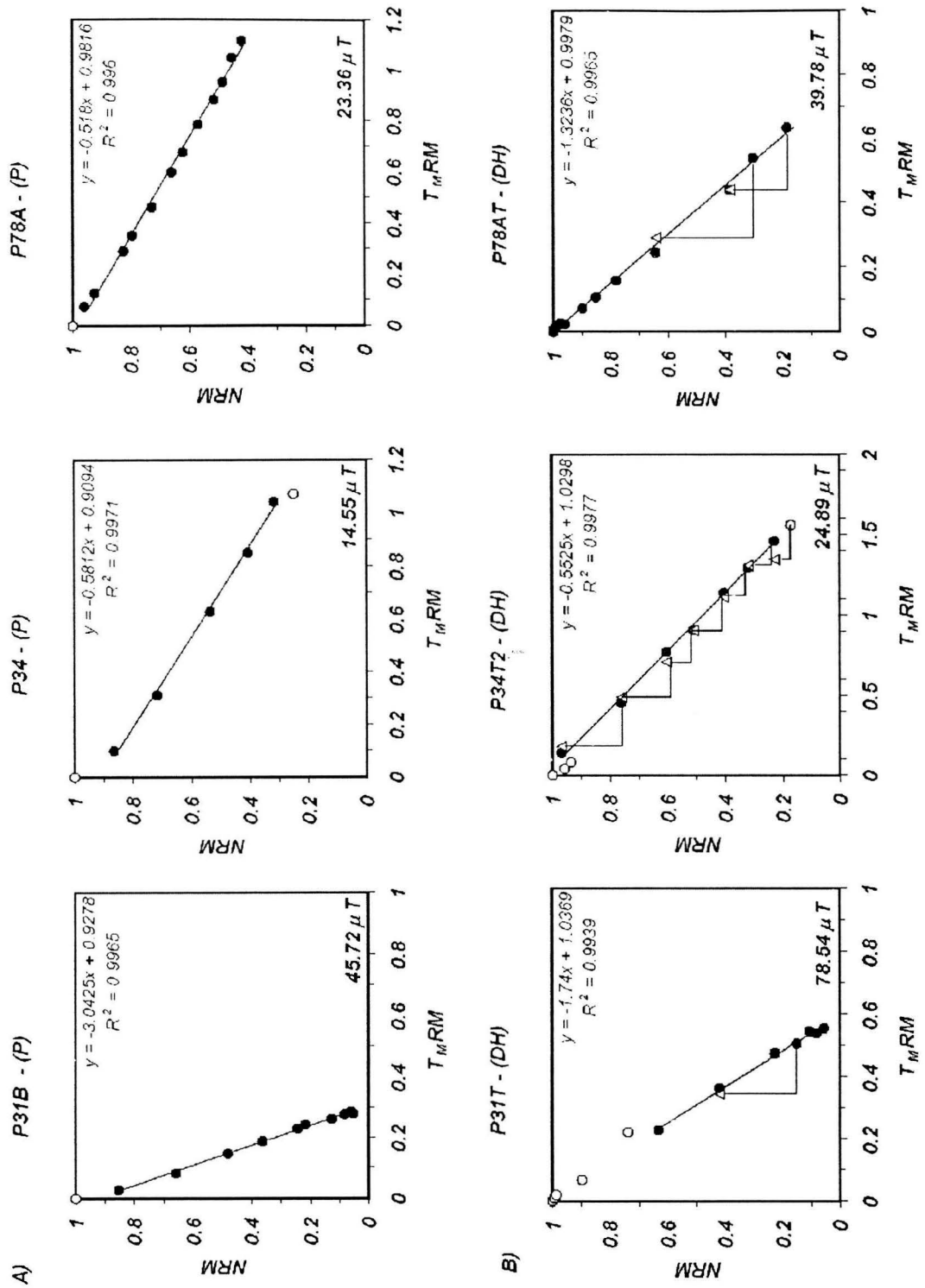

Fig. 3 Representative NRM-T_MRM plots (Arai plots) for Paricutin lavas obtained using the A) Kono and Ueno (1977) and B) Coe et al. (1978) methods.

Results

23 out of 34 samples (68%) yielded technically acceptable quality paleointensity determinations (Figure 3 and Table 1). The accepted minimum NRM fraction f, was 0.32 (mean value of 0.62) and the minimum quality factor, (Coe et al., 1978) q was 5, with a mean of 23. Results with less than four points and a regression coefficient r^2 of less than 0.99 on the slope of the Arai plot were rejected. In total, we rejected 11 samples that did not meet these criteria. With the perpendicular field method, the sum of the angles between the total magnetization vector and the NRM and T_MRM directions was monitored during each step, and if any increase above 90° was observed, the experiment was terminated, as this implied the primary NRM direction was not isolated or unstable. With the double 'heating' method, a maximum difference between the pT_MRM and the pT_MRM check of 20% was used.

Overall, the mean paleointensity estimate is calculated as 35 ± 19μT, with results ranging from 11 to 79μT. This is significantly different from the expected intensity of ~45μT, from observatory data (Figure 4), though similar to dispersion seen from the Thellier study (Figure 5) which gives a mean of 36 ± 20μT (Urrutia-Fucugauchi et al., 2004). Some samples taken from the same 25mm core, using both variants of the microwave method, yielded different results (e.g. samples P31, P34A, P78A – see Figure 3). This is different from other microwave paleointensity studies which show a high correlation between pairs of samples from the same 25mm core (Gratton et al., in prep.) and between the two methods (Hill et al., 2002). In the majority of cases, the double 'heating' method yields higher results than those obtained using the perpendicular field, suggesting that undetected alteration may have occurred in the latter case, resulting in a lower field estimate, due to increased TRM capacity.

Table 1

Accepted samples

Eruption	Sample	Site	F	Error	N	f	g	q	r^2	System	Method	F	Error
S5. Jan-Aug 1944	P31B	5	45.72	1.45	10	0.80	0.83	31.55	0.9965	14 GHz	P	42.17	24.60
S5. Jan-Aug 1944	P31Q	5	47.13	0.75	7	0.86	0.76	63.09	0.9995	14 GHz	P		
S5. Jan-Aug 1944	P31T	5	78.54	6.68	7	0.57	0.72	11.76	0.9939	14 GHz	DH		
S5. Jan-Aug 1944	P34	5	14.55	1.12	5	0.55	0.73	13.00	0.9971	14 GHz	P		
S5. Jan-Aug 1944	P34T2	5	24.89	0.90	7	0.74	0.81	27.72	0.9977	14 GHz	DH		
S6. Jun-Sep 1945	P37B2	6	15.48	0.69	9	0.68	0.79	22.59	0.9960	14 GHz	P	15.48	-
S7. Oct1944-Jan1945	P48A1	7	26.19	1.95	5	0.37	0.45	13.41	0.9995	8.2 GHz	P	43.24	20.12
S7. Oct1944-Jan1945	P48A3	7	24.46	1.10	11	0.70	0.81	22.24	0.9942	14 GHz	P		
S7. Oct1944-Jan1945	P53B	7	50.62	1.33	8	0.81	0.81	37.94	0.9982	14 GHz	P		
S7. Oct1944-Jan1945	P55A3	7	41.37	3.68	12	0.33	0.68	11.23	0.9961	14 GHz	P		
S7. Oct1944-Jan1945	P55AT2	7	73.55	2.67	12	0.85	0.86	27.58	0.9930	14 GHz	DH		
S8. Oct1944-Jan1945	P61B	8	34.76	1.16	8	0.77	0.74	30.03	0.9978	14 GHz	P	34.76	-
S10. Jan-Sep 1945	P71T	10	16.33	0.48	10	0.94	0.91	33.88	0.9938	14 GHz	DH	23.09	9.70
S10. Jan-Sep 1946	P71U	10	17.84	0.71	10	0.90	0.86	24.95	0.9925	14 GHz	DH		
S10. Jan-Sep 1945	P71Q	10	18.16	0.55	7	0.66	0.76	33.07	0.9989	14 GHz	P		
S10. Jan-Sep 1945	P78A	10	23.36	0.96	12	0.54	0.89	24.25	0.9960	14 GHz	P		
S10. Jan-Sep 1945	P78AT	10	39.78	1.03	14	0.81	0.82	38.60	0.9965	14 GHz	DH		
S11. Jan-Sep 1945	P81A	11	12.02	1.14	10	0.40	0.87	10.58	0.9915	14 GHz	P	30.53	21.99
S11. Jan-Sep 1945	P81AT	11	11.20	1.13	6	0.45	0.81	9.90	0.9946	14 GHz	DH		
S11. Jan-Sep 1945	P83A	11	46.34	3.03	8	0.46	0.81	15.31	0.9988	14 GHz	P		
S11. Jan-Sep 1945	P83AT	11	52.54	8.07	8	0.40	0.79	6.51	0.9858	14 GHz	DH		
S12. Feb-May 1945	P87BT	12	41.48	3.50	8	0.42	0.83	11.85	0.9948	14 GHz	DH	41.06	0.60
S12. Feb-May 1945	P91BT	12	40.64	7.04	4	0.32	0.61	5.78	0.9977	14 GHz	DH		

Rejected samples

Eruption	Sample	Site	F	Error	N	f	g	q	r^2	System	Method
S1. Sep-Dec 1943	P4B	1	36.00	12.32	11	0.18	0.86	2.92	0.9741	14 GHz	P
S1. Sep-Dec 1943	P4T2	1	30.10	8.93	10	0.27	0.83	3.37	0.9649	14 GHz	DH
S1. Sep-Dec 1943	P4T	1	31.50	5.64	7	0.25	0.84	5.59	0.9929	14 GHz	DH
S6. Jun-Sep 1945	P37B1	6	11.38	146.55	4	0.01	0.55	0.08	0.9894	8.2 GHz	P
S7. Oct1944-Jan1945	P48A2	7	26.37	17.79	7	0.16	0.79	1.48	0.9638	8.2 GHz	P
S7. Oct1944-Jan1945	P55A2	7	51.63	25.70	8	0.10	0.72	2.01	0.9917	8.2 GHz	P
S8. Oct1944-Jan1945	P59AB	8	6.90	69.30	4	0.17	0.61	0.10	0.9924	14 GHz	P
S8. Oct1944-Jan1945	P61BT	8	27.10	2.84	11	0.16	0.83	9.56	0.9983	14 GHz	DH
S10. Jan-Sep 1945	P71	10	5.97	1.99	8	0.28	0.82	3.00	0.9645	14 GHz	P
S12. Feb-May 1945	P87B	12	41.00	11.13	4	0.31	0.64	3.68	0.9942	14 GHz	P
S12. Feb-May 1945	P91B	12	52.80	5.07	8	0.28	0.84	10.42	0.9970	14 GHz	P

Microwave paleointensity results from the Paricutin Volcano. F: individual paleointensity estimate with associated error (1/q); F: flow mean paleointensity with Error (standard deviation); N: number of NRM-T_MRM points used for paleointensity determination; *f*, *g* and *q* are the fraction of NRM used, the gap factor and quality factor (Coe et al., 1978); r^2: regression coefficient of the slope; System: microwave system used (8.2 or 14GHz), Method used: P – perpendicular field, DH – double 'heating'.

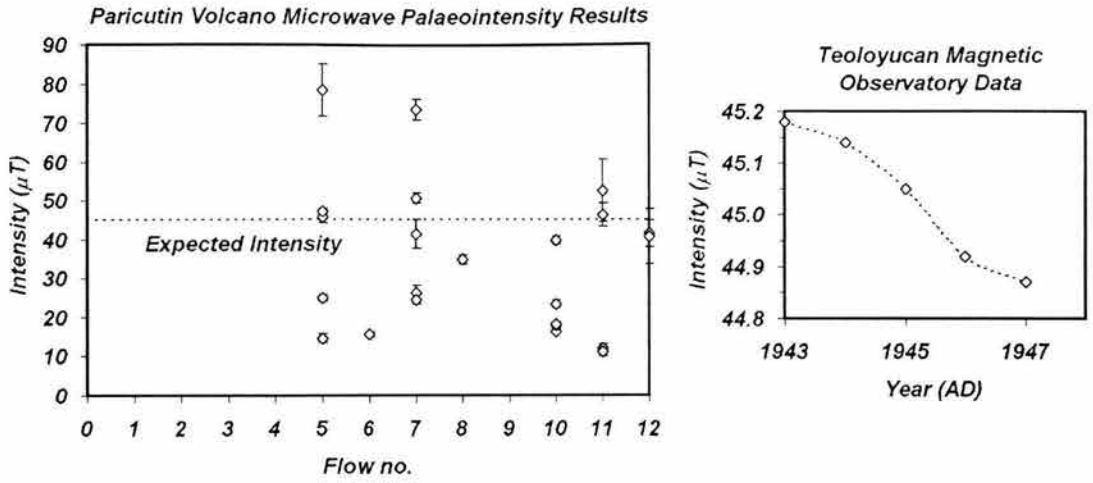

Fig. 4 Microwave paleointensity results for all studied Paricutin samples (see also Table 1) and total field intensity recorded at the Teoloyucan Geomagnetic Observatory during the study period.

Discussion

The mean values for flows 5, 7 and 12 are comparable with observatory data, though associated standard deviations for flows 5 and 7 are large (~50%). There are no significant differences in quality between results from these flows and those that give different results to the expected values. There have been several paleointensity studies of historic lavas that record problematic paleointensity results, including a previous investigation of the Paricutin flows (Gonzalez et al., 1997), which found similar dispersion of results using both Thellier and Shaw methods.

A through-flow study of the Holocene Xitle lava flow, Mexico by Böhnel et al. (1997) showed a high within-flow dispersion of paleointensity results, attributed to rock magnetic variations throughout the flow. A study of historical lava flows from Mt. Etna (Calvo et al., 2002) found that acceptable results (including positive pTRM checks) overestimated the field by 25%. This was attributed to multi-domain (MD) grains carrying the majority of the remanence. The majority of acceptable Paricutin flow results (including positive pT_MRM checks) both overestimate *and* underestimate the correct value, therefore MD behaviour is not likely to be only the cause of the wide-dispersion seen here.

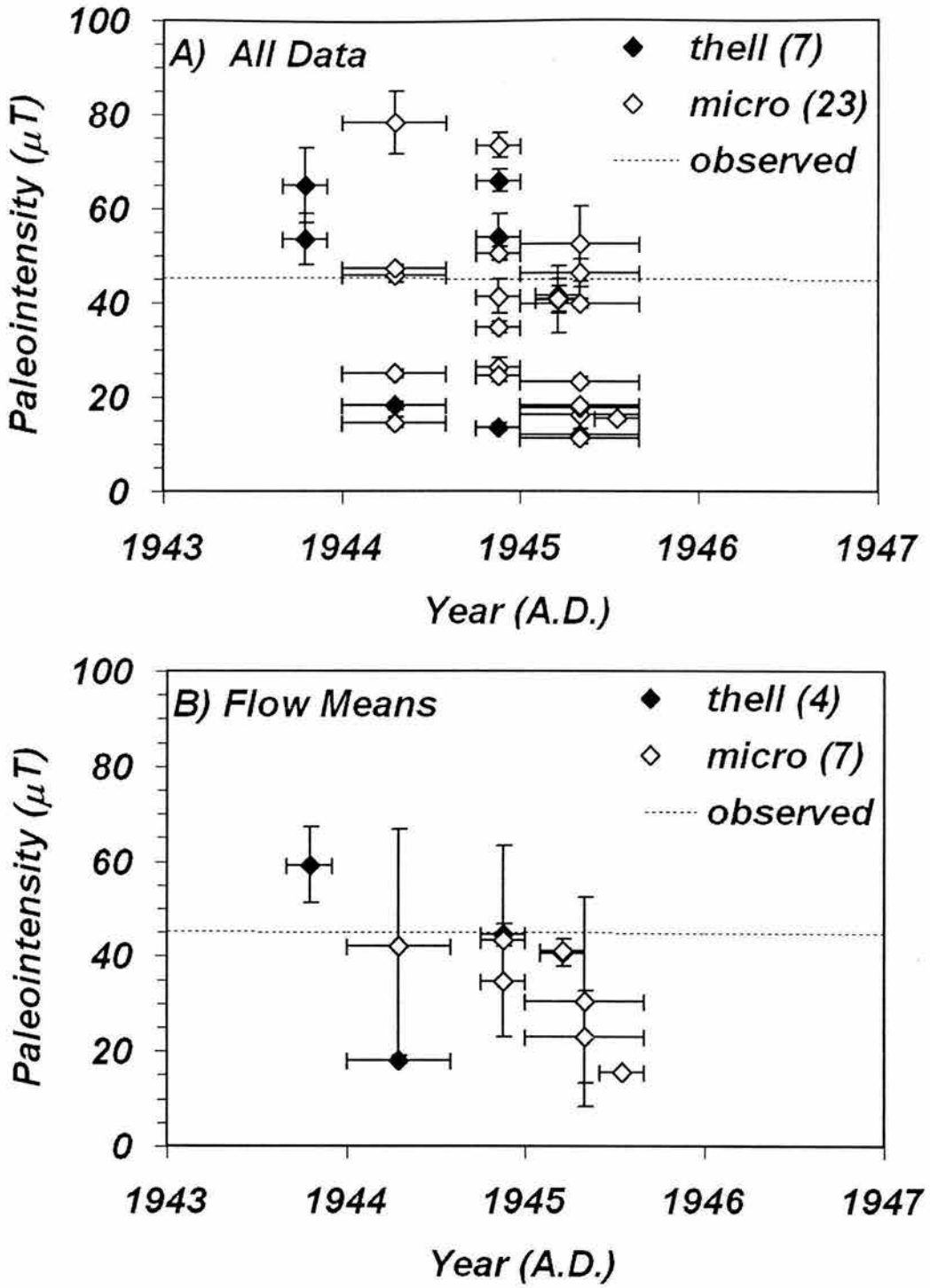

Fig. 5 Comparison of microwave and Thellier paleointensity results. A) Individual data, B) Flow mean values.

Another explanation for the results is that the TRM is of (thermo)chemical origin (CRM or TCRM). In a study of cooling Hawaiian lava lakes, Grommé et al. (1969) found zones in which NRM was held by minerals formed by subsolidus reactions at temperatures below their Curie point. Like the Paricutin lavas, Ti-poor titanomagnetites with visible ilmenite lamellaes were responsible for the remanence. Rolph (1997) studying the 1169 and 1971 eruptions of Mt. Etna and Hill and Shaw (2000) studying 1960 Kilauea (Hawaii) lava flows also suggested the reason for anomalous results could be due to CRM in some samples of their collection. Presently, it is almost impossible to distinguish between TRM and CRM due to the lack of any strict criteria. McClelland (1996) suggested that grain-growth CRM carried by magnetite or hematite could be distinguished from a TRM by analyzing a Thellier paleointensity experiment. A 'slow / fast growth CRM' may show a concave-up Arai plot, though Körner et al. (1998) and Goguitchaichvili et al. (1999) do not observe this concavity on artificially induced CRMs.

The number of determinations per flow may also be a factor in this high-dispersion. In this study, the average number of determinations per flow is less than two (counting multiple results from the same 25mm core as one determination), and this low number will not represent the total flow. Statistical analyses by Biggin et al. (2003) suggest that the present norm of determinations per flow should be trebled to gain a more representative estimate of the flow mean value.

Conclusions

Both microwave methods used in this study, and also the Thellier paleointensity methods have yielded widely dispersed paleointensity values from the historically observed geomagnetic intensity. This study demonstrates that even with the knowledge of the rock magnetic characteristics of the samples and the strength of the geomagnetic field during cooling of the lava, technically accurate paleointensity results using a variety of methods, may yield incorrect results. The simplest explanation for this discrepancy is that the NRM is not a pure TRM, though there is no hard evidence to support this. The study demonstrates that when both high within-flow dispersion and non-reproducibility within a 25mm core are observed, a reliable

paleointensity determination is not possible. The technically high quality of the results suggest that there is no set criteria that can discriminate between accurate and inaccurate paleointensity data.

Acknowledgments

We acknowledge the financial support of DGAPA-UNAM IN100403 and CONACYT grant n° 42661. The microwave measurements were carried out by Martin Gratton in the paleomagnetic laboratory of University of Liverpool.

References

Aitken, M. J., Pesonen, L.J., Leino, M., (1991). The Thellier paleointensity technique: Minisamples versus standard size, *J. Geomag. Geoelctr.*,V. 43, pp. 325-331.

Böhnel , H., Morales, J., Caballero, C., Alva, L., McIntosh, G., Gonzalez, S.,Sherwood, G., (1997). Variation of rock magnetic parameters and paleointensities over a single Holocene lava flow. *J. Geomag. Geoelectr.,* V. 49, pp. 523-542.

Biggin, A. J., Böhnel, H. N., Zúñiga, F. R., (2003). How many paleointensity determinations are required from a single lava flow to constitute a reliable average? *Geophys. Res. Lett.*, V. 30, DOI 10.1029/2003GL017146.

Biquand, D., (1994). Effet de la vitesse de refroidissement sur l' aimantation de thermoremanente: Etude experimentale, conséquences theoriques, Can. *J. Earth Sci.*, V. 31, pp. 1342-1352.

Bowles, J., Gee, J., Hildebrand, J., Tauxe, L., (2002). Archeomagnetic intensity results from California and Ecuador: Evaluation of regional data. *Earth Plan. Sci. Lett.*, V. 203, pp. 967-981.

Chauvin, A., (1989). Intensité du champ magnétique terrestre en periode stable et de transition, enregistrée par de sequences de coulées volcaniques du Quaternaire, *Ph.D thesis*, University of Rennes.

Calvo, M., M. Prévot, M. Perrin, J. Riisager, (2002). Investigating the reasons for the failure of paleointensity experiments: A study on historical lava flows from Mt. Etna (Italy). *Geophys. J. Int.*, V. 149, pp. 44-63.

Coe, R. S., (1967). The Determination of Paleo-Intensities of the Earth's Magnetic Field with Emphasis on Mechanisms which Could Cause Non-ideal Behaviour in Thellier's Method, *J. Geomag. Geoelectr.*, V. 19, pp. 157-179.

Coe, R., Grommé, S. & Mankinen, E.A., (1978). Geomagnetic paleointensity from radiocarbon-dated flows on Hawaii and the question of the Pacific nondipole low. *J. Geophys. Res.*,V. 83, pp. 1740-1756.

Day, R., M. Fuller, & V. A. Schmidt, (1977). Hysteresis properties of titanomagnetites: Grain-size and compositional dependence, *Phys. Earth Plan. Int.*, V. 13, pp. 260-267.

Dodson, M.H., & McClellend-Brown, E., (1980). Magnetic blocking temperature of single-domain graons during slow cooling. *J. Geophys. Res.*, V. 103, pp. 30561-30574.

Dunlop, D. & Ozdemir O., (1997). Rock-Magnetism, fundamentals and frontiers, *Cambrige University Press*, pp. 573.

Fox, J.M.W., Aitken, M.J., (1980). Cooling rate dependence of thermoremanent magnetization. *Nature*, V. 283, pp. 462-463.

Fries, C., J., (1953). Volumes and weights of pyroclastic material, lava and water erupted by Paricutin volcano, Mexico. *Trans. Am. Geophys. Union*, V. 34, pp. 603-616.

Garcia. Y., (1996), Variation de l'intensité du champ magnétique en France durant les deux derniers millénaires, *Ph.D thesis*, University of Rennes, pp. 353.

Goguitchaichvili, A., J. Morales, J. Urrutia-Fucugauchi, (2001). On the use of continuous thermomagnetic curves in paleomagnetism. *C.R. Acad. Sci., Earth and Planet. Sci.*, V. 333, pp. 699-704.

Goguitchaichvili, A., Prévot, M., Dautria, J.M., Bacia, M., (1999). Thermo-detrital and crystallo-detrital magnetizations in an Icelandic hyaloclastite. *J. Geophys. Res.*, V. 104, pp. 29219-29239.

Gonzalez, S., Sherwood, G., Böhnel, H., Schnepp. E., (1997). Palaeosecular variation in central Mexico over the last 30 000 years. *Geophys. J. Int.*, V. 130, pp. 201-219.

Goulpeau L., Lanos P., Langouet L., (1989) The anisotropy as a disturbance of the archeomagnetic dating method, Archeometry, proceedings of the 25th international Symposium, *Elsevier Publishers*, pp 45-58.

Gratton, M. N., Herrero-Bervera, E., Shaw, J., (2003). An absolute palaeointensity record from SOH1 lava core, Hawaii using the microwave technique, *in prep.*

Grommé, C. S., Wright, T.L., Peck, D.L., (1969). Magnetic properties and oxidation of Iron-Titanium oxide minerals in Alae and Makaopuhi lava lakes, Hawaii. *J. Geophys. Res.*, V. 74, pp. 5277-5293.

Haggerty, S. E., (1976). Oxidation of opaque mineral oxides in basalts. In*: Oxides Minerals, (Ed. D. Rumble) Mineral. Soc. Amer. Reviews in Mineralogy*, V. 3, pp. 300.

Hill, M. J. & Shaw, J., (1999). Paleointensity results for historic lavas from Mt. Etna using microwave demagnetization/remagnetization in a modified Thellier type experiment. *Geophys. J. Int.*, V. 139, pp. 583-590.

Hill, M. J. & Shaw., J., (2000). Magnetic field intensity study of the 1960 Kilauea lava flow, Hawaii, using the microwave paleointensity technique. *Geophys. J. Int.*, V. 142, pp. 487-504.

Hill, M. J., Gratton, M. N., Shaw, J., (2002). A Comparison of thermal and microwave palaeomagnetic techniques using lava containing laboratory induced remanence. *Geophys. J. Int.*, V. 151, pp. 157-163.

Koenisberger, J. G., (1938). Natural residual magnetism of eruptive rocks. *Terr. Magn. Atmos. Electr.,* V. 43, pp. 299-320.

Kono, M. & N. Ueno, (1977). Paleointensity determination by a modified Thellier method. *Phys. Earth Planet. Int.*, V. 13, pp. 305-315.

Körner, U., Prévot, M. & Poidras, T., (1998). CRM experiments and pseudo-paleointensity measurements on basaltic rocks with initially low Curie temperatures. *Annales Geophysicae, Suppl.*, 1 to V. 16, C210. (Abstract)

Kosterov, A. & M. Prévot, (1998). Possible mechanism causing failure of Thellier paleointensity experiments in some basalts. *Geophys. J. Int.*, **V.** 134, pp. 554-572.

Luhr, J.F. & Simkin, T. (Eds), (1993). Paricutin. The volcano born in a Mexican cornfield. *Geoscience Press, Inc., Arizona, USA*, 427 pp.

McClelland, E., (1984). Experiments on TRM intensity dependence on cooling rate. *Geophys. Res., Lett.*, V. 11, pp. 205-208.

McClelland, E., (1996). Theory of CRM acquired by grain growth and its implication for TRM discrimination and paleointensity determination in igneous rocks. *Geophys. J. Inter.*, V. 126, pp. 271-280.

Ordoñez, E., (1943). El volcan de Paricutin, Com. Imp. Coord. Inv. Cientif. *Anuario, Mexico City*, pp. 241-300.

Prévot, M., Mainkinen, R.S., Grommé, S., Lecaille, A., (1983). High paleointensity of the geomagnetic field from thermomagnetic studies on rift valley pillow basalts from the middle Atlantic ridge. *J. Geoph. Res.*, V. 88, pp. 2316-2326.

Rolph, T.C., (1997). An investigation of magnetic variation within two recent lava flows. *Geophys. J. Int.*, **V.** 130, pp. 125-136.

Shaw, J., Walton, D., Yang, S., Rolph, T.C., Share, J.A., (1996). Microwave archeointensities on Peruvian ceramics. *Geophys. J. Int.*, V. 124, pp. 241-244.

Segerstrom, K., 1965, Paricutin, (1965). Aftermath of eruption. *US Geological Survey Prof. Paper*, 550-C, 93-101.

Tauxe, L., Mullender, T. A. T., Pick, T., (1996). Pot-bellies, wasp-waists and superparamagnetism in magnetic hysteresis. *J. Geophys. Res.*, V. 95, pp. 12337-12350.

Thellier, E. & Thellier, O., (1959). Sur l'intensité du champ magnétique terrestre dans le passé historique et géologique. *Ann. Géophysique*. V. 15, pp. 285-376.

Urrutia-Fucugauchi, J., Alva-Valdivia, L., Goguitchaichvili, A., Rivas, M., Morales, J., (2004). Paleomagnetic, rock-magnetic and microscopy studies of historic lava flows from Paricutin volcano. *J. Geophys. Int.*, V. 156, pp. 431-442.

Walton, D., Shaw, J., Share, J., Hakes, J. (1993). Microwave magnetization. *Geophys. Res. Lett.*, V. 20, pp. 109-111.

Wilcox, R.E., (1954). Petrology of Paricutin Volcano, Mexico. *U.S. Geol. Surv. Bull.*, 965C, pp. 281-353.

Paleosecular Variation of Geomagnetic Full Vector from Vesuvius (Southern Italy): with Special Emphasis on the 1631 Eruption

Gennaro Conte[1], Jaime Urrutia-Fucugauchi[1], Avto Gogichaishvili[1] and Alberto Incoronato[2]

[1] Laboratorio de Paleomagnetismo y Geofisica Nuclear, Instituto de Geofísica, UNAM, Ciudad Universitaria, 04510 México, D.F., México.

[2] Dipartimento di Scienze della Terra, Universita' di Napoli, Largo S. Marcellino n° 10, 80138 Napoli, Italy.

Submitted in: Earth, Planets and Space.

Abstract

We carried out an integrated paleomagnetic, rock-magnetic and paleointensity study of fourteen uncertain-age lavas flows from the Somma-Vesuvius volcanic complex. The magnetic carriers consist in Ti-poor titanomagnetites with pseudo-single domain states. Characteristic magnetization directions determined from detailed stepwise alternating field and thermal demagnetizations give fourteen new well-defined flow unit mean directions. Thirty nine samples from seven lava flows yield reliable paleointensity estimates with the flow-mean virtual dipole moment (VDM) ranging from 7.86 to 13.5 ($10^{22}Am^2$). The mean paleomagnetic directions of eleven lava flows may be correlated with the Southern Italy Secular Variation Curve "SISVC" yielding new constraints on their ages.

Paleodirections for nine lava flows out of twenty-four analyzed (Caraccedo et al., 1993; Gialanella et al., 1993; Hoye, 1981; This Study) appear to be related to the AD 1631 eruption, as indicated by their direct correlation to the early seventeen century segment of the Italian paleosecular variation reference curve. This provides new evidence supporting that the AD 1631 episode was an explosive-effusive eruption.

Key Words: Paleosecular Variation, Vesuvius, 1631 Eruption, Paleointensity, Italy

Introduction

The Somma-Vesuvius volcanic complex, considering its proximity in a densely urban populated area, represents an example where to estimate of the hazard (probability of the occurrence of a disaster in space and time) is a determining factor. Several authors from purely volcanologic view point have studied some products and identified their events, but there are disagreements concerning their nature and distribution areas. In particular the "big eruption" of AD 1631 has been considered by Le Hon (1865) and Johnston Lavis (1884) as the major explosive and effusive event and this has been supported in recent works (Burri and Di Girolamo, 1975; Rolandi et al., 1991). In contrast, authors as Rosi and Santacroce (1986) and Arno et al. (1987) consider this eruption exclusively of explosive character (i.e. without lavas) and

attribute to the supposed lavas of the 1631 event to other eruptions occurred between the 968-1037. Paleomagnetism can help in the discrimination of the products in volcanic area and to contribute to hazard assessment. Paleomagnetic analysis to clear up this problem has been performed by several authors, but the conclusions are discordant too; Carracedo et al. (1993) and Tanguy et al., (1999, 2003) exclude that the eruption was effusive, while Gialanella et al. (1993) and Incoronato (1996) affirm occurrence of associated lavas with this eruption. The event of AD 1631 is not the only eruption in controversy; there are several volcanic units undated or uncertain presented in the geological map of the Somma-Vesuvius volcanic complex (Principe et al., 1987).

In this work, we report a detailed rock-magnetic, paleomagnetic and absolute paleointensity study of uncertain-age lavas flow from Somma-Vesuvius complex with the attempt to contribute to the knowledge on their nature and spatial distribution in the geological map (with particular attention to the AD 1631 eruption). In addition, we report new data to refine of Secular Variation Curve (SVC) for southern Italy.

Geological Setting and Sampling

The Campania plain represents one of the larger volcanic plateaus found in the Italian peninsula. Its formation was related with the tectonic activity that started in the upper Pliocene, following to the formation of Apennine belt. During the Quaternary, due to the subduction of the African plate beneath the Apennines chain, an intense and complex eruptive activity originated the large Roman-Campana Province (Di Girolamo, 1978). The main eruptive centers are localized in the Lazio (Vulsini, Vico, Sabatini) and Campania region (Roccamonfina, Campi Flegrei, islands of Ischia and Procida, and Somma-Vesuvius).

The Somma-Vesuvius is one of the more dangerous volcanic complexes in southern Italy, characterized mainly by explosive activity. Its eruptive history is well documented by historical documents since 79 d.C. The Somma-Vesuvius is formed by two superposed volcanic structures: Vesuvius volcano, with a conical shape truncated to the summit; and the older Somma volcano, which represent the caldera

of complex. The stratigraphical observations and the absolute dating of the some volcanic products intercalated between paleosoils, have evidenced several cycles of eruptive activity, which begins usually with a Plinian eruptions and have duration less than 2000 years. The oldest products of the Somma volcano are estimated as about 25 ka. In general, Somma-Vesuvius complex can be divided in three long periods (Arnó et al., 1987; Santacroce, 1987; Delibrias et al., 1978): 1). The first represents the longer and oldest period of the volcanic complex spending from 25 ka to 79 d.C. (the large plinian eruption), and is characterized by formation of the caldera; 2) The post-caldera activity, which includes many eruptions (at least eleven). Most famous of them are the 79 d.C. and 1631 'big' eruptions. 3) the third period comprises the eruptions between 1631 and 1944.

Generally, 10-12 specimens per site were collected using electric powdered drill and oriented with both magnetic and solar compasses prior to removal. A total of the 180 samples belonging to 14 individual lavas flow were obtained (Figure 1). The cores were later sliced into standard specimen cores (2.5 cm diameter, 2.1 cm high) in the laboratory obtaining 540 specimens.

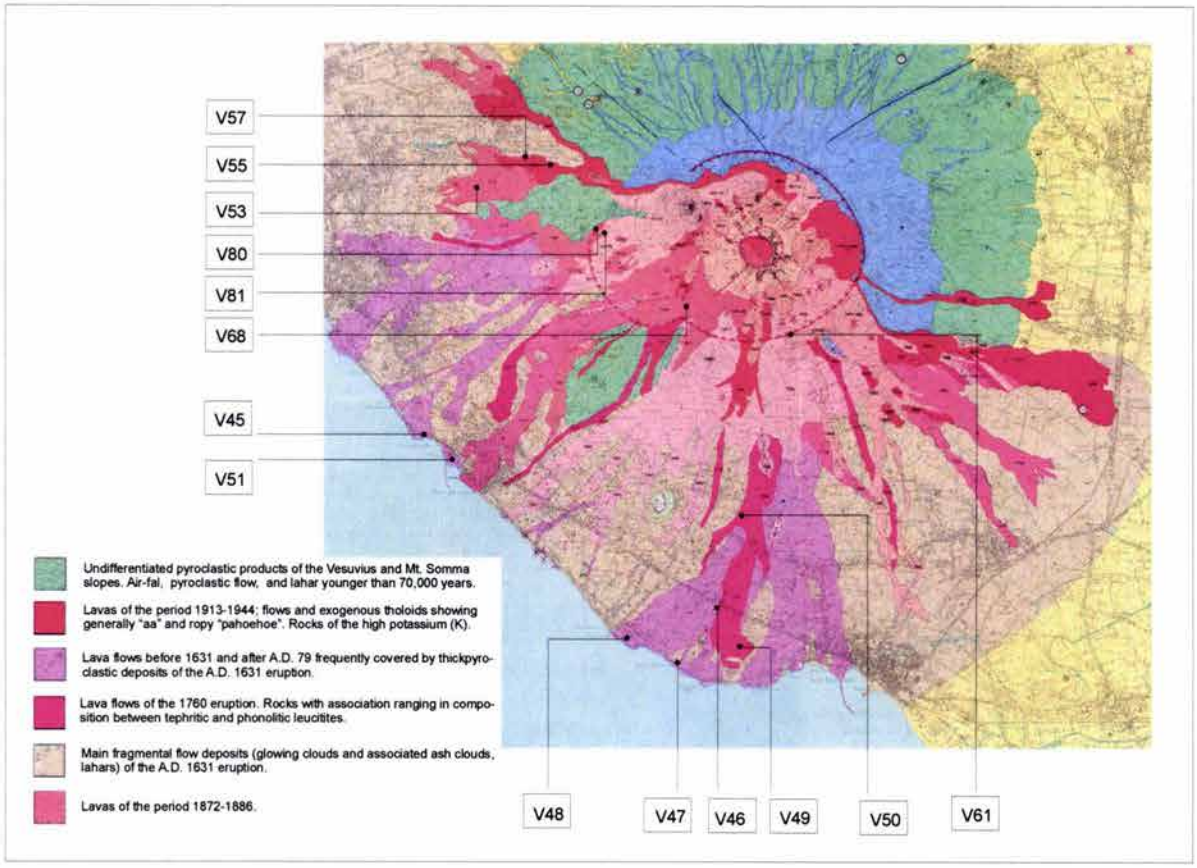

Fig. 1 Simplified geological map of Somma-Vesuvius volcanic complex showing the location of sites. (modified from Principe et al., 1987).

Magnetic Characteristics

Continuous susceptibility curves

One sample per site was heated in air up to 600°C at a heating rate of 10°C/min and then was cooled at the same rate in order to identify magnetic minerals responsible for remanent magnetization. The measurements were carried out using Bartington susceptibility meter MS2 equipped with a furnace. Curie temperature was determined by Prévot et al. (1983) method. These experiments indicate the presence of a single magnetic/ferrimagnetic phase with Curie temperature ranging from 560 to 580°C (Figure 2). We note that in some cases, the cooling and heating curves are not perfectly reversible. Low-Ti titanomagnetite seems to be responsible for remanence in all cases.

Hysteresis measurements

One sample per site was subjected to Hysteresis experiments using AGFM 'Micromag' apparatus in fields up to 1.4 Tesla. The hysteresis parameters (saturation remanent magnetization M_r, saturation magnetization M_s, and coercive force H_c) were calculated after correction for the paramagnetic contribution. Coercivity of remanence (H_{cr}) was determined by applying a progressively increasing back-field after saturation. Three typical hysteresis plots are showed in Figure 2; the curves are quite symmetrical in all cases. Near the origin no potbellied and wasp-waisted behaviors were detected (Tauxe et al., 1996), which probably reflects very restricted range of the opaque mineral coercivities. Judging from the ratios of the hysteresis parameters (H_{cr} / H_c ranges between 1.19 and 2.21 and M_r / M_s varies from 0.08 to 0.26), it seems that all samples fall in the pseudo-single-domain (PSD) grain size region (Day et al., 1977), probably indicating a mixture of multi-domain (MD) and a significant amount of single-domain SD grains (Figures 3 & 4). Isothermal remanent magnetization (IRM) acquisition curves indicate that the saturation is reached in moderate field of the order of 100-200 mT, which point, one more time, to some spinels as remanence carrier (most probably low-Ti titanomagnetites) (Figure 3).

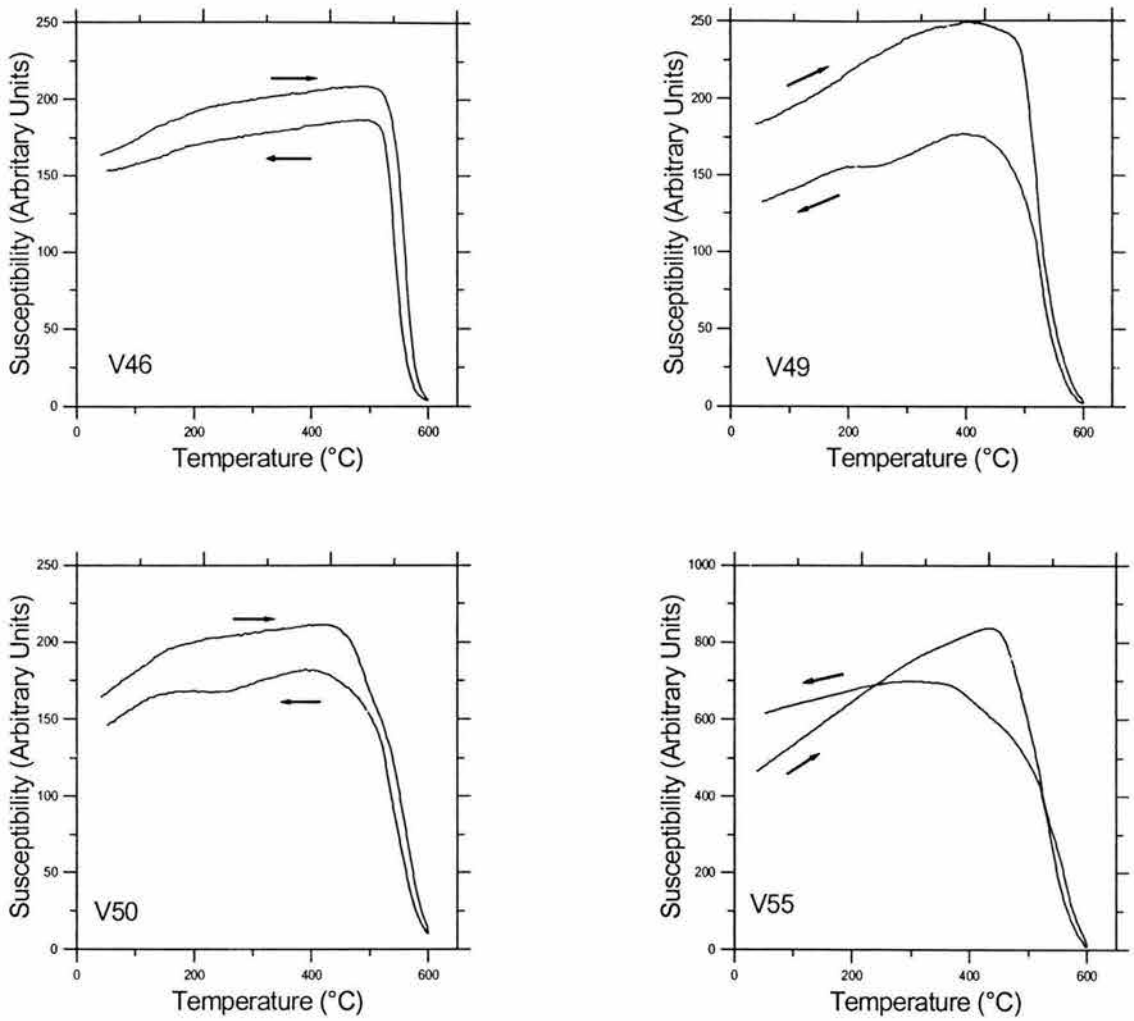

Fig. 2 Susceptibility vs. temperature (in air) curves of representative samples. The arrows indicate the heating and cooling curves.

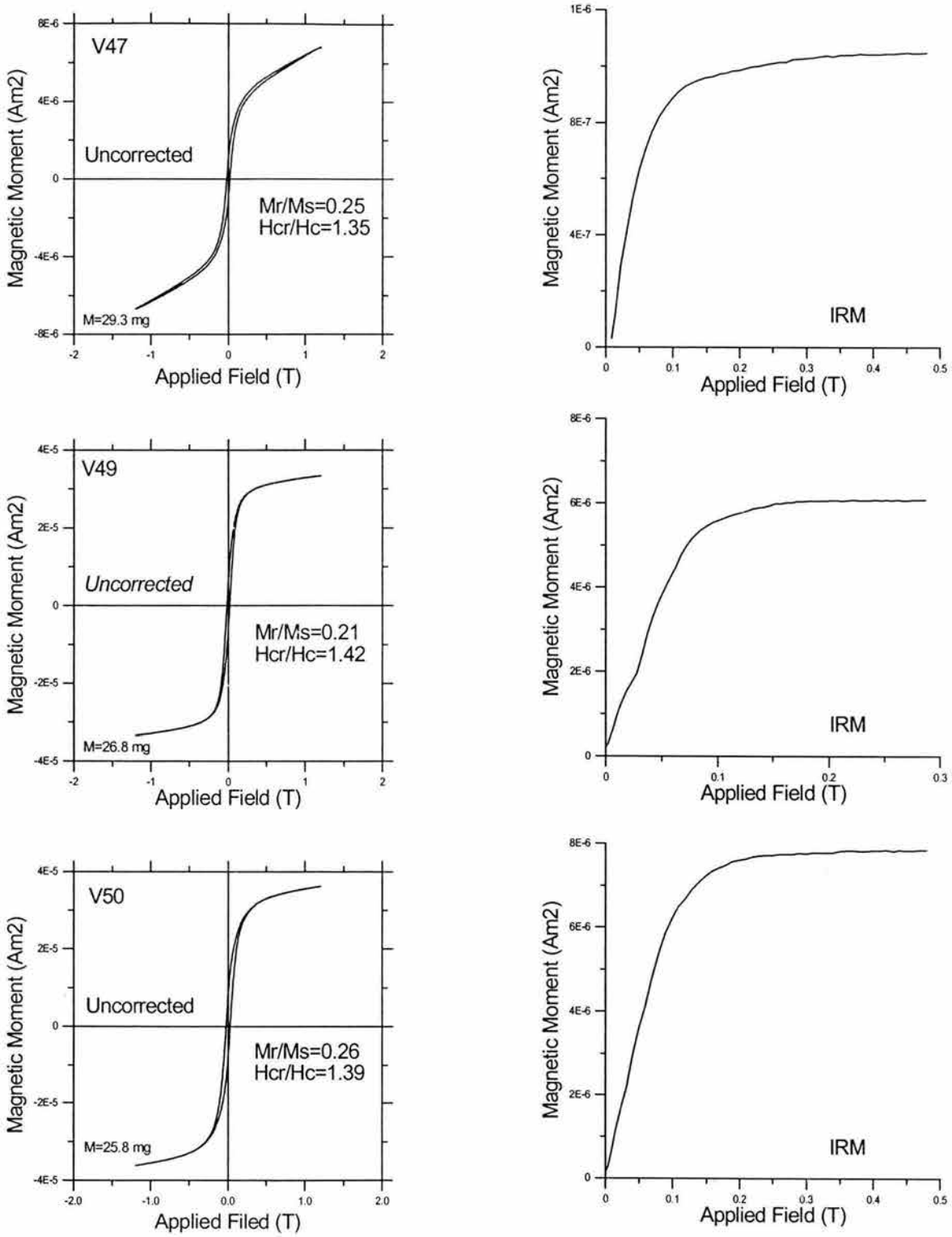

Fig. 3 Typical example of Hysteresis loop (uncorrected) and associated IRM (isothermal remanent magnetization) acquisition curves.

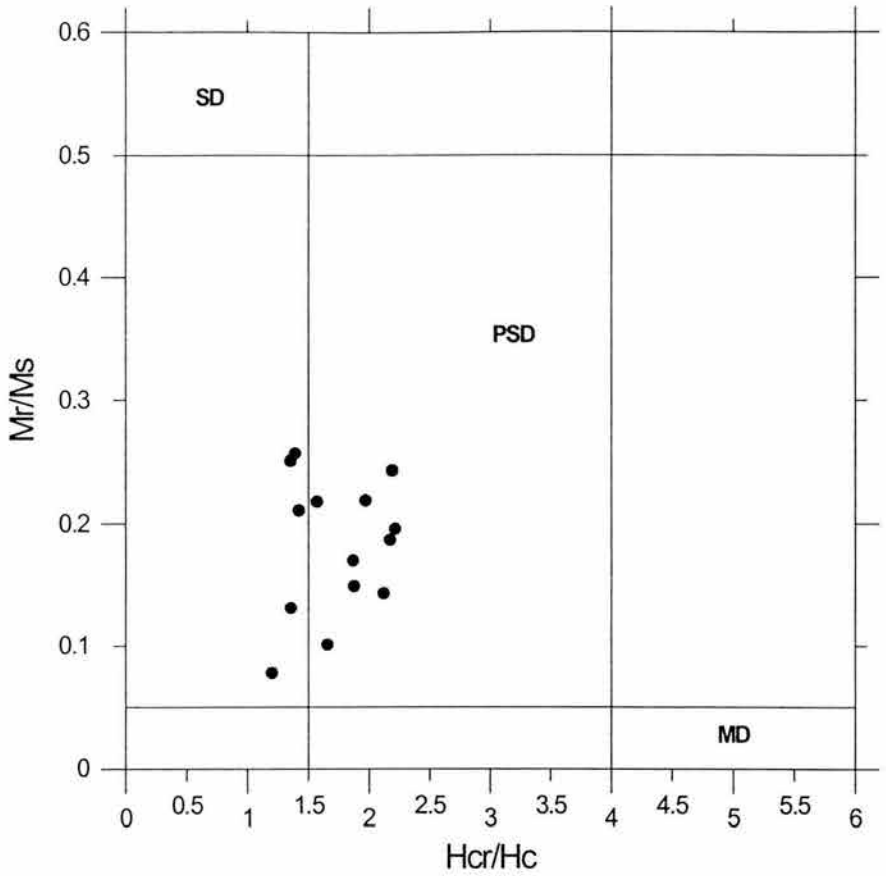

Fig. 4 Day plot (Day et al., 1977) with the hysteresis parameters ratios.

Paleodirectional determination

Laboratory procedures

The intensity and direction of natural remanent magnetization (NRM), of 10 to15 samples from each cooling unit, were measured with a JR-5A spinner magnetometer (nominal sensitivity ~ 10^{-9} Am^2). The coercivity spectrum, stability and vectorial composition of NRM were investigated by either progressive alternating field (AF) or stepwise thermal demagnetization. AF demagnetization was carried out in 8-10 steps up to maximums fields 70 or 100 mT using a *Molspin* AF-demagnetizer, while the thermal demagnetization was carried out in 12-14 steps up 560-600°C using a non-inductive Schonstedt furnace thermal demagnetizer.

Treatments

In total, all 184 specimens from 14 lava flows were demagnetized. In most of cases stable, univectorial paleomagnetic component was recognized (Figures 5, a-b). A generally small secondary component, probably of viscous origin, is sometime present and easily removed applying 200-250° C or 10-15 mT (V45-V51). The alternating field and thermal treatments carried out on the same cores, generally yield similar results (see samples V47 and V51). The greater part of remanent magnetization is removed at temperature between 520 and 560°C, which indicate, that low-Ti titanomagnetites is the main remanence carrier; while the median destructive field (MDF) ranges from 30 to 45 mT.

Results

The component analysis of remanent magnetization for individual specimens has been carried out using the linearity test suggested by Kirschvink (1980) taking from 4 to 9 points for the mean determination. Site-mean directions were calculated by vector addition giving unit weight to sample directions. Fisher statistics was used to estimate dispersion parameters (Fisher, 1953). Site-mean directions and their statistical parameters for all 14 sites, are summarized in Table 1.

Paleointensity Determination

Thellier Experiments

While procedures for the paleodirection studies are now more o less standardized, there still exist significant inter-laboratory differences on how to best obtain reliable estimates of the paleomagnetic field intensity. The Thellier method (Thellier and Thellier, 1959) in its modified form (Coe et al., 1967, 1978) has received the largest users group in last years (Juarez et al., 1998; Selkin and Tauxe, 2000; Alva-Valdiva et al., 2001; Goguitchaichvili et al., 2000). The method uses the fact that TRM is proportional with applied field in weak fields such as the geomagnetic (Nagata, 1943). The method involves heating samples twice at each temperature step: one in a zero magnetic field to remove a portion of NRM and second in a laboratory field to determine the partial thermoremanence (pTRM) gained. The ratio of NRM lost to pTRM gained is proportional to the ancient field.

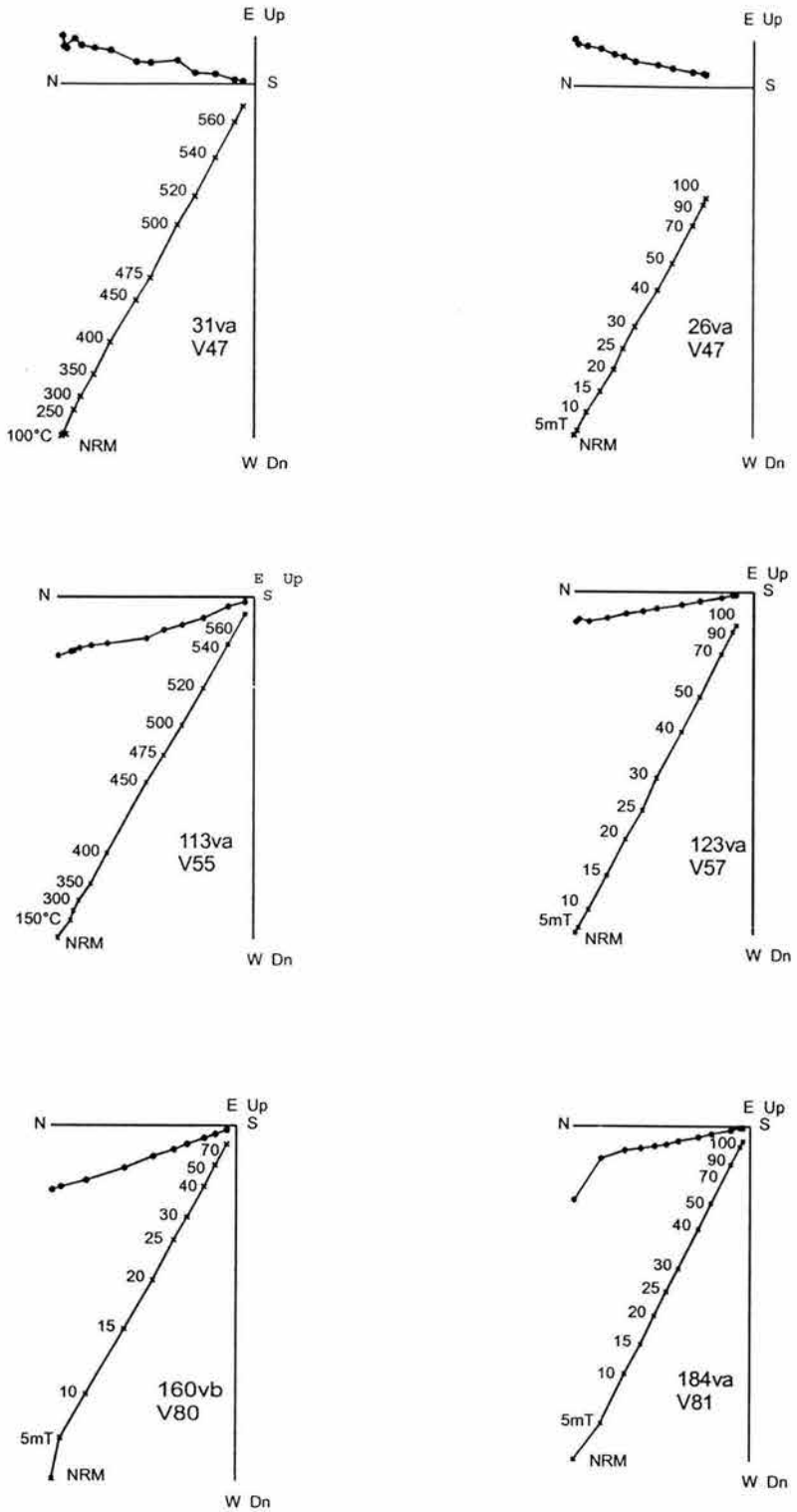

Fig. 5a Orthogonal vector plots of stepwise thermal and alternating field demagnetization (stratigraphic co-ordinates). The numbers refer to temperatures in °C or peak alternating fields in mT. o – projections into the horizontal plane, x – projections into the vertical plane.

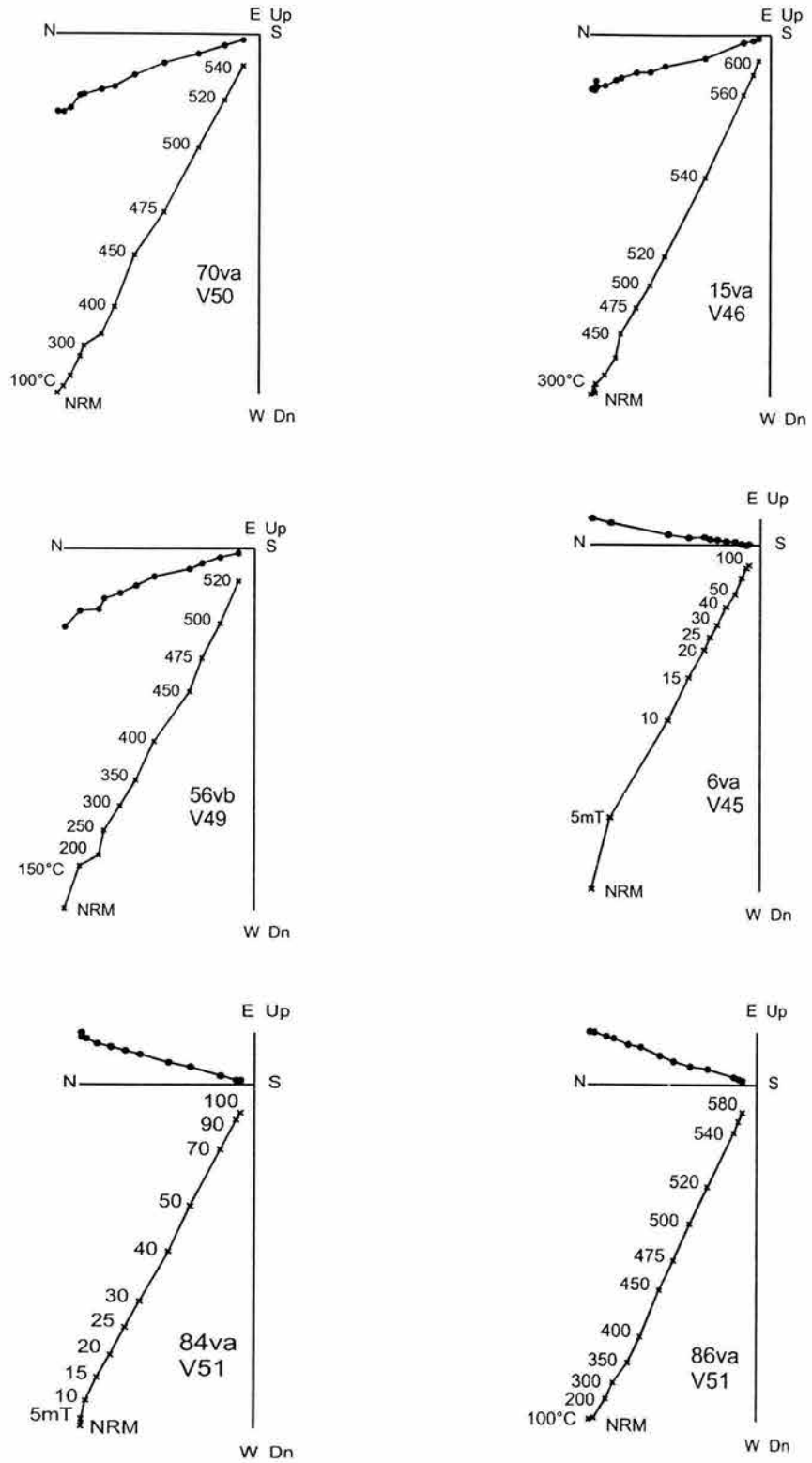

Fig. 5b Orthogonal vector plots of stepwise thermal and alternating field demagnetization (stratigraphic co-ordinates). The numbers refer to temperatures in °C or peak alternating fields in mT. o – projections into the horizontal plane, x – projections into the vertical plane.

Table 1

Site	*Coordinates*		*Age*	*n/N*	*Dec(°)*	*Inc(°)*	a_{95}(°)	*k*
	(°N)	*(°E)*						
V-45	40.81	14.34	1631	7/9	7.4	66.7	2.4	611
V-47	40.76	14.41	1631	9/13	11.5	61.6	1.5	1124
V-48	40.76	14.40	1631	10/15	13.8	65.1	2.6	340
V-51	40.78	14.36	1631	11/12	15.9	64.6	0.7	3863
V-46	40.77	14.41	1760	9/13	341.7	62.6	1.6	1085
V-49	40.76	14.42	1760	9/16	347.5	63.3	1.3	1569
V-50	40.77	14.42	1760	9/15	344.0	61.4	2.5	409
V-53	40.83	14.37	1872	11/15	348.5	56.4	0.9	2320
V-55	40.83	14.37	1872	8/12	347.6	54.4	1.0	2950
V-57	40.84	14.38	1872	11/13	347.5	57.6	1.1	1750
V-80	40.82	14.39	1858	11/13	345.3	56.0	1.7	725
V-61	40.81	14.44	1906	7/12	357.5	52.5	0.9	4306
V-68	40.81	14.41	1872/1886	8/12	345.2	59.2	1.9	862
V-81	40.82	14.39	1858/1895	9/12	347.9	59.8	1.1	2044
Mean: V-47, V-48, V-51			1631	3/2	13.6	63.8	3.3	1437
Mean: V-46, V-49, V-50			1760	3/3	344.1	62.5	2.6	2219
Mean: V-53, V-55, V-57			1872	3/3	347.9	56.2	2.5	2349

Paleodirectional results from the Vesuvius rocks: **N**: Number of treated samples, **n**: number of samples used for calculation, **Dec**: Declination, **Inc**: Inclination, **k** and α_{95}: Precision parameter and radius of confidence cone.

This technique was used in present study to determine absolute geomagnetic paleointensity. The heating and coolings were carried out, using a MDT 80 furnace and the laboratory field set to 30 microTesla at the Paleomagnetic Laboratory of National University (UNAM). Thirteen temperature steps were distributed between room temperature and 580°C. Temperature reproducibility between two steps was in general better than 2°C. During the experiment five control heating (so-called "pTRM" checks) were performed after every second step to check the thermal alteration (Coe et al., 1978).

Results

Altogether fifty-four samples from nine individual lava flows were pre-selected for Thellier paleointensity experiment because of stable one component magnetization accompanied with relatively high MDF values, elevated blocking

temperature, and reasonably reversible k-T curve. Some typical Arai-Nagata curves (Nagata et al., 1963) are shown Figures 6 a-b, and the results are given in Table 2.

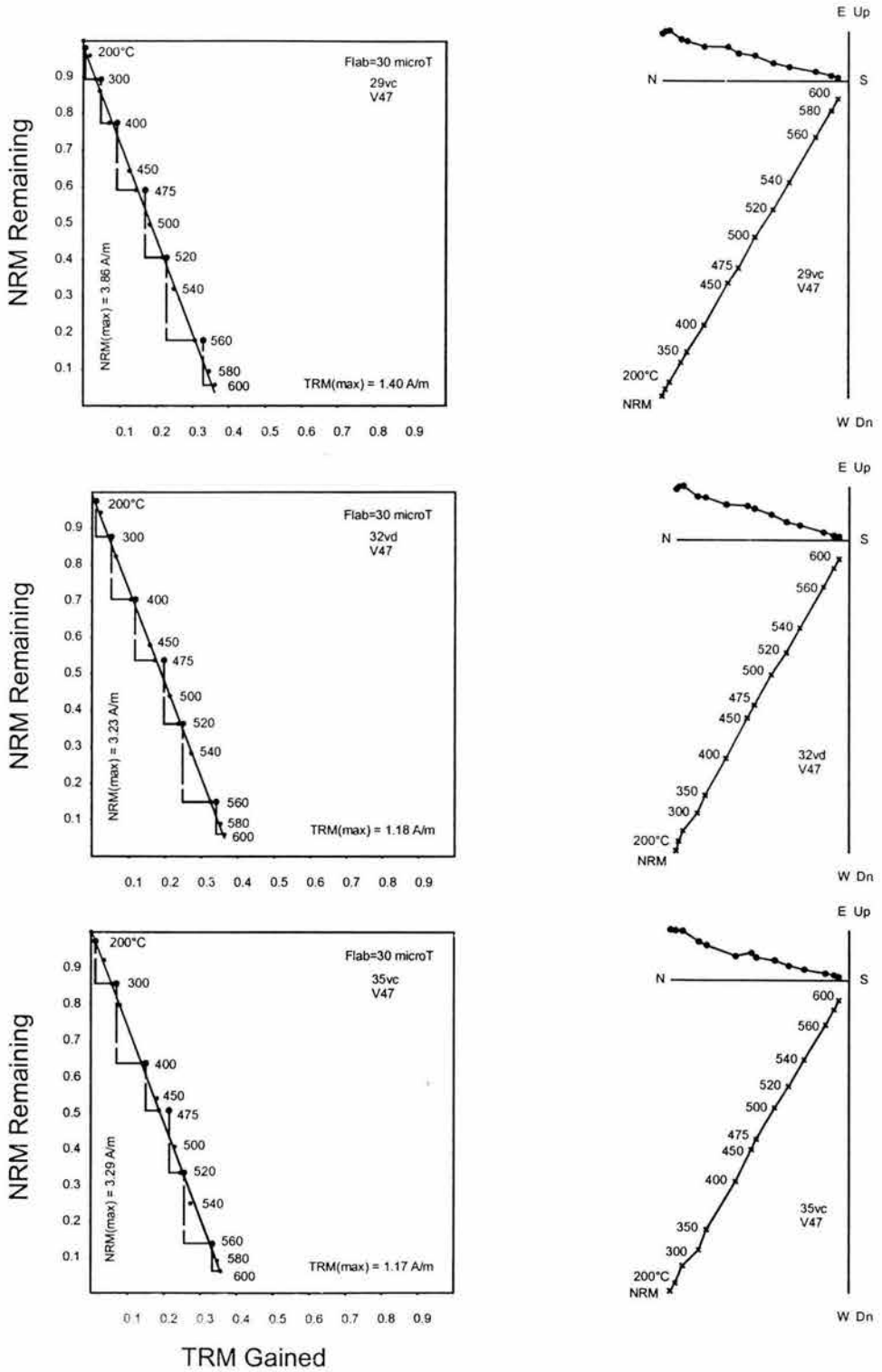

Fig. 6a The representative NRM-TRM plots and associated orthogonal diagrams for representative samples. For the orthogonal diagrams we used same notations as in Figure 5.

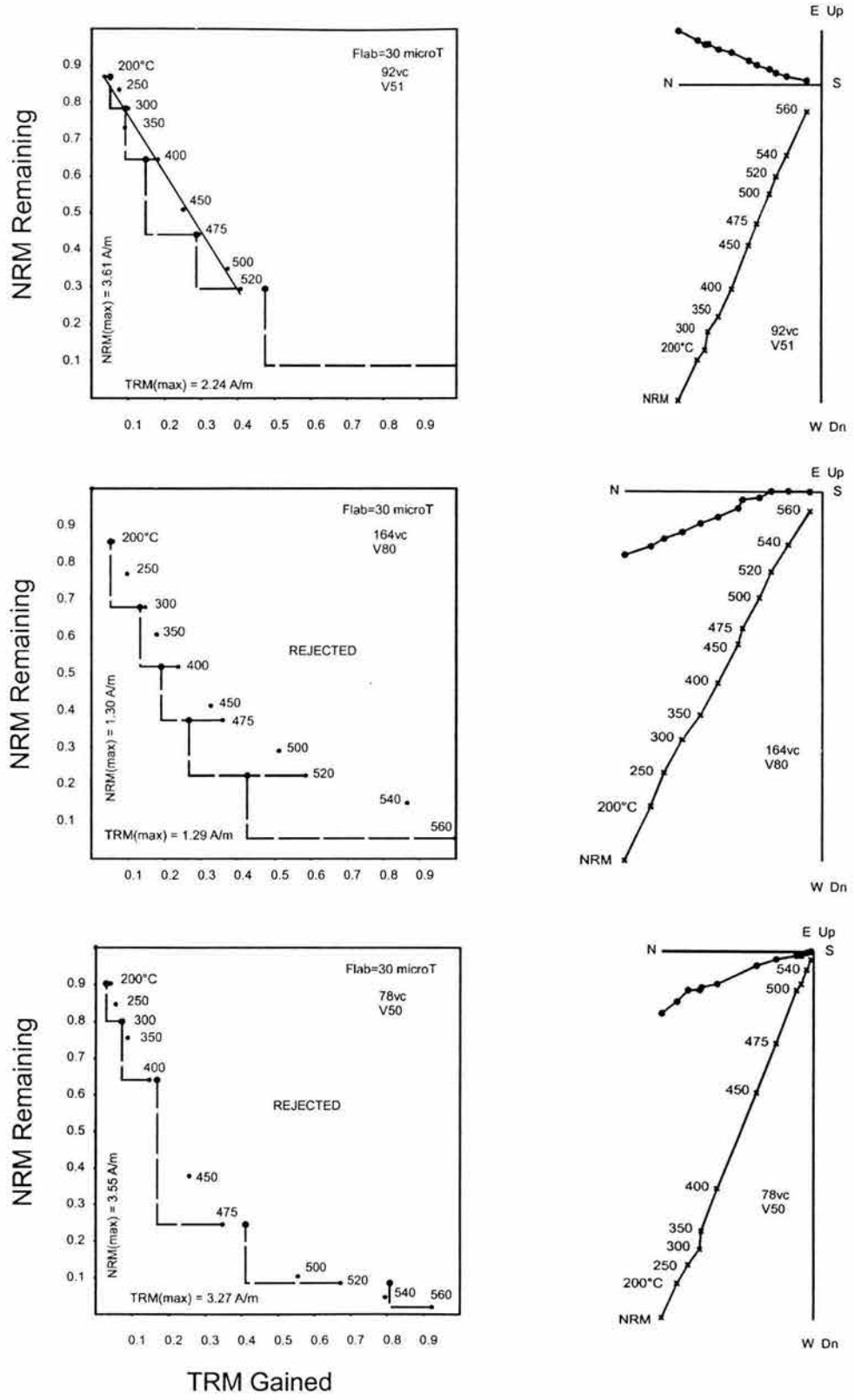

Fig. 6b The representative NRM-TRM plots and associated orthogonal diagrams for representative samples. For the orthogonal diagrams we used same notations as in Figure 5.

Table 2

Site (Age)	*Sample*	*N'*	T_{min}-T_{max}	*f*	*g*	*q*	$F_E \pm \sigma(F_E)$	*VDM*	*VDMe*
			°C				(μT)	$10^{22}Am^2$	$10^{22}Am^2$
V46 (1760)	V13	8	250-520	0.76	0.73	10.23	66.6 ± 3.6	11.3	**12.6 ± 1.3**
	V17	8	250-520	0.56	0.78	7.90	78.5 ± 4.4	13.3	
	V18	9	200-520	0.46	0.82	9.83	81.0 ± 3.1	13.2	
	V19	7	300-540	0.62	0.75	7.06	68.6 ± 4.5	11.1	
	V20	9	250-540	0.58	0.81	9.03	72.6 ± 3.7	12.3	
	V22	9	200-520	0.34	0.84	9.26	85.0 ± 2.6	14.2	
V47 (1631?)	V29	14	20-600	0.96	0.90	69.24	79.5 ± 0.9	13.7	***13.5 ± 0.4***
	V31	14	20-600	0.96	0.90	46.69	83.2 ± 1.5	14.0	
	V32	14	20-600	0.95	0.90	97.08	77.6 ± 0.7	13.3	
	V33	14	20-600	0.96	0.89	60.40	73.9 ± 1.1	12.9	
	V34	14	20-600	0.93	0.90	82.86	79.5 ± 0.8	13.7	
	V35	14	20-600	0.94	0.90	79.39	79.6 ± 0.8	13.5	
V51 (1631?)	V88	5	350-500	0.51	0.74	4.09	51.3 ± 4.7	8.34	***9.24 ± 1.8***
	V90	5	350-500	0.47	0.74	3.83	53.4 ± 4.9	8.48	
	V91	6	350-520	0.53	0.78	5.13	57.8 ± 4.7	9.24	
	V92	9	200-520	0.63	0.85	12.31	76.4 ± 3.3	12.3	
	V95	6	350-520	0.56	0.77	6.65	48.8 ± 3.2	7.89	
V53 (1872)	V97	13	200-600	0.99	0.87	21.26	44.3 ± 1.7	7.93	***7.86 ± 0.2***
	V99	13	200-600	0.98	0.87	17.98	44.9 ± 2.1	8.15	
	V100	13	200-600	0.97	0.87	22.23	43.4 ± 1.7	7.66	
	V105	14	20-600	0.99	0.88	25.58	42.8 ± 1.5	7.54	
	V106	14	20-600	0.99	0.89	24.51	43.9 ± 1.6	7.91	
	V108	14	20-600	0.98	0.88	21.22	44.6 ± 1.8	7.98	
V55 (1872)	V113	9	20-500	0.78	0.80	8.25	63.9 ± 4.8	11.9	***10.1 ± 2.8***
	V118	9	200-520	0.68	0.83	25.87	71.7 ± 1.6	13.2	
	V119	6	300-500	0.62	0.77	7.76	42.5 ± 2.6	7.68	
	V122	7	300-520	0.69	0.80	9.78	40.1 ± 2.3	7.56	
V57 (1872)	V127	7	300-520	0.58	0.79	6.22	78.9 ± 5.8	13.5	***10.5 ± 1.7***
	V128	9	200-520	0.72	0.84	18.08	57.3 ± 1.9	10.1	
	V129	9	200-520	0.77	0.82	16.50	48.8 ± 1.9	8.44	
	V132	9	200-520	0.74	0.82	13.27	64.5 ± 2.9	11.4	
	V133	9	200-520	0.77	0.82	16.08	55.4 ± 2.2	9.78	
	V134	8	250-520	0.82	0.81	13.07	54.4 ± 2.8	9.84	
V61 (1906)	V136	9	200-520	0.70	0.83	12.90	51.5 ± 2.3	9.75	***9.28 ± 0.7***
	V137	9	200-520	0.65	0.83	12.53	50.2 ± 2.1	9.51	
	V139	9	200-520	0.54	0.81	7.55	51.9 ± 3.0	9.86	
	V142	5	300-475	0.42	0.66	4.66	51.6 ± 3.1	9.74	
	V145	7	200-475	0.45	0.76	2.40	43.8 ± 6.3	8.22	
	V147	6	350-520	0.61	0.78	7.68	45.0 ± 2.8	8.59	

Paleointensity results from the Vesuvius lavas, n is number of NRM-TRM points used for paleointensity determination, Tmin-Tmax is the temperature interval used, *f*, *g* and *q* are the fraction of extrapolated NRM used, the gap factor and quality factor (Coe et al., 1978) respectively. Fa is the individual paleointensity estimate with associated error, Fe is site mean paleointensity, VDM and VDMe are individual and average virtual dipole moments.

The criteria that we used for individual paleointensity determination are basically similar to those reported by Conte et al. (2004) and can be described as follows. We only accepted determinations that fulfil the following criteria: (1) obtained from at least six NRM-TRM points corresponding to a NRM fraction larger than 1/3, (2) yielding quality factor (Coe et al., 1978) of about 5 or more, and (3) with positive 'pTRM' checks i.e. the deviation of "pTRM" checks was less that 15% (Table 2). Only thirty-nine samples, from seven individual lava flows, yielded acceptable paleointensity estimates. For these samples the fraction of NRM *f* used for paleointensity determination ranges between (0.34-0.99) and the quality factor *q* from (2.4-97.1) generally greater than 5. Moreover the NRM end points, obtained from the Thellier experiments at each step, is reasonably linear and point to the origin (Figures 6 a-b, right side); no deviation of the direction NRM left toward the applied laboratory field was observed. The principal reasons for rejecting paleointensity determination were typical "concave-up" behavior (Dunlop and Özdemir, 1997, Levi, 1977) detected in some cases (sample 78vc and 164vc in Figure 6b).

Discussion and Conclusion

The average directions of each unit were determined assuming a Fisherian distribution with α_{95} ranging from 0.7° to 2.6 (Table 1). This points to a very high quality paleomagnetic data. Thirty-nine samples yielded acceptable paleointensity estimates, being the first published for Mount Vesuvius (Table 2). Fraction of NRM *f* used for paleointensity determination ranges between 0.47-0.99 and the quality factor *q* from 3.8-97.1, generally greater than 5. NRM end points obtained from the Thellier experiments at each step are reasonably linear and point to the origin (Figures 6a-b); no deviation of NRM left direction towards applied laboratory field was observed. These points to high technical quality of paleointensity determinations. Obtained VDMs (virtual dipole moments), ranging from 7.86±0.2 to 13.5±0.4 ($10^{22}Am^2$), are higher than the present day geomagnetic field strength.

As far as the paleodirections is concerned they are to be compared with a SVC for the area. Two of such a curves are available: the SISVC (Southern Italy Secular Variation Curve) (Incoronato et al., 2002; Incoronato and Del Negro, 2004) and the

SIVC (South Italian Volcanic Curve) (Tanguy et al., 2003) largely derived from Tanguy et al. (1999). These curves are constructed from different procedures, extensively discussed in Incoronato et al. (2002) and (Incoronato and Del Negro (2004), that are recalled here only briefly.

The SISVC relies on:

1. Analysis of the entire coercivity/blocking temperature spectra by subjecting each specimen to complete demagnetization in order to check the presence of magnetization components.
2. Information on the magnetic carrier.
3. Separation of different magnetization components achieved by PCA. In dealing with lava flows emplaced a few hundred years ago only, very low MAD have been used in order to separate primary components of magnetization from secondary ones, acquired in such a small time interval of a few hundred years only, although this caused many specimens or sites to be rejected.
4. Relocation of geomagnetic/magnetization directions, via the inclined geocentric dipole, performed within a few hundred kilometers only.

The bulk of the data on which the SIVC relies derives from NRM measurements and measurements of partial PAFD; no PCA analysis, Zijderveld diagrams and information on magnetic carriers were available.

Taking into account the different procedures leading to these SVCs, the SISVC will be used for further discussion of the results.

As test for our result, we plotted the paleodirections determined of all investigated lava flows over the secular variation curve for the area. All data showed the compatible paleodirections with the SISVC (Figure 7) and their ages may be easily retrieved. Two sites, however (V68 and V81) yielded distinct mean directions. At this stage of investigation it is unclear whether these lavas are erupted during other time intervals or the data have no geomagnetic significance.

Concerning the 1631 eruption, we re-analyzed the whole data-set of paleomagnetic directions previously published (Hoye, 1981; Gianella et al. 1993, Carracedo et al. 1993; Tanguy et al., 1999) and added 4 new, high quality results

(sites V45, V47, V48, and V51 of present study). These directions are compared with SISVC and the directions furnished by 1631 pyroclastic lava flow by Carracedo et al., (1993). The difference found between the paleodirections retrieved from reference curve and pyroclastic flow (unambiguously pertaining to this eruption) seems to be related to the mechanism of remanence acquisition in pyroclastic lavas as already underlined by Carracedo et al. (1993) (Figures 8 and 9). Strictly speaking, only lava flow V48 from the present study matches with the corresponding segment of the reference curve.

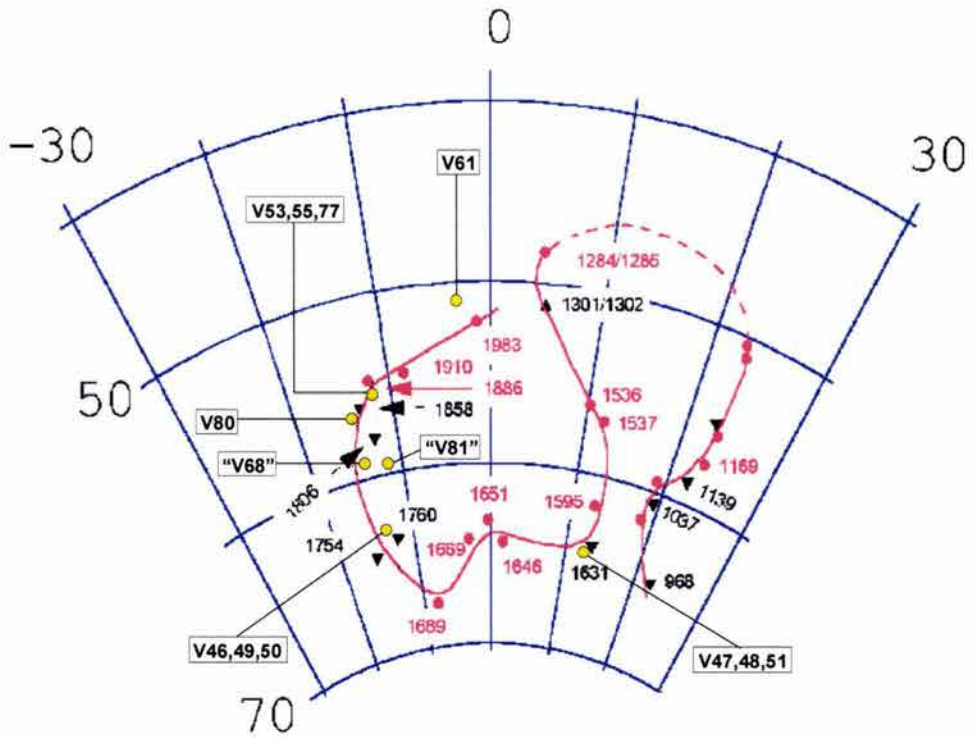

Fig 7 Site-mean characteristic paleodirections from Vesuvius lava flows referred to the Southern Italy secular variation curve (Incoronato et al., 2002).

●	Etna relocated to Vesuvio	Incoronato et al., 2002
▲	Arso (Ischia)	
▼	Vesuvio	
▼	Vesuvio (1754)	Tiano, 2001
○	This Study	see tab. 1

Although two lavas, (V47 and V51) which may be considered as coeval flows yielded similar paleodirections close to the reference curve, they should be considered as distinct cooling units as indicated by their different paleointensities. Site V45 has significantly different paleodirections compared to the reference curve. The lava flows from Carracedo et al.'s (1993) study yield highly scattered directional results. Two sites (V16 and V20) may be also related to the 1631 eruption, while all flows (excepting two: sites 9 and 11) studied by Gialanella et al. (1993) give concordant directions with the reference, as far as reported in his work. The same is true for site A of Hoye (1981). In summary, paleodirections of eight lava flows from twenty-two flows studied coincide within associated uncertainties with the corresponding segment of the Southern Italy secular variation curve. Thus, this major event in Vesuvius volcanic history should be considered as an explosive- effusive eruption.

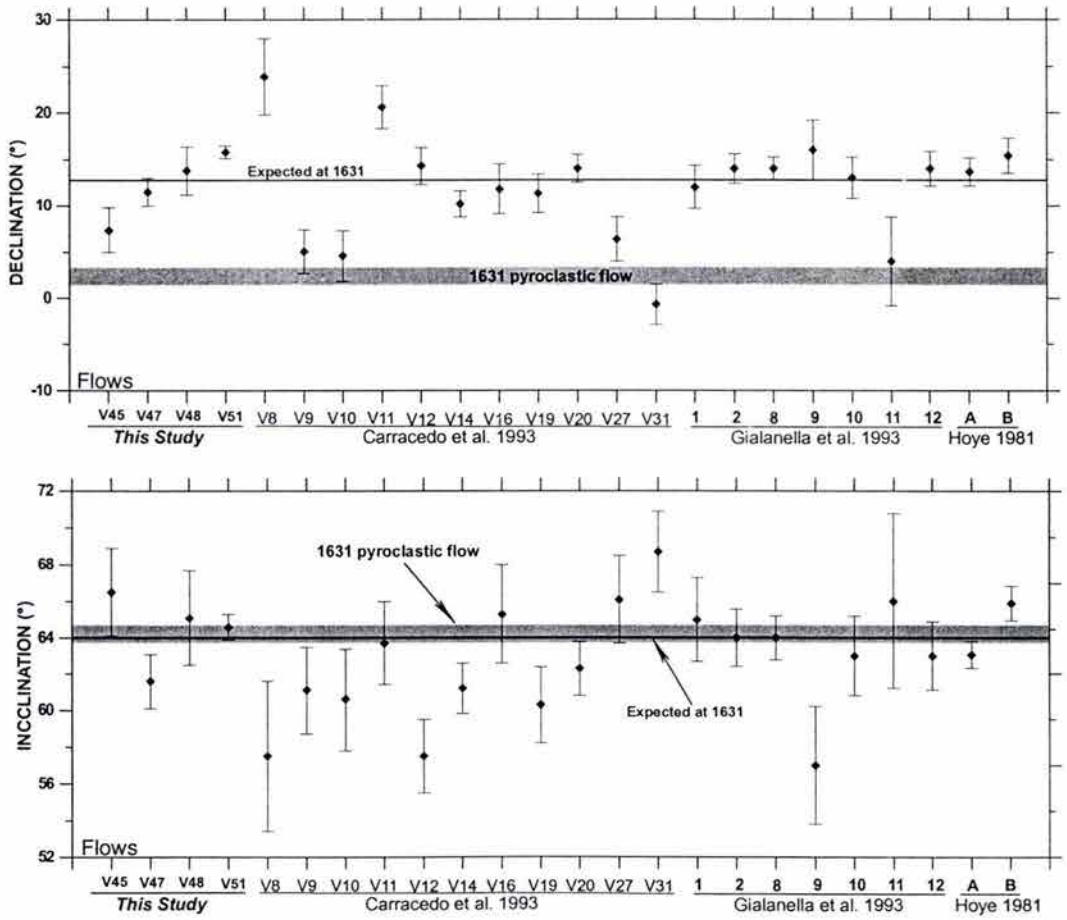

Fig. 8 Summary of characteristic unit mean paleodirections obtained from the Vesuvius '1631' lava flows (see also text).

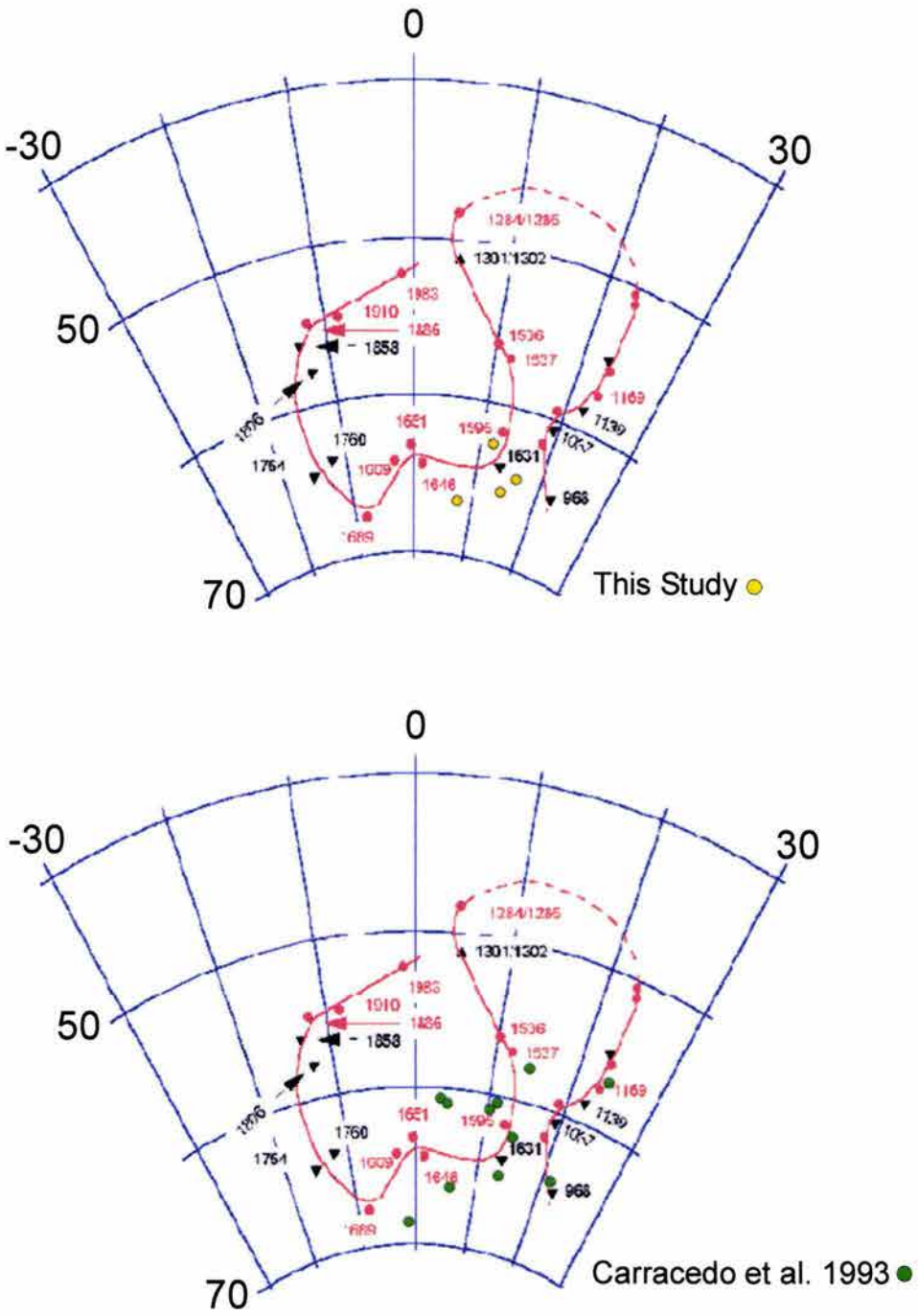

Fig. 9 Site-mean characteristic paleodirections from Vesuvius lava flows presumably related to the 1631 eruption referred to the Southern Italy secular variation curve (Incoronato et al., 2002).

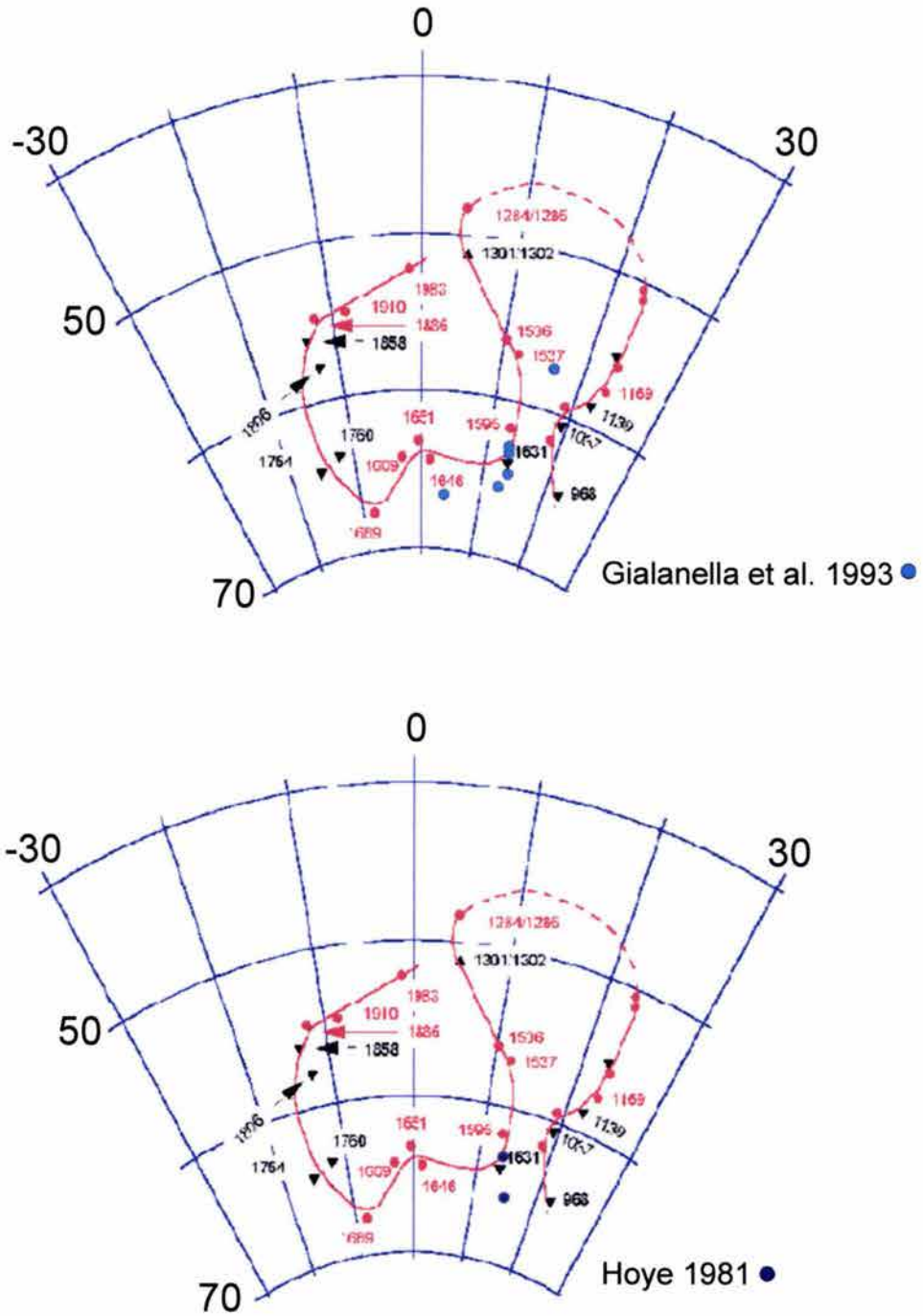

Fig. 9 (*Continued*)

References

Alva-Valdivia L., Goguitchaichvili A., Urrutia-Fucugauchi J., and Morales. (2001). Further constraints for the Pliocene geomagnetic field strangth: New results from the Los Tuxtla volcanic field (Mexico). *Earth Planets Space*, V. 53, pp. 873-881.

Arnó V., Principe C., Rosi M., Santacroce R., Sbrana A. & Sheridan M. F. (1987). Eruptive history. In Santacroce R. (Ed.) "Somma- Vesuvius" *Quaderni de "La ricerca scientifica"*. C. N. R. 114, 8, pp. 243.

Burri C., and Di Girolamo P. (1975) Contributo alla conoscenza delle lave della grande eruzione del Vesuvio del 1631. *Rend. Soc. Ital. Mineral. Petrol.,* 30 (2), pp. 705-739.

Carracedo J., Principe C., Rosi M., and Soler V. (1993). Time correlation by palaeomagnetism of the 1631 eruption of Mount Vesuvius. Volcanological and volcanic hazard implications. *Journal of Volcanology and Geothermal Research,* 58, pp. 203-209.

Coe R. (1967). The determination of paleo intensities of the Earth's field with emphasis on mechanism which could cause non-ideal behavior in Thellier's method. *Journal of Geomagn. and Geolectr.,* V. 19, pp. 157-179.

Coe R., Gromme S. and, Mankinen E. A. (1978). Geomagnetic paleointensity from radiocarbon-dated lava flows on Hawaii and the question of the Pacific non-dipole Low. *Journal of Geophysical Research,* 83, pp. 1740-1756.

Day R., Fuller M., and Schmidt V. A. (1977). Hysteresis properties of titanomagnetites: Grain size and compositional dependence. *Physics of the Earth and Planetary Interiors,* 13, pp. 260-267.

Delibrias G., Di Paola G., Rosi M., and Santacroce R. (1979). La storia eruttiva del complesso vulcanico Somma-Vesuvio ricostruita nelle successioni piroclastiche del M.te Somma. *Rend. Soc. It. Mineral. Petrol.*, V. 35, pp. 411-438.

Di Girolamo P. (1978). Geotectonic setting of Miocene-Quaternary volcanism in and around the Easten Tyrrhenian sea border (Italy) as deduced from major element geochemistry. *Bull. Volcanol.*, V. 41, pp. 229-250.

Dunlop D. J., and Ozdemir O. (1997). Rock-magnetism Fundamentals and frontiers. *Cambridge, UK, Cambridge University Press*, pp. 573.

Fisher, R. A., (1953). Dispersion on the sphere. *Proc. R. Soc. London. Ser.* A 217, pp. 295-305.

Gialanella R., Incoronato A., Russo F., and Nigro G. (1993). Magnetic stratigraphy of Vesuvius products. I-1631 lavas. *Journal of Volcanology and Geothermal Research,* 58, pp. 211-215.

Goguitchaichvili A., Chauvin A., Roperch P., Prevot M., Vergra M., Moreno H. (2000). Paleomagnetism of the Miocene Farellones formation in Chile. *Geophys. Journal Int.* 140, pp. 357-374.

Hoye G. S. (1981). Archaeomagnetic secular variation record of Mount Vesuvius. *Nature,* 291, pp. 216-218.

Incoronato A. (1996). Magnetic stratigraphy procedures in volcanic areas: the experience at Vesuvius. Palaeomagnetic and Tectonics of the Mediterranean Region. *Geological Society Special Publication* 105, pp. 367-371.

Incoronato A., and Del Negro C. (2004) - Magnetic Stratigraphy Procedures At Etna. In: Bonaccorso A., Calvari S., Coltelli M., Del Negro C. & Falsaperla S. (eds.) "The Mt. Etna Volcano". *AGU Geophysical Monograph Series* V. 143, pp. 263-271.

Incoronato A., Angelino A., Romano R., Ferrante A., Sauna R., Vanacore G., and Vecchione C. (2002). Retrieving geomagnetic secular variations from lava flows: evidence from Mount Arso, Etna and Vesuvius (southern Italy). *Geophys. Journal Int.,* 149, pp. 724-730

Johnston Lavis H. J. (1884). The geology of the Mt. Somma and Vesuvius: being a study of volcanology. Q. J. Geol. Soc. london, V. 40, pp. 135-149.

Juarez M. T., Tauxe L., Gee J. S., Pick T. (1998). The intensity of the Earth's magnetic field over the past 160 million years. *Nature 394*, pp. 878-881.

Kirschvink, J. L., (1980). The least-squares line and plane and the analysis of palaeomagnetic data. *Geophys. J. R. Astr. Soc.* 62, pp. 699-718.

Le Hon M. (1865). Histoire complete de la grande eruption du Vesuve de 1631. *Bulletin de l'Acadamie des Sciences, Lettres et Beaux Arts, Belge*, V. 20, pp. 483-538.

Levi, S., (1977). The effect of magnetite particle size on paleointensity determination of the geomagnetic field. *Phys. Earth Planet. Inter.*, 13, pp. 245-259.

Nagata T., (1943) The natural remanent magnetism of volcanic rocks and its relation to geomagnetic phenomena. *Bull. Earthq. Res. Inst.*, V. 21, pp. 1-196.

Nagata T., Fisher R. M., Momose K. (1963). Secular variation of the geomagnetic total force during the last 5000 years. *Journal of Geophysical Research,* 68, pp. 5277-5281.

Prévot M., Mankinen R. S., Gromme S., and Leccaille A. (1983). High paleointensity of the geomagnetic field from thermomagnetic studies on rift valley pillow basalts from the middle Atlantic ridge. *Journal of Geophysical Research,* 88, pp. 2316-2326.

Principe C., Rosi M., Santacroce R., Sbrana A. (1987). Explanatory Notes to the Geological Map of Vesuvius. *Quaderni de La ricerca scientifica, CNR, Rome 114* V. 8 pp. 11-51.

Rolandi G. Barrella A., Borrelli A., and D'Alessio G. (1991). The 1631 Vesuvian eruption. *Int. Conf. on Active Volcanoes and Risk Mitigation. Abst.,* 91.

Rosi M. and Santacroce R. (1986). L'attivita' del Somma-Vesuvio precedente l'eruzione del 1631. Dati stratigrafici e vulcanologici. In: Albore Livadie C. (ed.) Tremblement de terre, eruptions volcaniques et vie des hommes dans le campanie antique. *Biblioteque d'Institute Français Naples*, 7, pp. 15-33.

Santacroce R. (1987). Somma-Vesuvius. *CNR Quader. Ric. Scient.*, 114, V. 8, pp. 251

Selkin P. A., Tauxe L. (2000). Long-term variations in palaeontensity. *Philos. Trans. R. Soc. London* A 358, pp. 1065-1088.

Tanguy J. C., M. Le Goff, V. Chillemi, A. Paiotti, C. Principe, S. La Delfa and G. Patanè (1999) Variation séculaire de la direction du champ géomagnétique enregistrée par les laves de l'Etna et du Vésuve pendant les deux derniers millénaires. *C. R. Ac. Sc. Paris, Sciences de la Terre et des planètes*, 329, pp. 557-564.

Tanguy J. C., M. Le Goff, V. Chillemi, A. Paiotti, C. Principe, S. La Delfa and G. Patanè (2003) Archeomagnetic dating of Mediterranean volcanics of the last 2100 years: validity and limits. Earth and Planet. Sc. Lett., 211, pp. 111-124.

Tauxe L., Mullender T.A.T., Pick T. (1996) Pot-bellies, wasp-waists and superparamagnetismo in magnetic hysteresis. *Journal of Geophysical Research,* 95, pp. 12337-12350.

Thellier E. and Thellier O. (1959). Sur l'intensite de champ magnetique terrestre dans le passe historique et geologique. *Ann. Geophys,*. V. 15, pp. 285-376.

Zijderveld, J. D. A.. (1967). A. C. demagnetization of rocks: analysis of results, in Methods in Palaeomagnetism. E*ds Colinson, D. W., Creer, K. M. & Runcorn, S. K., Elsevier, Amsterdam.* pp. 254-286.

TERCERA PARTE

Conclusiones

CONCLUSIONES

Las investigaciones sobre las variaciones espacio-temporales del campo geomagnético han permitido identificar y cuantificar las variaciones geomagnéticas de largo periodo incluidas en la variación paleosecular, excursiones y cambios de polaridad. La cronología de cambios de polaridad para el Fanerozóico define la ocurrencia de periodos de diversa duración caracterizados por polaridad normal o reversa (denominados crones) y dos periodos de larga duración (conocidos como super-cron normal del Cretácico y super-cron reverso Kiaman o Permo-Triásico). Estas variaciones temporales del campo geomagnético proveen un sistema de referencia espacio-temporal de utilidad para estudios geocronológicos y correlación estratigráfica. En este proyecto doctoral se ha investigado la variación paleosecular del campo geomagnético a diferentes escalas (que incluyen periodos de los últimos miles de años y los últimos dos millones de años) en las zonas central de México y meridional de Italia. En México se investigaron las secuencias volcánicas en el estratovolcán Popocatepetl y algunos conos cineríticos del campo volcánico Michoacán-Guanajuato. En Italia se estudiaron los flujos recientes del complejo volcánico Somma-Vesuvio. Además de la contribución al conocimiento de la variación paleosecular en estas dos zonas y periodos seleccionados, se han investigado varios otros problemas de interés en paleomagnetismo y volcanología. Por ejemplo, en el estudio en Italia, se realizaron muestreos en flujos de lava del complejo Somma-Vesuvio posiblemente relacionados a la erupción del 1631. Esta erupción del Vesuvio ha sido tema de controversia, en particular sobre el carácter de la actividad: puramente explosiva o explosiva-efusiva. Las investigaciones realizadas en México e Italia presentan una aportación adicional en comparación con estudios paleomagnéticos convencionales. En nuestros estudios se trató de determinar experimentalmente la dirección y la paleointensidad del campo geomagnético. Por este motivo es presentado como estudio paleomagnético integral. La determinación de paleointensidades presenta en general una mayor dificultad que la cuantificación de las paleodirecciones, lo que presenta retos adicionales en la pre-selección de muestras para los experimentos de paleointensidad y en la obtención de datos

analíticos de calidad. Las investigaciones incluyen además estudios detallados de la mineralogía magnética y de los portadores de la magnetización remanente y su estado de dominio magnético. Estos estudios aportan información crítica para la selección de muestras para las determinaciones de paleointensidad.

La determinación de la mineralogía magnética, por medio de experimentos como mediciones de susceptibilidad magnética de alta temperatura, ciclo de histéresis magnética y magnetización remanente isotermal (IRM) revelaron que los minerales portadores de la magnetización remanente, en la mayoría de los casos sea para Central México e Italia, están representados por titanomagnetitas pobres en titanio y predominantemente de dominio pseudo-sencillo.

Los sitios muestrados alrededor del complejo volcánico Popocatépetl, presentan una polaridad normal de acuerdo con los datos previos (Carrasco et el., 1986), confirmando entonces una edad para el complejo volcánico no más atrás de 0.78 M.a. (Brunhes Chron). Combinando todos los datos disponibles en literatura el valor de paleodirección promedio es de D=345.7, I=35.4, K=21, α_{95}=5.8, N=15 el cual se desvía ligeramente en el sentido contrario de las manecillas del reloj respecto al valor actual del campo geomagnético. Los análisis geoquímicos (elementos mayores y trazas) testimonian el carácter calco-alcalino de algunos de los volcanes de la Faja Volcánica Trans-Mexicana, típico de ambiente de subducción, mientras los experimentos de paleointensidad con técnica Thellier-Thellier (Thellier & Thellier, 1959) y sus modificaciones (Coe et al., 1967, 1978) dan resultados de buena calidad para 14 muestras sobre 25 pre-seleccionadas pertenecientes a cuatro flujos independientes. El valor promedio del momento dipolar virtual (VDM) es de 7.2±1.4 ($10^{22}Am^2$), el cual es ligeramente más bajo que el valor actual del campo geomagnético ($8*10^{22}Am^2$).

Los resultados de paleodirección del campo volcánico Michoacán-Guanajuato se acercan a los esperados publicados en diferentes partes del mundo para este periodo, con un valor promedio de dirección de D=357.9, I=28.4, α_{95}=7.3, N=20. Sin embargo el estudio de paleointensidad fue limitado, y se obtuvieron resultados satisfactorios solamente para dos flujos independientes. La determinación de la variación paleosecular (PSV) para los sitios muestrados en este trabajo

proporcionaron un valor de S_f=15.4, Su=19.6 y Sl=12.7 (limite inferior y superior respectivamente) el cual es decisivamente más alto respeto al modelo teórico de McFadden et al. (1988, 1991). El motivo de esa discrepancia podría ser relacionado al poco número de sitios estudiados respeto al intervalo de tiempo en consideración (0-2,10 Ma). Tomando en cuenta todos los datos disponibles para la Faja Volcánica Trans-Mexicana, se obtuvo un conjunto de 151 datos, donde más del 60% son de edades menores a 70,000 años. Seleccionando estos datos tomando en cuenta un angulo de corte (cutoff-angle) de 30° y un α_{95}<15° se calculó la variación paleosecular y se obtuvo un valor de S_f=13.3, S_u=14.8 y S_l=12.1, el cual se ajusta muy bien al modelo de referencia de McFadden et al., (1988, 1991) para la latitud de México Central. Por lo tanto, el presente trabajo excluye que México Central pertenece a la zona de baja magnitud no-dipolar del Pacifico como ha sido propuesto por algunos autores (Doell & Cox, 1971, 1972).

Los experimentos de paleointensidad por medio de técnica de microondas con lavas del volcán Paricutin, desgraciadamente dieron resultados muy diferentes entre de ellos y respecto a los esperados suponiendo como causas la presencia de multi-dominios MD o eventual CRM o TCRM.

En cuanto al complejo volcánico Somma-Vesuvio, lo datos obtenidos, se ajustan muy bien a la curva de referencia para Italia meridional (Incoronato et al., 2002; Incoronato & Del Negro, 2004), en especial modo aquellos supuestos de la erupción del 1631 que ha sido material de especulación y desacuerdo entre de varios autores. Los experimentos de paleointensidad, proporcionan datos de buena calidad sin embargo, estos son muy altos respecto a los esperados con valores de VDM entre de 7.86±0.2 a 13.5±0.4 ($10^{22}Am^2$).